Doctoral Dissertations   Graduate School

12-2014

The role of NAG-1 in Tumorigenesis

Kyung-Won Min
University of Tennessee - Knoxville, kmin1@vols.utk.edu

To the Graduate Council:

I am submitting herewith a dissertation written by Kyung-Won Min entitled "The role of NAG-1 in Tumorigenesis." I have examined the final electronic copy of this dissertation for form and content and recommend that it be accepted in partial fulfillment of the requirements for the degree of Doctor of Philosophy, with a major in Comparative and Experimental Medicine.

<div align="right">Seung J. Baek, Major Professor</div>

We have read this dissertation and recommend its acceptance:

Xuemin Xu, Michael F. McEntee, Ranjan Ganguly, Daniel P. Kestler

<div align="right">Accepted for the Council:</div>

<div align="right">Carolyn R. Hodges</div>

<div align="right">Vice Provost and Dean of the Graduate School</div>

(Original signatures are on file with official student records.)

The role of NAG-1 in Tumorigenesis

A Dissertation Presented for the

Doctor of Philosophy

Degree

The University of Tennessee, Knoxville

Kyung-Won Min

December 2014

ACKNOWLEDGEMENTS

ABSTRACT

This dissertation explores the nature of a divergent member of the Transforming Growth Factor-β [beta] superfamily, the non-steroidal anti-inflammatory drugs activated gene (NAG-1), as it relates to its regulation and biological activity in cancer context. Our lab has extensively studied on the molecular mechanism by which phytochemicals and NSAIDs induce apoptosis correlation with NAG-1 expression in human colorectal cancer (CRC) cells. Significant data from *in vitro* studies suggest that NAG-1 has an anti-tumorigenic activity which elicits apoptosis in a cyclooxygenase (COX)-independent manner in CRC cells. Indeed, NAG-1 transgenic mice developed less aberrant polyp foci (APC) compared to those of control counterpart in chemically- , genetically induced colorectal cancer models. However, it has been reported that NAG-1 has a tumor-promoting activity in a different cancer type such as prostate cancer and in *chapter 1*, a literature review for the regulation and the role of NAG-1 in the context of cancer will be discussed. Human pancreatic cancer cells treated with the PPARγ [gamma] ligand MCC-555 showed the feature of apoptosis with associated with NAG-1 induction. MCC-555 induces KLF4 expression via PPARγ-independent pathway, which in turn induces NAG-1 transactivation by which KLF4 binds to NAG-1 promoter region, suggesting NAG-1 is also implicated in apoptosis in human pancreatic cancer cells (*Chapter 2*). During the study on the signaling pathway and target genes affected by NAG-1, we observed nuclear expression of NAG-1. Nuclear NAG-1 moderates TGFβ signaling by interfering binding of Smad complex to DNA, leading to the inhibition of cell migration and invasion induced by TGFβ signaling (*Chapter 3*). Taken together, the studies

presented in this dissertation suggest that NAG-1 maybe a driver factor for apoptosis

not only in CRC cells, but in pancreatic cancer cells, and this effect might arise from the

activity of nuclear NAG-1 which attenuates Smad signaling required for cancer survival

and progression.

TABLE OF CONTENTS

LIST OF TABLES

LIST OF FIGURES

LIST OF ABBREVIATIONS

APC	adenomatous polyposis coli
ATF3	activating transcription factor 3
ATP	adenosine triphosphate
bFGF	basic fibroblast growth factor
CDK5	cyclin-dependent kinase 5
C/EBPβ	CCAAT/enhancer binding protein β
ChIP	chromatin Immunoprecipitation
COX	cyclooxygenase
CRC	colorectal cancer
CRM1	chromosome region maintenance 1
CTGF	connective tissue growth factor
ECM	extracellular matrix
EGFR	epidermal growth factor receptor
EGR-1	early growth response protein 1
GAPDH	glyceraldehyde 3-phosphate dehydrogenase
GDF15	growth differentiation factor 15
GSK3	glycogen synthase kinase 3 beta
HMGB1	high-mobility group protein B1
HSP90	heat shock protein 90
KLF4	Kruppel-like factor 4
LTBP	latent TGF-beta binding protein
MAZ	myc-associated zinc finger protein
MMP	matrix metalloproteinases
NAD	nicotinamide adenine dinucleotide
NAG-1	nonsteroidal anti-inflammatory drug-activated gene-1
NGS	next-generation sequencing
NPC	Nuclear pore complex
NSAID	nonsteroidal anti-inflammatory drug
PPARγ	peroxisome proliferator-activated receptor gamma
Smad	mothers against decapentaplegic homolog 2
SS	sulindac sulfide
TA	tolfenamic acid
TG2	transglutaminase 2
TGFβ	transforming growth factor beta
TIMP3	tissue inhibitor of metalloproteinase 3
WGA	wheat germ agglutinin

INTRODUCTION

This dissertation explores the nature of a divergent member of the Transforming Growth Factor-β superfamily, the non-steroidal anti-inflammatory drugs activated gene (NAG-1), as related to its regulation and biological activity within cancer context. Our lab has extensively studied this divergent member of the Transforming Growth Factor-β superfamily on the molecular mechanism by which phytochemicals and NSAIDs induce apoptosis correlation with expression of this gene in human colorectal cancer (CRC) cells. Significant data from *in vitro* studies suggest that NAG-1 has an anti-tumorigenic activity which elicits apoptosis in a cyclooxygenase (COX)-independent manner in CRC cells. Indeed, NAG-1 transgenic mice developed fewer aberrant polyp foci (APC) compared to those of control counterpart in chemically- , genetically induced colorectal cancer models. However, it has been reported that NAG-1 has a tumor-promoting activity in a different cancer type such as prostate cancer. It has been demonstrated that the cellular context including epigenetic status and protein expression profiling in cancer is the crucial key which tunes cellular behavior to proper response to stimulus. There is the need to study NAG-1 in other cancer type which in NAG-1 might elicit a different biological consequence.

The regulation and the role of NAG-1 in the context of cancer will be discussed within *chapter 1* literature review. Since NAG-1'role in pancreatic cancer has not been well documented, we employed pancreatic cancer cells to study if NAG-1 can be induced in this cancer type. Human pancreatic cancer cells treated with the PPARγ-ligand MCC-555 showed the feature of apoptosis with associated with NAG-1 induction. MCC-555 induces KLF4 expression via a PPARγ-independent pathway, which in turn

induces NAG-1 transactivation through the binding of KLF4 to the NAG-1 promoter region, suggesting NAG-1 is also implicated in apoptosis in human pancreatic cancer cells (*Chapter 2*). During the study on the signaling pathway and target genes affected by NAG-1, we observed nuclear expression of NAG-1. Nuclear NAG-1 moderates TGFβ signaling by interfering with the binding of the Smad complex to DNA, leading to inhibition of cell migration and invasion induced by TGFβ signaling (*Chapter 3*).

 Taken together, the studies presented in this dissertation suggest that NAG-1 maybe a driver factor for apoptosis not only in CRC cells, but in pancreatic cancer cells, and this effect might arise from the activity of nuclear NAG-1 through attenuation of Smad signaling required for cancer survival and progression.

CHAPTER 1

NAG-1 in cancer

1.1 Introduction

Nonsteroidal anti-inflammatory drug (NSAID) activated gene-1 (NAG-1), a TGF-β superfamily gene, was discovered and identified by several different groups, referring as macrophage inhibitory cytokine - 1 [1], placental transformation growth factors (PTGFB) [2], prostate-derived factor (PDF) [3], growth differentiation factor 15 (GDF15) [4], or placental bone morphogenetic protein (PLAB) [5]. Because the method strategies used for finding this protein arise from different cellular context, NAG-1 may have a multiple facet to response to different environmental questions. In the context of cancer as with other members of the TGFβ superfamily, both an anti-tumorigenic and pro-tumorigenic potential of NAG-1 have been demonstrated [6], yet it's the molecular mechanism(s) remain to be resolved, including elucidation of NAG-1's downstream signal pathway and its receptor(s).

Transcriptional regulation of NAG-1 has been well studied, compared to the biological consequence induced by NAG-1 expression. It has been reported that dietary compounds, NSAID(s) and PPARγ ligands induce the activation of up-stream signal molecule such as p53, EGR-1 and KLF4, responsible for NAG-1 trans-activation in various cancer cell lines. In this case, NAG-1 expression seems to be implicated in the inhibition of tumor cell growth.

Upon discovery of dynamic protein localization, NAG-1 could be subjected to study its cellular localization, although it has been characterized as a secretion protein like other TGF-β superfamily proteins. Since secretion protein observed in intra-cellular region [7], it is plausible that NAG-1 also has second location where it resides in and

performs a different function, which in part could explain divergent roles of NAG-1 in cancer. By dissecting NAG-1's role on molecular level(s) during tumorigenesis, NAG-1 may serve as a potential biomarker/or a therapeutic target for the diagnosis and treatment during cancer progression.

1.2 Transcriptional regulation of NAG-1

Many trans-acting transcription factors that control NAG-1 induction have been identified, including p53, early growth response gene-1 (EGR-1), Sp1, activating transcription factor-3 (ATF-3) and Kruppel-like factor 4 (KLF4). A variety of dietary compounds, NSAIDs and PPARγ ligands have been reported to induce NAG-1 expression through the activation of these transcription factors in various cancer cell lines.

p53 is classified as a tumor suppressor gene and plays a pivotal role in apoptosis, genomic stability and controlling cell cycle. NAG-1 promoter contains p53 binding sites and NAG-1 expression can be mediated by p53 expression induced by natural products, leading cell growth arrest and apoptosis in cancer cells [8]. EGR-1 plays a role in the regulation of cancer cell growth and differentiation and EGR-1 is a direct regulator of multiple tumor suppressors [9], though EGR-1 also possesses tumor-promoting effect in prostate cancer [10], suggesting that EGR-1' role in cancer is dependent on cellular context. EGR-1-binding sites are located within region -73 to -51 of the NAG-1 promoter and have an important role in the transactivation of PPARγ ligand-induced NAG-1 expression [11].

ATF3 is a member of the ATF/CREB superfamily and its expression is dramatically induced in response to extracellular signals [12]. Recently, it has been reported that NAG-1 can be induced by cooperation of transcriptional machinery. In colorectal cancer cells, capsaicin, a natural product of red peppers induces nuclear accumulation of GSK3β which phosphorylates C/EBPβ. ATF3 plays a role as a bridge protein to make complex with activated C/EBPβ by capsaicin for enhancing binding affinity of C/EBPβ onto NAG-1 promoter and activates transcription of NAG-1 gene [13].

KLF4 is a zinc finger transcription factor, and its high expression level has been observed in postmitotic, differentiated epithelial cells of the skin and the gastrointestinal tract [14, 15]. Ectopic expression of KLF4 leads to cell-cycle arrest by the ability of KLF4 to express p21 [16], and KLF4 suppresses cyclin D1 at the transcriptional level [17], suggesting that KLF4 may serve as a tumor suppressor. Loss of expression of KLF4 has been observed in human tumor associated with a more aggressive phenotype [18], and conditional KLF4-knockout mouse model develop hyperplasia and polys in their stomachs [19], suggesting KLF4 can indeed function as a tumor suppressor gene. It has been reported that NAG-1 is up-regulated byKLF4 activation. KLF4 expression by a PPARγ ligand controls the NAG-1 promoter activity in human and mouse colorectal cancer [20]. In chapter 2, KLF4 as a trans-acting element for NAG-1 expression in pancreatic cancer cells will be discussed.

1.3 The controversial role of NAG-1 in cancer development

Even though NAG-1 expression is under control of tumor suppressor proteins such as p53, Egr-1 and KLF4, its implication in cancer development is still unclear. The anti-tumorigenic and pro-tumorigenic effects of NAG-1 seem to be context dependent. The high serum level of NAG1 in colorectal cancer patient has been reported, and NAG-1 serum level was proposed as a prognostic marker for disease progression [21]. NAG-1 shows a tumor suppressor effect in cell culture system [22]. The study with NAG-1 transgenic mice demonstrates NAG-1 has the anti-tumorigenic activity in chemical induced or genetic colorectal cancer models [23]. In prostate cancer, NAG-1 has been shown to induce growth arrest in DU145 human prostate carcinoma cells and implicated in apoptosis by caspase-3 activation [24]. Ectopic expression of NAG-1 in PC-3 cells inhibited proliferation and the growth of these cells in a xenograft tumor model [25]. However, significant data also have shown that NAG-1 induces prostate cancer cell migration and invasion [26]. NAG-1 also increases cell proliferation of LNCaP cells through ERK activation [27]. Plasma levels of NAG-1 was associated with prostate tumor progression and NAG-1 expression has been observed in human prostate cancers [28, 29], suggesting that NAG-1 might be a target for a diagnostic maker in prostate cancer. Elucidating biological regulation, downstream pathways and target genes of NAG-1 could decipher the dichotomy of NAG-1 in cancer progression.

1.4 The diverse subcellular localization of proteins and its implication in new biological function of NAG-1 in cancer context

The idea of one gene - one protein - one function has become too simple to explain the cellular complexity since 20,000 -25,000 human protein-coding genes are currently estimated. Although alternative splicing mechanism could partially explain this discrepancy, it still requires another way for our understanding of cellular complexity. A growing number of multifunctional proteins in which the two functions are found in a single polypeptide chain, are being identified and give us a new insight for deciphering a complex modern cell.

Emerging data on cellular localization of proteins unravels additional activities of proteins by changing their subcellular localization apart from the region where proteins are first destined. One single cellular compartment (cytoplasmic, nuclear, plasma membrane or extracellular region) in which each protein primarily resides and functions was considered to characterize a protein in the classical view [30]. However, unexpected subcellular localization of such proteins changes this classical view, and gives us one of mechanism for multifunctional protein which may represent a new mechanism through which cells overcome the limited amount of genomic information to fulfill a complex biological behavior.

Although such proteins were identified and categorized based on a single activity, each is now known to display multiple, independent functions beyond those from which they were identified originally, and these multifunctional proteins are also referred to as "Moonlighting proteins" [31]. Moonlighting refers to a single protein that

has multiple functions that are not result of gene fusions, families of homologous

proteins, splice variants, or promiscuous enzyme activities. It is speculated that

ancestral moonlighting proteins originally possessed a single function but through

evolution, acquired additional functions [32]. In addition to a change in cellular location,

moonlighting proteins can switch between functions due to a change in temperature, a

change in the redox state of the cell, a change in oligomeric state of the protein,

interactions with different polypeptide chains in different protein complexes, or changes

in the cellular concentration of a ligand, substrate, cofactor, or product [33, 34].

Although these switching conditions are all considered as mechanism(s) for

moonlighting, this review is to only catalog well known proteins in which a change of

subcellular localization contributes to additional function of proteins (Fig. 1.1).

1.4.1. Transcription factor

1.4.1.1. p53 tumor suppressor protein

p53, a well- known tumor-suppressor protein, accumulates in the nucleus in

response to DNA damage, oncogene activation or other cellular stresses, where it acts

as a nuclear transcription factor by binding to specific DNA sequence to regulate a

variety of genes [35, 36]. In addition to this nuclear activity, p53 has also been reported

to exhibit a different biological activity in the cytoplasmic region than that of a

transcription factor [37]. Wherein mutant p53 losing transcriptional activity still has the

ability to induce apoptosis [38].

In the extracellular region

- TG2
- Hsp90
- HMGB1
- MMP
- bFGF
- GAPDH
- CCN2

In the nucleus

- p53
- GAPDH
- TG2
- HMGB1
- bFGF
- MMP
- CCN2

In the cytoplasm

- p53
- GAPDH
- TG2
- Hsp90

◯ - multifunctional protein
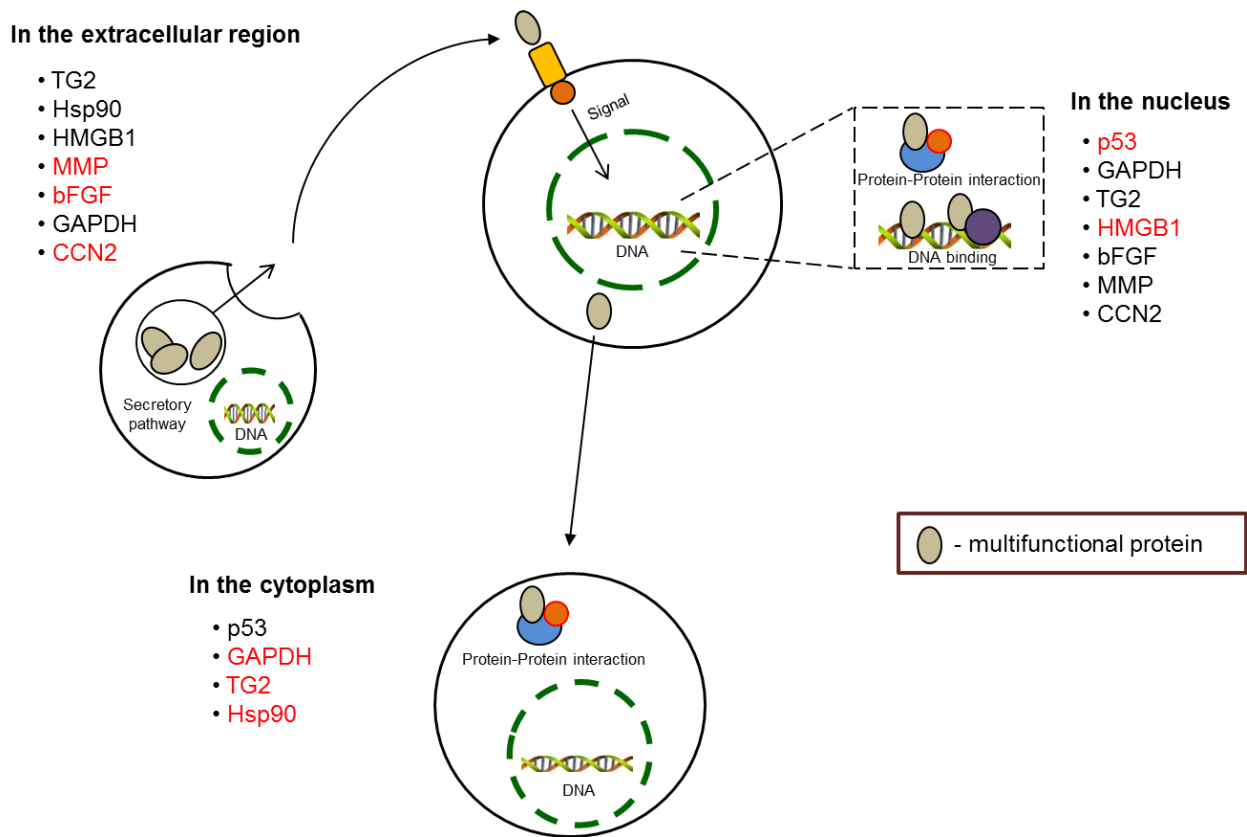
Figure 1.1 Multifunctional proteins

A protein can be localized in multiple subcellular regions. Altered subcellular localization results in a different function. Red colored proteins indicate that they originally reside in the subcellular region where they are categorized in. TG2, transglutaminase 2; Hsp90, heat shock protein 90; HMGB1, high-mobility group protein B1; MMP, matrix metalloproteinase; bFGF, basic fibroblast growth factor; GAPDH, glyceraldehyde 3-phosphate dehydrogenase; CCN2, connective tissue growth factor.

There are reports that p53 rapidly accumulates to the mitochondria under a variety of stress conditions [39]. The mitochondrial membrane is one of intracellular compartment where cytoplasmic p53 is located under a stress condition and induces mitochondrial outer membrane permeabilization by triggering the release of pro-apoptotic factors such as Bax and Bak, [40, 41]. This indicates that the pro-apototic effects of cytoplasmic p53 are independent of transcription. Post-translational modification of p53 and protein interactions can dictate destination of p53 [39, 42]. Together, it is likely that apoptosis induced by p53 arise from combined activities of the cytoplasmic and nuclear proteins.

1.4.1.2. Smads

Smad transcription factors are downstream mediator of TGFβ superfamily cytokines, and eight Smad proteins have been identified in human and mouse [43]. Smad1, Smad2, Smad3, Smad5 and Smad8 are substrates for TGFβ receptors, referred to as receptor-regulated Smads, or R-Smads. Smad4 interact with R-Smads as a common partner for all Rsmads, also referred to as Co-Smad. Smad6 and Smad7 are inhibitory Smads, also referred to as I-Smad that attenuates the interaction between Smad-receptor or Smad-Smad interaction [44]. R-Smads constantly shuttle between the cytoplasm and the nucleus in the basal state to monitor if TGFβ receptors are activated. Upon ligands binding, phosphorylated R-Smad by its receptor can be recognized by Co-Smad (Smad4). This this complex can then enter the nucleus more rapidly to regulate appropriate gene expression together with other DNA-binding cofactors based on specific cellular context [45, 46]. This is originally characterized by the role of R-Smads

12

and Smad4 in the nucleus as a transcription factor mediating TGFβ signaling. However, Smad proteins could also act as an adaptor protein in the cytoplasm to regulate other signal pathways. Notably, Dvl-1, Erbin, and Par-3 have been identified as Smad3 binding proteins using a yeast two-hybrid screen, suggesting that Smads can directly interact with these proteins, not as a transcription factor, but to regulate cell polarity [47]. Smad3 also binds to collagen types I, III, and V implying another aspect of smad proteins, not served as a transcriptional factor in the developing orofacial region [48]. Smad4 binds to Hoxa9 proteins in the cytoplasm to prevent nuclear translocation of Hoxa9, suggesting a protective role of Smad4 against nuclear activation by Hoxa9 and leukemia transformation [49]. This indicates that monitoring activation of TGFβ receptor is not the only task which Smad proteins perform for ultimately regulation of gene expression. Remarkably, Smad proteins interact with different components of other pathway in the cytoplasm [50], as an adaptor or an anchor protein for fine tuning and cross-talking of TGFβ signal with other signaling pathways.

1.4.2. Cytoplasmic proteins

1.4.2.1. Hsp90

Heat shock protein 90 (Hsp90) is a molecular chaperone of cytoplasmic proteins, mediating the ATP-dependent folding, stabilization, intracellular disposition and proteolytic turnover of proteins [51, 52]. However, Hsp90 is also a secreted and cell surface protein. The Hsp90 secreted form is considered a pro-tumorigenic protein as

blocking this form showed significant inhibition of tumor metastasis while serum level of

Hsp90 positively correlates with tumor malignancy in clinical cancer patients [53].

Extracellular Hsp90 interacts with and stabilize matrix metalloproteinase-2 (MMP-2) that

contributes to angiogenesis and cancer cell invasiveness [54, 55]. Secreted Hsp90 has

also been reported to regulate and alter E-cadherin function in prostate cancer, giving

rise to EMT [56], indicating it can be a diagnostic marker for tumor malignancy. In

addition to this unexpected role of Hsp90 in the extracellular region, while Hsp90 has

also been found in the nucleus [57] and could regulate several nuclear events [58].

1.4.2.2. Transglutaminase 2

Transglutaminase 2 (TG2), a ubiquitous member of the mammalian

transglutaminase family, can catalyzes protein cross-linking via transamidation of

glutamine residues to lysine residues in a Ca^{2+}-dependent manner [59]. Besides its

classical protein crosslinking activity, TG2 possesses several other functions in a

different cellular compartment including G protein, cell adhesion, kinase activities. TG2

is predominantly a cytoplasmic protein, but increasing evidences indicate that TG2

dynamically translocate depending on cellular context [60], even though molecular

mechanism(s) underlying dynamic translocation of TG2 to various subcellular

compartments remains elusive. In addition to transglutaminase (TGase) activity,

cytosolic TG2 has been shown to be involved in signal transduction. TG2 activates NF-

κB pathway to elicit anti-apoptotic effects in ovarian cancer cells [61]. TG2 can function

as a G protein (G_h) on the plasma membrane which has a unique GTP binding pocket

and GTP hydrolysis activity, suggesting TG2 may be implicated in receptor signaling [62]. Membrane TG2 was also shown to have a kinase activity. TG2 isolated from membrane fractions was found to phosphorylate insulin-like growth factor-binding protein-3 (IGFBP-3) [63]. Translocation of TG2 from the cytoplasm to the nucleus has been reported in various cell types [64-66] which shows how a versatile protein TG2 is. Although elevation of intracellular calcium levels promoted TG2 translocation to the nuclear compartment [66], biological function of nuclear TG2 is still unclear. Emerging evidence indicates the importance of nuclear TG2 in regulating gene expression via post-translational modification of transcriptional factors (via crosslinking and phosphorylation) and histone proteins. These include E2F1 [67], hypoxia inducible factor 1[68], Sp1[69] and all four mammalian core histones (H2A, H2B, H3 and H4) [70]. Although TG2 has been originally identified as an intracellular enzyme, TG2 even was found in extracellular space. Extracellular TG2 acts as a matrix stabilizer through its protein cross-linking and as an important cell adhesion protein involved in cell survival [71]. Extracellular TG2 has been reported to associated with multiple integrins of the β_1 and β_3 subfamilies implicated in cell adhesion and spreading [72]. TG2 also interacts with extracellular matrix-associated fibronectin (FN). FN-bound TG2 with increased resilience to MMP degradation maintains cell adhesion by interacting with cell surface heparin sulfate chains of syndecan-4 [73]. These substantial observations indicate that various activities of TG2 are differentially regulated depending on its subcellular localization.

1.4.2.3. GAPDH

Glyceraldehyde-3-phosphate dehydrogenase (GAPDH) catalyzes an important energy-yielding step in glycolysis in which GAPDH coverts glyceraldehyde-3-phosphate to D-glycerate 1,3-bisphospate in the presence of inorganic phosphate and nicotinamide adenine dinucleotide (NAD), mediating formation of NADH and adenosine triphosphate (ATP). In addition to this originally identified function as a "housekeeping" protein in the cytoplasm, emerging data exhibits numerous activities apart from energy production [74, 75]. GAPDH is translocated to the nucleus upon exposure to a stressor such as oxidative stress leading to cell death/dysfunction [76]. This nuclear translocation is mediated by S-nitrosylation at Cys-150, allowing GAPDH to bind to Shia spanning nuclear localization signal, resulting in nuclear translocation of this GAPDH-Siah complex. Nuclear GAPDH is further acetylated at Lys 160 by the acetyltransferase p300/CREB binding protein (CBP) through direct protein interaction, which in turn stimulates the acetylation and catalytic activity of p300/CBP, leading to induce its target genes including the tumor suppressor p53 [77]. Various functions of GAPDH in the nucleus that deviate from cell death have also been reported. GAPDH directly interacts with APE1 involved in the base excision DNA repair pathway. GAPDH reactivate endonuclease activity of APE1 to cleave a basic site and to regulate the redox state of a number of transcriptional factors such as p53, AP-1, c-Jun, cFos and NF-κB [78]. GAPDH binds to and makes complex with Oct-1-p38/GAPDH to regulate transcription required for S-phase progression in cell cycle [79]. Nuclear GAPDH also plays a role in maintaining and protecting telomeric DNA from chemotherapy-induced rapid

degradation [80]. Through these finding, GAPDH is not only believed to be involved in glycolysis as a cytoplasmic protein, but also participated in gene regulation as a nuclear factor.

1.4.3. Nuclear protein

1.4.3.1. *HMGB1*

High mobility group box-1 (HMGB1) belongs to three families (HMGA, HMGB and HMGN), and members of each family have been identified as the second most abundant chromatin proteins, participating in gene regulation and cellular differentiation [81]. Moreover, they contribute to the fine tuning of transcription in response to rapid environmental changes by interacting with nucleosomes, transcription factors, nucleosome-remodeling machines, and with histone H1 [82]. HMGB1 regulates transcription by binding with nucleosomes to loose packed DNA and remodel the chromatin, which facilitates the binding of other proteins to DNA. HMGB1 was previously thought to function only as a nuclear factor. However, this protein was recently discovered to be a crucial cytokine that mediates the response to infection, injury and inflammation [83]. HMGB1 was found to be released by cultured macrophages more than 8 hours after stimulation with endotoxin, TNF, or IL-1. Releasing HMGB1 was considered as a cytokine involved as a late-acting mediator for lethal shock (endotoxemia) because HMGB1 release occurs considerably later than secretion of the classical early pro-inflammatory mediator TNF and IL-1 [84]. HMGB1 bind to the receptor for advanced glycation end-products (RAGE) and to the Toll-like

receptors (TLRs) for activating the inflammatory process in immune and endothelial cells [85, 86], and has been intensively reviewed. Secretion of HMGB1 seems not to be restricted to immune cells since epithelial gastric and colon cancer cell lines also release HMGB1 [87].

1.4.4. Plasma membrane proteins

1.4.4.1. E-Cadherin

E-cadherin is a class I transmembrane glycoprotein which plays an important roles in cell adhesion, forming adherens junctions and facilitating the formation of the entire epithelial junctional complex. This identifies function of this protein as a cell membrane protein [88, 89]. E-cadherin contain 5 cadherin repeats (EC1 ~ EC5) within the extracellular domain that bind calcium ions to form a stiffened linear molecule, one transmembrane domain, and an intracellular domain that interacts with the catenins and a variety of actin-binding proteins to anchor the cadherin–catenin complex to the actin cytoskeleton [88]. β-catenin is a protein that binds to intracellular domain of E-cadherin and intense studies have shown that β-catenin can localize in the nucleus and play a key role in signal transduction in the canonical Wnt signaling pathway [90]. E-cadherin can also block growth factor–mediated proliferation signaling (contact inhibition of growth), thereby maintaining tissue integrity and preserving tissue function [91]. Decrease in E-cadherin attenuates strong cell-cell interactions supporting cancer progression and metastasis [92]. Since lowering the strength of cellular adhesion within a tissue gives rise to cancer cell motility, enabling cancer cells to cross the basement

membrane and invade surrounding tissues. Reduced expression of E-cadherin is indicative of unfavorable clinical outcome in several malignant diseases [93]. These findings support the notion that E-cadherin may be a tumor-suppressor protein. However, emerging roles of nuclear E-cadherin as a modulator of tumor growth survival, and motility, triggering cancer progression, have been reported as E-cadherin may also possess oncogenic functions. E-cadherin has been shown to be cleaved by γ-secretase wherein the E-cadherin cytoplasmic fragment translocates to the nucleus and regulate gene expression [94]. This implies that oncogenic functions of E-cadherin may arise from cleaved translocated form in the nucleus. Nuclear E-cadherin fragment interacts with CTF2 to suppress the induction of apoptosis [94]. *In vivo* studies have shown that detection of aberrant nuclear E-cadherin correlates with lymph node spread and liver metastases in pancreatic endocrine tumors [95]. In addition to γ-secretase, several proteases, matrix metalloproteinases (MMP-3, MMP-7, MMP-9, and MT1-MMP) have also been reported to converts the mature 120 kDa E-cadherin into an extracellular N-terminal 80-kDa fragment and an intracellular C-terminal 38-kDa fragment [96]. Interestingly, the extracellular fragment is released from the plasma membrane and diffuses into the extracellular environment and even the bloodstream to serve as a paracrine/autocrine signaling molecule [97].

1.4.4.2. TGF-β receptor I

TGFβ receptors are type I transmembrane proteins which possess serine/threonine kinase activity. In the canonical pathway, active TGF-β1 binds to cell

surface receptor kinases TGF-β type I (TβRI) and type II receptors (TβRII). Upon ligand binding to TβRII, TβRII further phosphorylates and activates TβRI, which in turn propagates the signals by phosphorylating Smad proteins [98], which are aforementioned, to regulate cell differentiation, morphogenesis, tissue homeostasis and regeneration. This function as a cell membrane receptor for sensing and propagate signal is originally identified the role of TGFβ receptors. Since TNF-alpha converting enzyme (TACE) has recently been shown to cleave TβRI and releases ectodomains, which was demonstrated to cause a decrease in TGFβ signaling [99], *Yabing Mu's* group has further investigated and have shown that TGFβ induces Lys63-linked polyubiquitination of TβRI via TRAF6 to promote cleavage of TβRI by metalloprotease TNF-alpha converting enzyme (TACE), resulting in translocation of the intracellular domain of TβRI to the nucleus [100]. After the liberated intracellular domain (ICD) of TβRI is translocated to the nucleus, it associates with the transcriptional regulator p300 to activate genes involved in tumor invasion, such as Snail and MMP2, suggesting how TGFβ promotes tumor progression. n. Another recent report has shown that ligand-stimulated TβRI is translocated to the nucleus in association with importin β1, nucleolin, and Smad2/3 inHER2-transformed cells. In the nucleus, TβRI specifically recognizes RNA targets and regulates RNA processing in the nucleus [101].

1.4.4.3. EGFR

The epidermal growth factor receptor (EGFR) is a member of the EGFR tyrosine kinase family, which consists of EGFR (ErbB1/HER1), HER2/neu (ErbB2), HER3

(ErbB3) and HER4 (ErbB4) triggering intracellular signaling pathway by phosphorylating downstream signal molecules such as the RAS/MAPK, PI(3)K/Akt, PLCγ/PKC, and Jak/STAT. EGFR stimulates downstream cell signaling cascades that influence cell proliferation, apoptosis, migration, survival and complex biological processes. There are many reports that EGFR has been consistently detected in the nuclei of cancer cells from primary tumor specimens and highly proliferative tissues [102, 103], suggesting a second function of EGFR as a nuclear factor in addition to traditional cytoplasmic signaling. Research over the last decade has demonstrated the mechanism(s) of transport of EGFR to the nucleus. The EGFR family members (EGFR, ErbB2, ErbB3, and ErbB4) have conserved tripartite nuclear localization signal (NLS) which can be recognized by importin β1 for shuttling EGFR to the nucleus [104]. EGFR is described to undergo COPI-mediated retrograde trafficking from the Golgi to the ER [105] then EGFR is translocated to the inner nuclear membrane (INM). Molecular mediators for nuclear translocation of EGFR include dynamin, importins and Sec61 [106], and CRM1 exportin may be involved in the nuclear export of EGFR [107]. Upon entry into the nucleus, the EGFR can function in ways distinct from the receptor tyrosine kinase on plasma membrane. Many reports have indicated a role of nuclear EGFR, which act as a co-transcription factor by interacting with transcription factors including E2F1 and STAT3 [108-110]. These findings suggest that the subcellular distribution of EGFR contribute to elicit different biological outcomes and need to be taken into consideration in the field of EGFR studying.

1.4.5. Secreted proteins

1.4.5.1. MMPs

Matrix metalloproteinases (MMPs) were originally identified as zinc-dependent endopeptidases that act in the extracellular matrix. Most studies on the MMPs have been traditionally associated with the degradation and turnover of most of the extracellular matrix (ECM) components, contributing to tissue destruction, remodeling and pathological process such as tumor cell invasion [111, 112]. Emerging data have uncovered nontraditional roles for MMPs in the extracellular space as well as in the nucleus [113]. The biological role of intracellular located MMPs and mechanism(s) for protein trafficking are still unclear, although recent studies have demonstrated some of their functions in intracellular regions and mechanism(s) for protein trafficking. The presence of MMP-2 in the nucleus of cardiac myocytes has been reported. Poly (ADP-ribose) polymerase (PARP) may be a nuclear substrate of MMP-2 suggesting a possible role of nuclear MMP-2 in PARP degradation [114]. MMP-3 is also found in the nucleus of several cultured cell types and in human liver tissue sections. MMP-3 may have the putative NLS at position 107 to 113 in amino acid sequence which is responsible for nucleus entry. Nuclear expression of MMP-3 is associated with an increased rate of apoptosis although the mechanism is unclear and may serve as an anti-tumorigenic protein [115]. Additional putative NLS in MMP-3 have been found and show another role in the nucleus as a transcriptional factor. MMP-3 binds to a transcription enhancer in the connective tissue growth factor (CCN2/CTGF) promoter and activates transcription of CCN2/CTGF [116] which promotes physiological

chondrocytic proliferation and ECM formation, suggesting a novel role of MMP3 in the development, tissue remodeling, and pathology of arthritic diseases through CCN2/CTGF modulation. MMP-12 is known as macrophage metalloelastase which contributes to degradation of extracellular matrix during inflammatory tissue destruction. However MMP-12 can be translocated into the nucleus where it binds to the NFKBIA promoter, driving transcription [117]. Intracellular MMP-12 mediates NFKBIA transcription, leading to IFN-α secretion and host protection from virus-infection. The recent findings of nuclear localization of MMPs open new avenue in which MMPs cleave and activate intracellular peptides as well as induce specific gene expression.

1.4.5.2. NAG-1
This will be discussed in Chapter III.

1.5. Summary Conclusion

The list of multifunctional proteins and their new biological role are continuing to grow. Changing subcellular localization contributes to giving proteins additional functions that are seen in the proteins described above (Tab. 1.1). Remarkably, disease progression may not only arise from gene mutation and expression of splice variants, but also through dysregulation of protein sorting system which controls protein localization in the cell.

Table 1.1 Examples of multifunctional proteins shown in this review.

Name	Primary subcellular localization and function	Additional subcellular localization and function
p53	• Nucleus; Transcription factor	• Mitochondria; Promoting mitochondrial membrane permeabilization
Smads	• Nucleus; Transcription factor	• Cytoplasm; Adaptor protein
Hsp90	• Cytoplasm; Molecular chaperone	• Extracellular region; Regulator for angiogenesis and cell invasiveness
TG2	• Cytoplasm; Catalyzes protein cross-linking	• Nucleus; Regulates gene expression Extracellular region; • Implicates in cell adhesion and spreading
GAPDH	• Cytoplasm; Glycolytic enzyme	• Nucleus; Participates in gene regulation
HMGB1	• Nucleus; Binds to nucleosomes	• Extracellular region; Inflammatory cytokine
E-cadherin	• Cell surface; Plays a role in cell adhesion	• Nucleus; Implicates in gene regulation
TβRI	• Cell surface; Type I transmembrane protein	• Nucleus; Participates in gene regulation
EGFR	• Cell surface; Membrane receptor tyrosine kinase for EGF	• Nucleus; Co-transcription factor
MMPs	• Extracellular region; Secretion protein involved in proteolysis	• Nucleus; Regulates gene expression
NAG-1	• Extracellular region; Secretion protein involved in apoptosis	• Nucleus; Implicates in gene regulation

CHAPTER 2

A peroxisome proliferator-activated receptor ligand MCC-555 imparts anti-proliferative response in pancreatic cancer cells by PPAR gamma-independent up-regulation of KLF4

The results discussed in this chapter have been published in *Toxicology and Applied Phamacology*, Volume 263, Issue 2, 1 September 2012, Pages 225–232

2.1 Abstract

MCC-555 is a novel PPARα/γ dual ligand of the thiazolidinedione class and was recently developed as an anti-diabetic drug with unique properties. MCC-555 also has anti-proliferative activity through growth inhibition and apoptosis induction in several cancer cell types. Our group has shown that MCC-555 targets several proteins in colorectal tumorigenesis including nonsteroidal anti-inflammatory drug (NSAID)-activated gene (NAG-1) which plays an important role in chemoprevention responsible for chemopreventive compounds.

NAG-1 is a member of the TGF-β superfamily and is involved in tumor progression and development; however, NAG-1's roles in pancreatic cancer have not been studied. In this report, we found that MCC-555 alters not only NAG-1 expression, but also p21 and cyclin D1 expression. NAG-1 and p21 expression was not blocked by PPARγ-specific antagonist GW9662, suggesting that MCC-555-induced NAG-1 and p21 expression is independent of PPARγ activation. However, decreasing cyclin D1 by MCC-555 seems to be affected by PPARγ activation. Further, we found that the GC box located in the NAG-1 promoter play an important role in NAG-1 transactivation by MCC-555. Subsequently, we screened several transcription factors that may bind to the GC box region in the NAG-1 promoter and found that KLF4 potentially binds to this region.

Expression of KLF4 precedes NAG-1 and p21 expression in the presence of MCC-555, whereas blocking KLF4 expression using specific KLF4 siRNA showed that both NAG-1 and p21 expression by MCC-555 was blocked.

In conclusion, MCC-555's actions on anti-proliferation involve both PPARγ-dependent and -independent pathways, thereby enhancing anti-tumorigenesis in pancreatic cancer cells.

2.2 Introduction

Pancreatic cancer is a major cause of cancer-related deaths in developed countries and has the highest mortality rate among major cancers. Pancreatic cancers may cause only vague symptoms before being detected, and chemotherapeutic regimens for this disease have provided very limited improvements in tumor regression and overall survival rates after diagnosis [118]. Although the precise pathogenesis of pancreatic cancer remains unclear, common mutations in several cell proliferation-related genes have been described: mutation of K-ras, p16, p53, and Smad4 genes has been identified in sporadic pancreatic tumors [119].

The peroxisome proliferator-activated receptors (PPARs) are members of the nuclear receptor superfamily and function as ligand-activated transcription factors. PPARs function in a variety of roles including cell differentiation, metabolism, immune function and cell growth. Thiazolidinediones, synthetic PPARγ ligands, are used to treat patients with type 2 diabetes, and current studies have shown that thiazolidinediones also have anti-tumorigenic activity in a wide variety of cancer cells [120-123]. Intense

studies on the role of PPARγ ligands in colorectal cancer cells have showed that PPARγ activation may be implicated in the inhibition of cell proliferation genes and induction of apoptosis in colorectal cancer cells [122, 124, 125]; however, effects and molecular targets of PPARγ ligands in pancreatic cancer cells have not been studied in detail.

MCC-555 (RWJ-241947) is a novel class of thiazolidinediones and was recently established as an anti-diabetic drug in animal models of Type 2 diabetes, and is more effective in the anti-diabetic potency compared to other PPARγ ligands. Like other thiazolidinediones, MCC-555 binds to PPARγ and increases transcriptional activities, but its binding affinity for PPARγ is relatively weak compared to other PPARγ-specific agonists [126]. MCC-555 effects not only PPARγ as effective anti-diabetic agents but also PPARα as anti-hyperlipidemic agents [127]. MCC-555 has been reported to be over 50-fold more potent than rosiglitazone in decreasing blood glucose levels in rodent models of type 2 diabetes and 5- to 10-fold less effective than rosiglitazone in inducing adipogenesis in mouse preadipocytes [128, 129]. These effects may be explained by the ability of MCC-555 to act as a PPARγ agonist, partial agonist, or antagonist, depending on cell context [130]. The same scenario may apply to the effect of MCC-555 on anti-proliferative activity. MCC-555 has an anti-tumorigenic activity against prostate cancer [131] and colorectal cancer [126] in both PPARγ-dependent and -independent manners. It has been shown that dual ligands exhibit better activity with respect to cell growth inhibition, compared to the PPARγ specific agonists [132], Thus, it is expected that dual ligands for PPAR may provide a better outcome to prevent cancer. Since the anti-proliferative potency of MCC-555 has not been examined in pancreatic cancer

cells, we extended our knowledge to pancreatic cancer to investigate whether MCC-555 affects anti- cancer activity along with several molecular targets affected in tumorigenesis.

MCC-555 and other PPARγ ligands modulate the expression of various genes such as NAG-1, p21, cyclin D1, and KLF4 through a PPARγ-dependent or -independent pathway [125, 133, 134]. We have reported that KLF4 is the key regulator that induces NAG-1 by MCC-555 in colorectal cancer cells [135]; however, in this study, we found a novel *cis*-acting element where KLF4 binds to the NAG-1 promoter in pancreatic cancer cells. KLF4 is a well-known transcription factor that induces p21 and suppresses cyclin D1 [136, 137]; however, KLF4 seems to not be involved in cyclin D1 down-regulation in the presence of MCC-555. Therefore, the mechanisms by which MCC-555 induces cell growth inhibition may be associated with both PPARγ dependence and independence and affects multiple targets in pancreatic cancer cells.

2.3 Materials and Methods

2.3.1 Cell lines, reagents, antibodies, and DNA constructs

Human pancreatic cancer cell lines BxPC3 and AsPC-1 were purchased from American Type Culture Collection (Manassas, VA). Both cell types were maintained in RPMI1640 medium. The culture media contained 10% fetal bovine serum (Hyclone), 50 U/ml penicillin and 50 μg/ml streptomycin. MCC-555, ciglitazone, rosiglitazone, troglitazone, 15-deoxy-$\Delta^{12,14}$-prostaglandin J$_2$, and GW9662 were purchased from

Cayman Chemical Co. (Ann Arbor, MI), and all chemicals were dissolved in dimethylsulfoxide (DMSO). Anti-human NAG-1 antibody was previously described [138]. Antibodies against KLF4, Sp1, Sp3, ZF9, BTEB1, MAZ, cyclin D1 and actin were purchased from Santa Cruz Biotechnology (Santa Cruz, CA), whereas p21 antibody was purchased from Cell Signaling Technology (Beverly, MA). The NAG-1 promoter constructs pNAG-1-3500/+41, pNAG-1-1086/+41, pNAG-1-474/+41, pNAG-1-133/+41 and the internal deletion mutant clones derived from pNAG-1-133/+41 were described previously [139-141].

2.3.2 Cell proliferation analysis

Cell proliferation was investigated using the CellTiter 96 Aqueous One Solution Cell Proliferation Assay (Promega, WI). Cells were plated in a 96-well plate at 1,000 cells/well in four replicates. Cells were then stimulated with different doses of MCC-555 in the presence of 1% serum. After two days treatment, 20 μl of CellTiter 96 Aqueous One Solution was added to each well, and the plate was incubated for 1 h at 37ºC. Absorbance at 490 nm was recorded in an enzyme-linked immunosorbent assay plate reader (Bio-Tek Instruments, Winooski, VT).

2.3.3 Caspase 3/7 enzyme activity

Enzyme activity of caspase 3/7 was analyzed using the Caspase-Glo 3/7 Assay kit (Promega) according to the manufacturer's protocol. Briefly, cells were seeded onto a 96-well plate at 5,000 cells/well in four replicates. The cells were then treated with 10

µM MCC-555 in the absence of serum. After 24 hours, 100 µl of caspase-Glo 3/7 Reagent was added into each well, and the plate was incubated for 1 hour at room temperature. Luminescence was measured using an FLX800 microplate reader (Bio-Tek).

2.3.4 Cell cycle analysis

Cells were plated at $4x10^5$ cells/well in 6-well plates, and then treated with MCC-555 (10 µM) for 24 hours. The cells (attached and floating cells) were then harvested, washed with phosphate-buffered saline (PBS), fixed by slow addition of 1 ml cold 70% ethanol and stored at -80ºC. The fixed cells were pelleted, washed with 50% and 30% ethanol in PBS, and stained with 0.5 ml of 70 µM propidium iodide containing 1 mg/ml RNase for 15 min at room temperature. Ten-thousand cells were examined by flow cytometry using a Becton Dickinson fluorescence-activated cell sorter equipped with CellQuest software, by gating on an area vs. width dot plot to exclude cell debris and cell aggregates.

2.3.5 TUNEL assay

Apoptosis in the BxPC-3 cells was determined by the terminal deoxynucleotidyl transferase (TdT)-mediated dUTP–biotin nick end labeling (TUNEL) staining method using an in situ cell detection kit (TACS 2 TdT Blue kit, Trevigen, Gaithersburg, MD) according to the manufacturer's instructions. Briefly, the cells on coverslips were fixed with 3.7% formaldehyde and permeabilized with proteinase K solution. The slides were

then immersed in quenching solution and 1 X terminal deoxynucleotidyl transferase (TdT) labeling buffer and incubated in labeling reaction mix containing TdT dNTP mix and TdT enzyme. After 1 hour, the cells were immersed in strep-HRP solution for 10 min and then were incubated in TACS-blue label solution. The slides were counterstained with Nuclear Fast Red solution, and the stained slides were observed and photographed using light microscopy.

2.3.6 Western blot analysis

Western blot analysis was performed as described previously [135]. Briefly, cells were starved overnight, and treated with MCC-555 at the indicated time and dose in serum-free media. Cell lysates were obtained using RIPA buffer containing protease inhibitor cocktail (Calbiochem, San Diego, CA). Protein concentration was determined by bicinchoninic acid protein assay (Pierce, Rockford, IL). Proteins were separated on SDS/polyacrylamide gel electrophoresis and transferred to nitrocellulose membranes (Osmonics, Minnetonka, MN). The membranes were incubated with a specific primary anti-serum in tris-buffered saline containing 0.05% Tween 20 (TBS-T) and 5% non-fat dry milk at 4°C overnight. After three washes with TBS-T, the blots were incubated with peroxidase conjugated immunoglobulin G for 1 hour at room temperature, visualized using ECL (Amersham Biosciences, Piscataway, NJ) and quantified by Scion Image Software (Scion Corp., Frederick, MD).

2.3.7 Real-Time RT-PCR Analysis

Total RNA was isolated from BxPC3 and AsPC-1 cells using RNA isolation kit (OMEGA Bio-Tek, Norcross, GA), and 1 µg of RNA was reverse-transcribed with an iScript cDNA kit (BioRad, Hercules, CA) according to the manufacturer's instruction. PCR was carried out using Absolute qPCR SYBR Green Mix (Thermo Scientific, UK) with primers for human *NAG-1, p21, cyclinD1* and *GAPDH* as follows: NAG-1, forward 5'-ATGCCCGGGCAAGAACTC-3' and reverse 5'-CATATGCAGTGGCAGTC-3'; p21, forward 5'-GCGACTGTGATGCGCTAAT-3' and reverse 5'-TAGGGCTTCCTCTTGGAGAA-3'; cyclin D1, forward 5'-ATGGAACACCAGCTCCTGTGCTGC-3' and reverse 5'-TCAGATGTCCACGTCCCGCACGT-3'; GAPDH, forward 5'-GGGCTGCTTTTA ACT CTGGT-3' and reverse 5'-TGGCAGGTTTTTCTAGACGG-3'.

Gene expression levels were calculated and GAPDH was used as a control gene, using MyiQ thermal cycler (Bio-RAD). Vehicle-treated samples were set to 1 and fold change are represented as mean ± S.D.

2.3.8 Transient transfection and luciferase reporter assays

BxPC3 cells were plated in 12-well plates at 2×10^5 cells/well. The next day, plasmid mixtures containing 0.5 µg of *NAG-1* promoter linked to luciferase and 0.05 µg of *pRL-null* vector were transfected by PolyJet transfection reagent (Signagen, Rockville, MD) according to the manufacturer's protocol. After transfection, cells were treated with DMSO or MCC-555 (10 µM) in serum-free media for 24 hours. Cells were

harvested in 1 x passive lysis buffer (Promega), and luciferase activity was measured using DualGlo Luciferase Assay Kit (Promega). The results were normalized to *pRL-null* luciferase activity.

2.3.9 RNA interference

Klf4 siRNA was purchased from Santa Cruz Biotechology and control siRNA was purchased from Ambion. BxPC-3 cells were transfected with 10 µM of *KLF4* or control siRNA using PepMute siRNA Transfection reagent (Signagen), according to the manufacturer's protocol. After transfection for 24 hours, cells were serum starved overnight and treated as indicated. Total protein was subjected to Western blot analysis as described.

2.3.10 Chromatin immunoprecipitation

Cells were fixed with 1% formaldehyde for 10 minutes at 37ºC and sonicated four times for 10 seconds. Cell lysates (0.2 ml) were diluted with 0.8 ml of immunoprecipitation buffer (0.1 % SDS, 1 % Triton X-100, 0.1 % Na-deoxycholate and 140 mM NaCl) and immunoprecipitated with 10 µg specific antibodies for normal IgG or KLF4 at 4ºC overnight. The chromatin-associated DNA was eluted, reverse cross-linked by heating at 65ºC for 4 hours and treated with proteinase K at 45ºC for 2 hours. DNA was purified by phenol/choloroform extraction, and precipitated DNA was amplified using the following primer pairs: forward 5'- CCAGAAATGTGCCCTAGCTT-3' and reverse 5'-GAGCTGGGACTGACCAGATG-3'. PCR products (202 bp) were resolved on

2% agarose gel and visualized under UV light.

2.3.11 Statistical analysis

SAS for windows (v9.2; SAS institute, Inc.) statistical analysis software was used. For multiple group comparisons, analysis of variance with Tukey's multiple comparison test was used to compare mean values. The Student t test was used to analyze differences between samples. Results were considered statistically significant at * $P <$ 0.05, ** $P < 0.01$, and *** $P < 0.001$.

2.4 Results

2.4.1 MCC-555 induces cell growth arrest and apoptosis in pancreatic cancer cells

The effects of PPARγ agonists on cancer are mediated in PPARγ-dependent and/or -independent manners, depending on cell types or ligand structures [142]. In this study, we have investigated the therapeutic properties of MCC-555 in human pancreatic adenocarcinoma cells. BxPC-3 cells were treated with MCC-555 for 2 days, and we observed the reduction of cell proliferation in MCC-555 treated cells in a dose dependent manner, compared to DMSO-treated cells (Fig. 2.1A). To investigate whether MCC-555 arrests cell cycle, we stained cells with propidium iodide and examined cell cycle status. Treatment with MCC-555 resulted in a significant increase in cells arrested at the G1 phase (Fig. 2.1B), consistent with previous reports that PPARγ ligands arrest
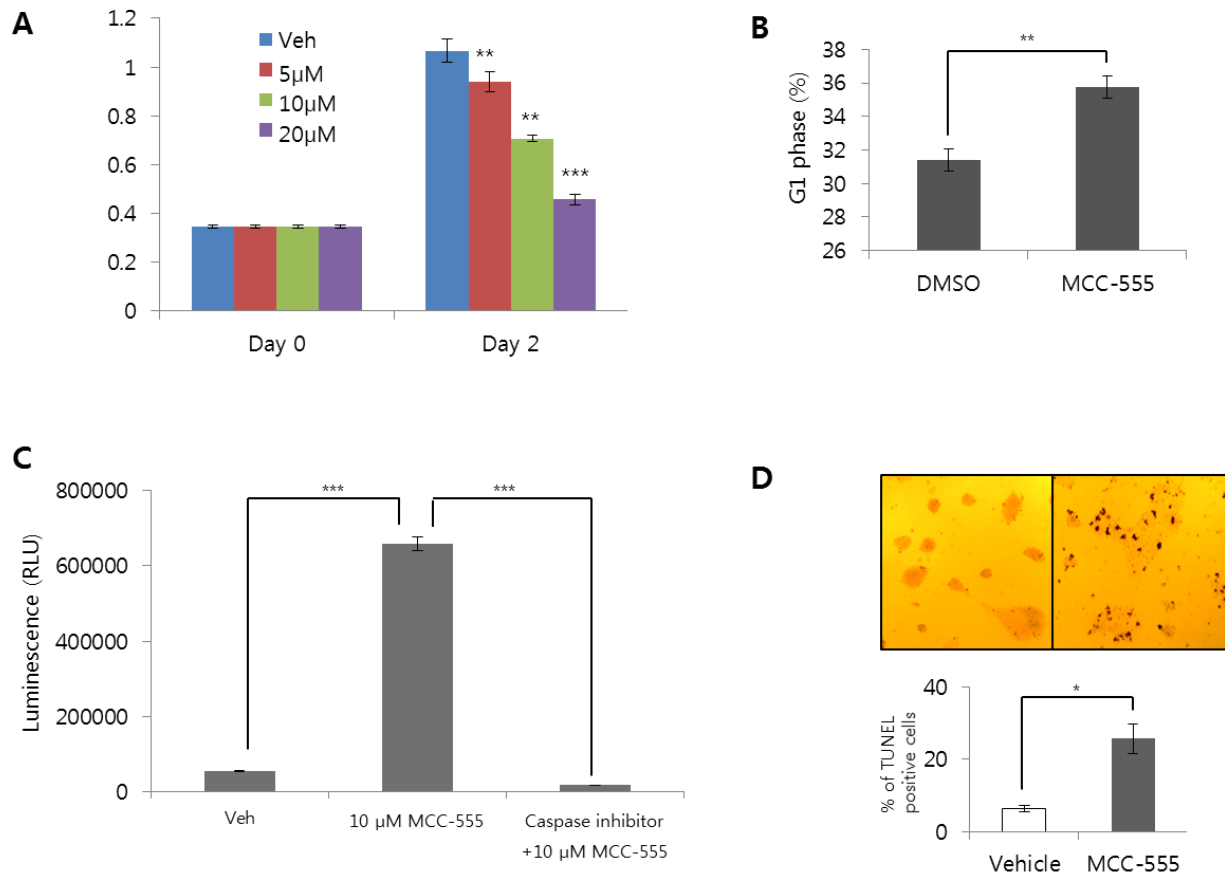
Figure 2.1 MCC-555 inhibits cell proliferation and induces apoptosis in human pancreatic cancer cells.

A, BxPC-3 cells were treated with vehicle or MCC-555 in a dose depedent manner. Cell growth was measured using the CellTiter 96 Aqueous One Solution Cell Proliferation Assay. Values are expressed as mean ± S.D. of four replicates. *P* < 0.01** *and P* < 0.001***, compared to vehicle-treated cells. **B**, Flow cytometric analysis of vehicle- or MCC-555-treated BxPC-3 cells. Cell were treated with vehicle or MCC-555 for 24 h and stained with propidium iodide as decribed in Materials and Methods. Percentage of G1 is expressed as mean ± S.D of three replicates. *P* < 0.01**. **C**, Caspase 3/7 enzymatic activity was measured as described in Materials and Methods. BxPC-3 cells were pretreated with either vehicle or caspase inhibitor (10 μM, Z-VAD-FMK) for 30 min, and then were stimulated with MCC-555. Values are expressed as mean ± S.D of three replicates. *P* < 0.001***. **D**, Apoptosis was analyzed by TUNEL assay using BxPC-3 cells treated with 10 μM MCC-555 for 24 h (40X). The graph indicates the percentage of MCC-555-treated cells versus the vehicle-treated cells from the reading of three randomly defined areas. *P* < 0.05*.

cell cycle at the G1 phase in other cells [143, 144]. To examine whether MCC-555 affects apoptosis of human pancreatic cancer cells, we performed caspase 3/7 activity and TUNEL assay using BxPC-3 cells treated with either DMSO or MCC-555 (10 µM). As shown in Fig. 2.1C, MCC-555 treatment significantly increased caspase 3/7 activity, and addition of caspase inhibitor with MCC-555 resulted in decreasing caspase 3/7 activity, indicating that MCC-555-induced apoptosis is mediated by caspase 3/7 activity. We also performed TUNEL assay to detect apoptotic cells in the presence of MCC-555. As shown in Fig. 2.1D, MCC-555 enhanced TUNEL positive cells in MCC-555-treated cells, compared to vehicle-treated cells. Taken together, MCC-555 seems to increase cell cycle arrest and apoptosis in pancreatic cancer cells; these results appear to account for the cell growth arrest as seen in Fig. 2.1A.

2.4.2 MCC-555 induces NAG-1 and p21, and suppresses cyclin D1 expression

To elucidate the molecular mechanism(s) by which MCC-555 induces cell cycle arrest and apoptosis in human pancreatic cancer cells, we analyzed the expression of pro-apoptotic gene NAG-1, and cell cycle regulators p21 and cyclin D1. It has been reported that several PPARγ agonists induce NAG-1 expression, which exerts anti-cancer activity in colorectal cancer cells [124, 145]. Likewise, expression of cyclin D1, and p21 are altered in the presence of PPARγ ligands [146, 147]. BxPC-3 cells were treated with several PPARγ agonists, including MCC-555, rosiglitazone (RGZ), 15-deoxy-$\Delta^{12,14}$-prostaglandin J$_2$ (PGJ$_2$), and troglitazone (TGZ). MCC-555 and TGZ
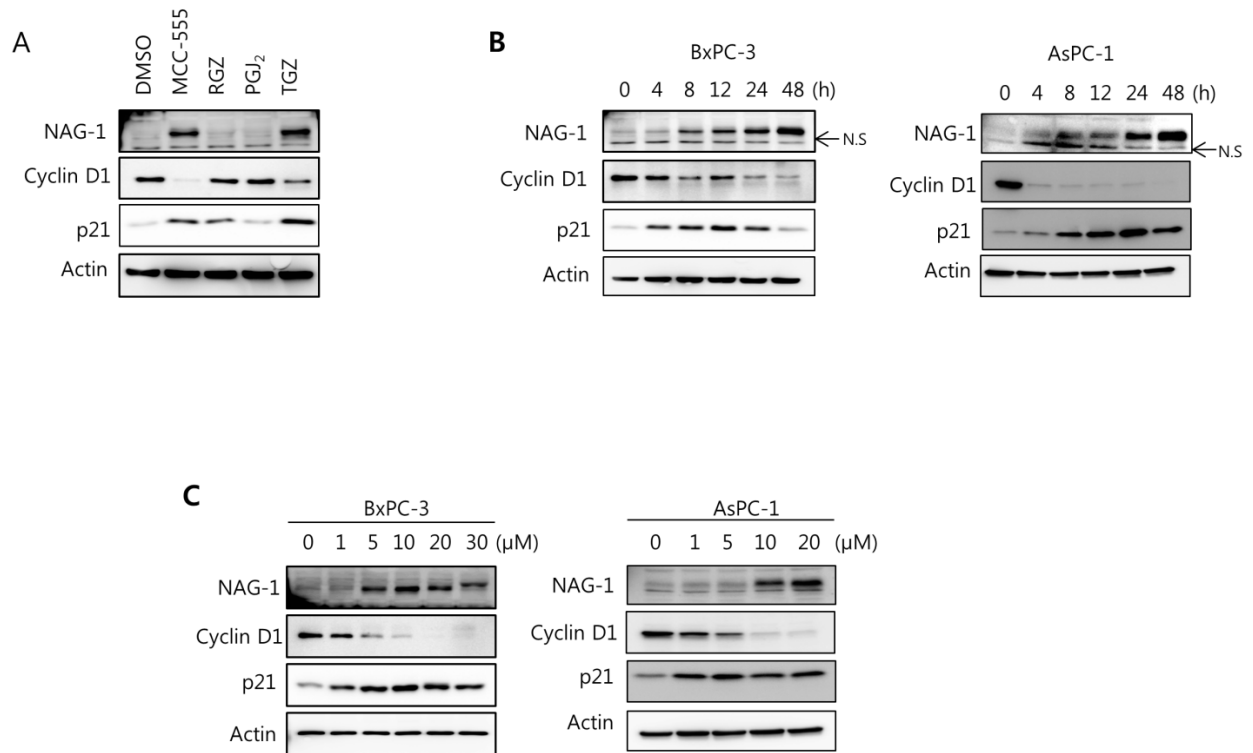
Figure 2.2 MCC-555 induces NAG-1 and p21, and suppresses cyclin D1 expression.

A, BxPC-3 cells were treated with DMSO or 10 μM of various PPARγ ligands for 24 h, and Western blot was performed with antibodies for NAG-1, p21, Cyclin D1 and Actin. **B, C**, BxPC-3 and AsPC-1 cells were treated with 10 μM of MCC-555 at the indicated times and were treated with the indicated doses for 24 h. Western blot was performed with antibodies for NAG-1, p21, Cyclin D1 and Actin. N.S., non-specific.

dramatically induced NAG-1 expression compared to other PPARγ agonists. MCC-555

and TGZ also induced p21 as well as suppressed cyclin D1 expression (Fig. 2.2A). In

this report, we focus on MCC-555's effects since TGZ was withdrawn from the market

due to the prevalence of adverse liver effects [148]. NAG-1 and p21 were induced by

MCC-555 not only in BxPC-3 cells, but also in other pancreatic cancer cells AsPC-1 in a

dose- and time-dependent manner, whereas cyclin D1 was suppressed by MCC-555 in

both cells in a dose- and time-dependent manner (Fig. 2.2B and C). Long-term

treatment (48 h) of MCC-555 exhibits the reduction of p21 protein in both cell lines,

probably due to cytopathic effects.

2.4.3 Cyclin D1, but not NAG-1 and p21 expression is involved in PPARγ activation

We examined whether NAG-1, p21 and cyclin D1 expression by MCC-555 is

regulated by PPARγ transcription factor activation. First, qRT-PCR results showed that

these transcripts were dose-dependently altered by MCC-555 in BxPC-3 and AsPC-1

cells (Fig. 2.3A). It has been reported that BxPC-3 and AsPC-1 cells express PPARγ,

and treatment with PPARγ agonists induces apoptosis and differentiation in these cells

[149, 150]. To determine whether NAG-1, p21 and cyclin D1 expression by MCC-555 is

dependent on PPARγ activation, PPARγ antagonist GW9662 was used to treat the cells.

As shown in Fig. 2.3B, NAG-1 and p21 induction by MCC-555 were not blocked by

GW9662 treatment, but reduction of cyclin D1 by MCC-555 was inhibited by GW9662
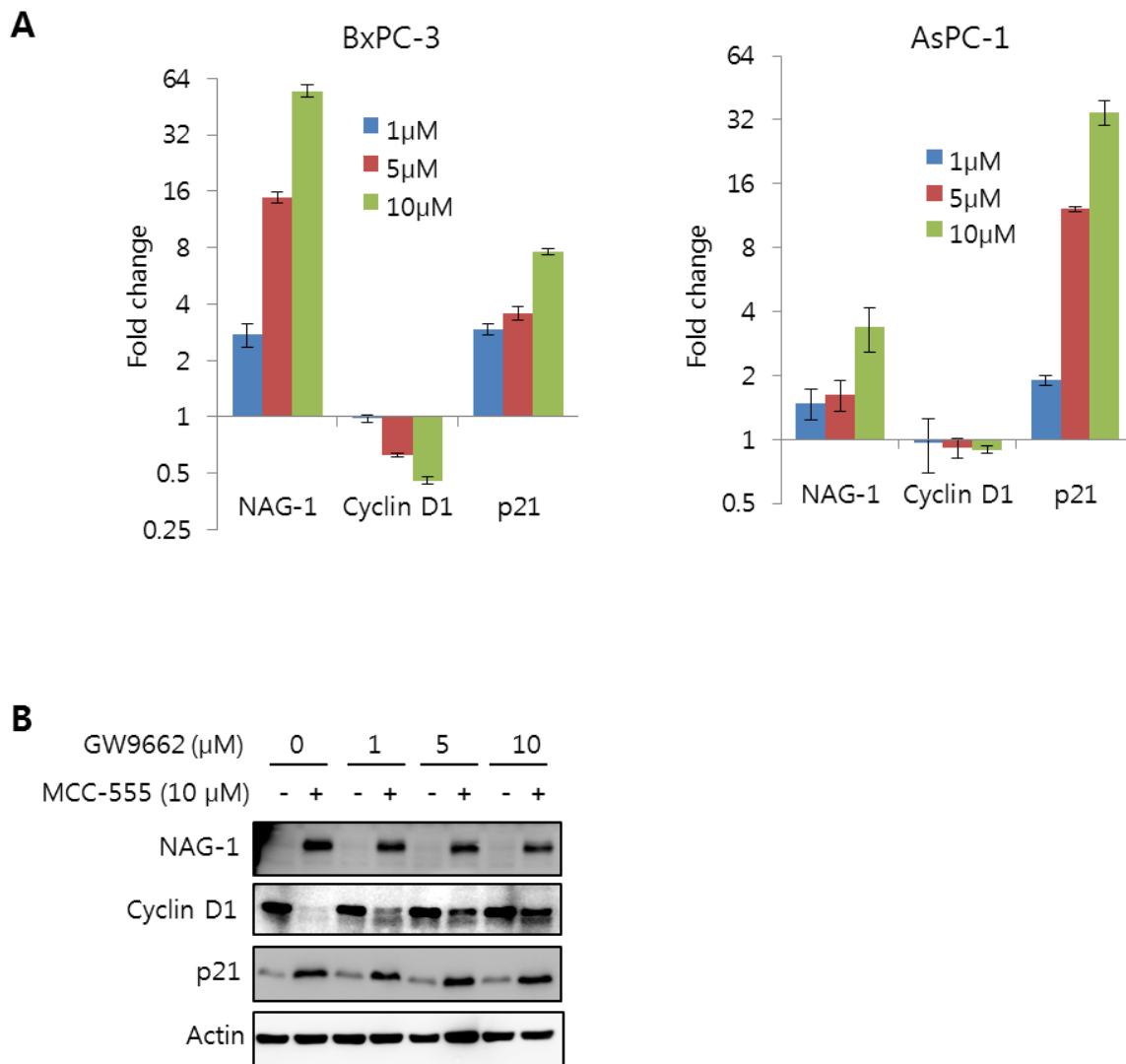
Figure 2.3 Cyclin D1, but not NAG-1 and p21, expression is involved in PPARγ activation.

A, Total RNAs were isolated from BxPC-3 and AsPC-1 cells after MCC-555 treatment. The expression of transcripts for NAG-1, p21 and Cyclin D1 was analyzed by qRT-PCR, normalized to GAPDH. Fold change compared to vehicle-treated cells are represented, vehicle-treated cells are set as 1. Error bars represent the mean±S.D of three replicates. **B**, Effects of PPARγ antagonist on MCC-555-induced NAG-1 and p21 up-regulation, and MCC-555-induced Cyclin D1 down-regulation. BxPC-3 cells were pretreated with GW9662 for 30 min at the indicated dose and then the cells were treated with 10 μM of MCC-555 for 24 h. Total proteins were isolated for Western blot analysis. Equal loading was confirmed by Actin.

treatment, indicating that NAG-1 and p21 induction by MCC-555 is independent of

PPARγ activation, whereas cyclin D1 suppression by MCC-555 is dependent on PPARγ

activation.

2.4.4 The GC box region in -133/+41 NAG-1 promoter is responsible for NAG-1 transactivation

Unlike cyclin D1 and p21 regulation by PPARγ ligands, NAG-1 expression by

PPARγ ligands in pancreatic cancer cells has not been studied in detail. Therefore, we

decided to further examine the transcriptional regulation of NAG-1 affected by MCC-

555. BxPC-3 cells were transfected with the four serial deletion constructs of the human

NAG-1 promoter, and then were treated with MCC-555. Treatment with MCC-555

resulted in increasing the promoter activity in all of the constructs tested (Fig. 2.4A).

Therefore, the -133/+41 promoter region was further analyzed using the TFSEARCH

site (http://www.cbrc.jp/research/db/TFSEARCH.html) and TESS

(http://www.cbil.upenn.edu/cgi-bin/tess/tess33?RQ=SEA-FR-Query). There are several

cis-acting elements in this region including activating transcription factor 3 (ATF3), MYC-

associated zinc finger protein (MAZ), retinoic acid receptor α (RAR-α), xenobiotic

response element binding factor (XF-1) and specificity protein 1 (Sp1) binding sites. To

investigate the responsible site in MCC-555-mediated transcriptional regulation of NAG-

1, we used internal deletion clones in which the aforementioned transcription binding

sites were deleted. As shown in Fig. 2.4B, transfection with a double deletion clone

lacking the two potential Sp1 binding sites (or GC box) significantly attenuated MCC-
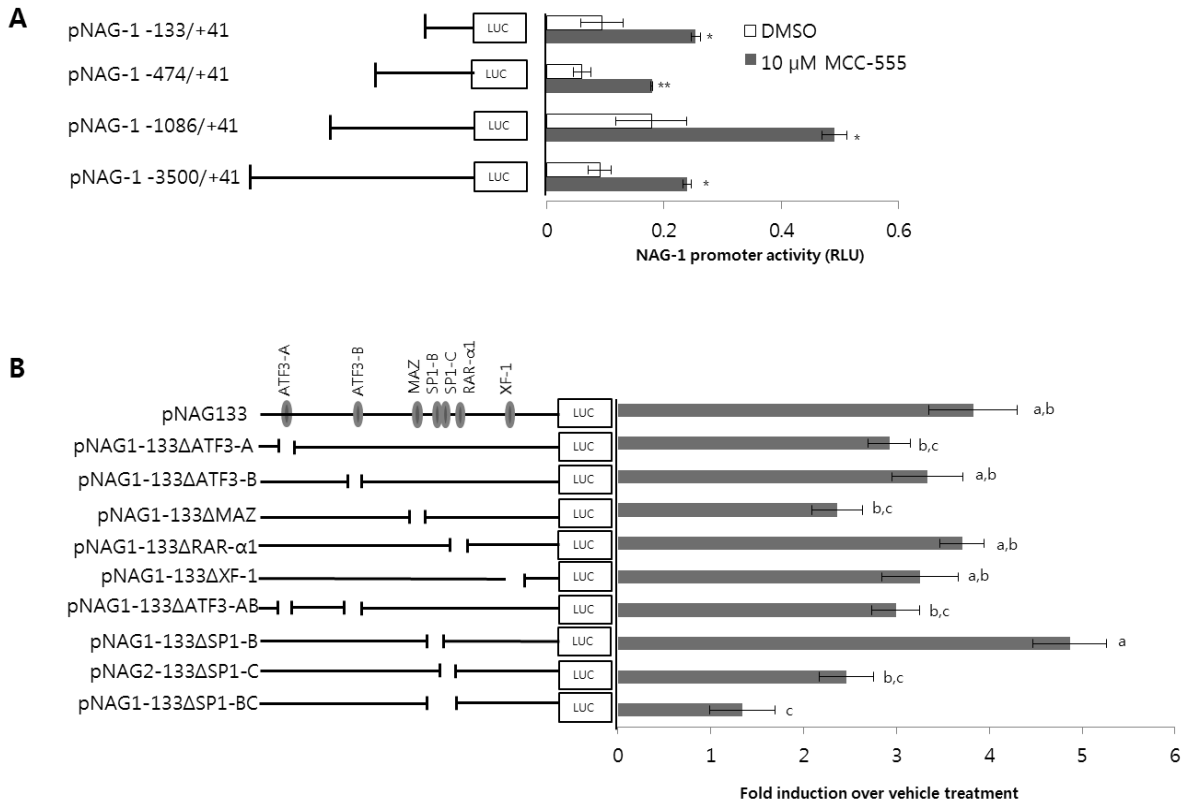
Figure 2.4 Identification of the cis-acting elements responsible for MCC-555-induced *NAG-1* transactivation.

A, Indicated constructs of the NAG-1 promoter (0.5 μg) and *pRL*-null (0.05 μg) were transfected into BxPC-3 cells for overnight. The transfected cells were exposed to MCC-555 for 24 h. The promoter activity was measured as a ratio of firefly luciferase activity/Renilla luciferase activity. The results are the mean ± S.D of three replicates. $P < 0.05^*$ and $P < 0.01^{**}$, compared to DMSO treated sample. RLU, relative luciferase unit. **B**, BxPC-3 cells were transfected with each internal deletion construct of *-133/+41 NAG-1* and then treated with vehicle or 10 μM MCC-555 for 24 h. The x-axis shows fold induction relative to vehicle-treated samples. Data were analyzed using Tukey's multiple comparison test; mean with same letters indicate no significance *(P < 0.05)*.

555-induced promoter activity, compared to wild-type promoter, suggesting that these two GC box sites are important in MCC-555-induced NAG-1 expression in pancreatic cancer cells.

2.4.5 KLF4 is a key molecule to regulate MCC-555-induced NAG-1 and p21 expression

To determine what *trans*-acting elements are involved in these GC boxes, we decided to examine the expression of proteins that could bind to these sites. Sp or several Sp-related transcriptional factors could bind to these GC boxes. The results indicate that expression of Sp transcription factors (Sp1 and Sp3) was not altered; only KLF4 was increased by MCC-555 in a dose-dependent manner, implying that KLF4 expression by MCC-555 could be responsible for NAG-1 expression in human pancreatic cancer cells (Fig. 2.5A). This is consistent with the previous report, indicating that MCC-555 increases KLF4 expression in human colorectal cancer cells [135]. Other zinc-finger proteins including ZF9 and MYC-associated zinc finger protein (MAZ) were marginally expressed in pancreatic cancer cells, whereas basic transcription element-binding protein 1 (BTEB1) was highly expressed; however, MCC-555 does not affect their expression. If KLF4 regulates NAG-1 expression in responding to MCC-555, KLF4 expression should be an earlier event than NAG-1 expression. As shown in Fig. 2.5B, KLF4 expression preceded NAG-1 expression in the presence of MCC-555. To confirm KLF4's role in MCC-555-induced NAG-1 expression, specific KLF4 siRNA was utilized. The results clearly indicate that blocking KLF4 expression resulted in the reduction of

NAG-1 and p21 expression (Fig. 2.5C). Interestingly, blocking KLF4 expression did not affect MCC-555-induced cyclin D1 suppression, suggesting that KLF4 expression may not be involved in MCC-555-induced cyclin D1 suppression. Finally, a ChIP assay was performed to confirm that KLF4 binds to the NAG-1 promoter in responding to MCC-555 (Fig. 2.5D).

2.5 Discussion

Pancreatic cancer is the fourth leading cause of cancer deaths, and the survival rate is very poor compared to other cancers. Since conventional therapeutic approaches do not decrease the incidence of mortality of this deadly cancer, we have paid more attention to alternative research including identification of molecular target approaches for an increasing survival rate.

The PPARγ agonists affect cell proliferation, differentiation, and apoptosis in a PPARγ-dependent and/or -independent manner, and thereby represent a potentially important family of therapeutic compounds for cancer treatment. Many studies describe the beneficial effects of the PPARγ agonists for treatment of lung [151], ovarian [152], breast [153] and colorectal [124] cancers *in vitro* and *in vivo*. Recently, clinical success in cancer prevention research and diabetic treatment with PPARγ agonists was overshadowed by reports of several side effects that include obesity, cardiotoxicity, and liver toxicity [154]. However, Choi et al., reported CDK5 is a new molecular target of the PPARγ ligand [155], and this finding could reverse the negative swing of the PPARγ ligand in diabetic research. As a similar token, identification of novel targets induced by
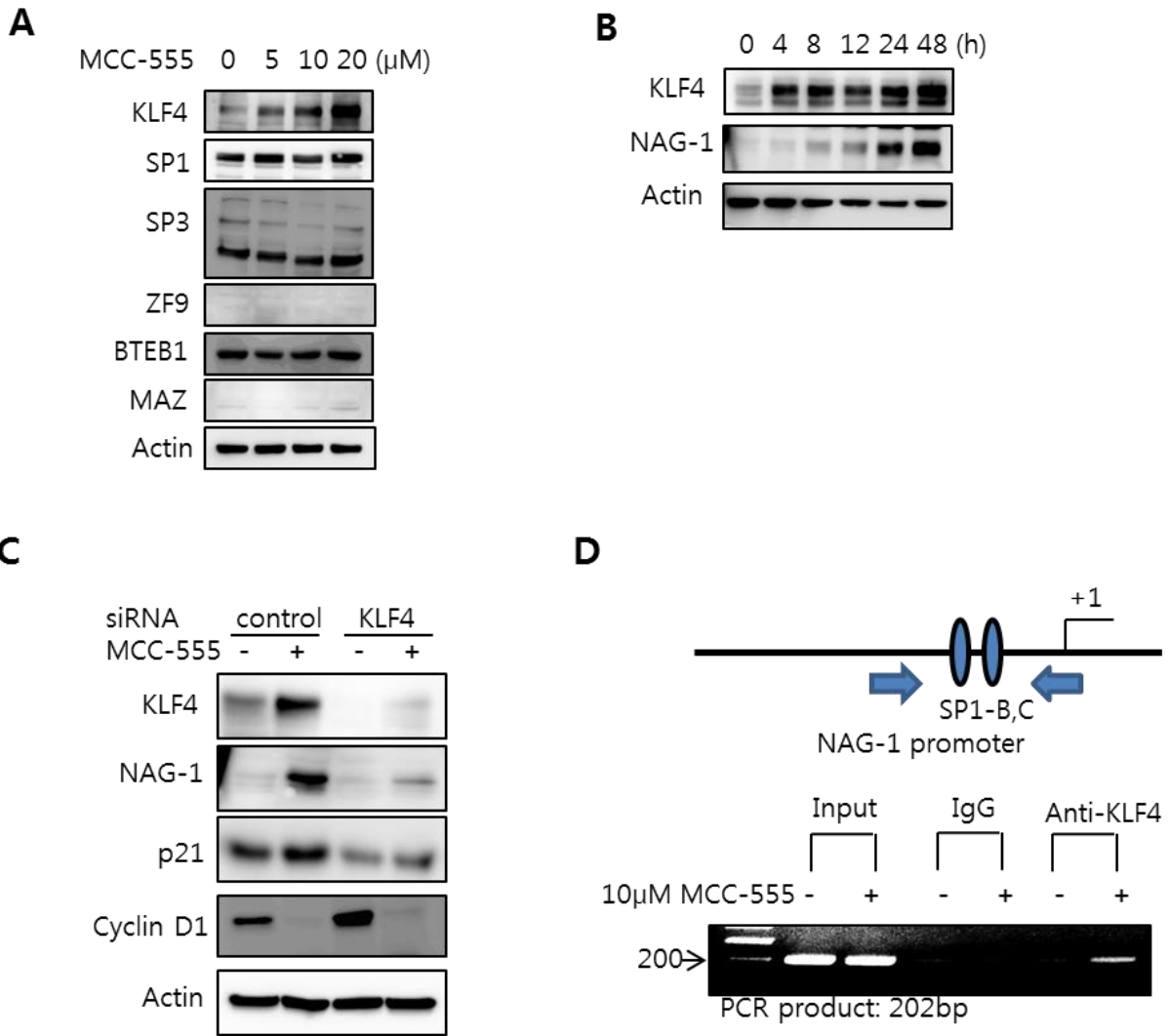
Figure 2.5 MCC-555-induced KLF4 is responsible for NAG-1 and p21 expression.

A, B, BxPC-3 cells were treated with MCC-555 at indicated time and dose. Protein lysates were harvested and subjected to Western blot analysis using KLF4, Sp1, Sp3, Zf9, BTEB1, MAZ, NAG-1, and Actin antibodies. **C**, BxPC-3 cells were transfected with either control or KLF4 siRNA using PepMute siRNA Transfection reagent according to the manufacturer's protocol. Cells were serum starved overnight and treated with DMSO or MCC-555 for 24 h, followed by Western analysis. **D**, Chromatin immunoprecipitation assay was performed using a DNA-protein complex treated with 10 μM MCC-555 for 6 h as described in Materials and Methods. The Sp1 binding sites of the human *NAG-1* promoter (-133/+41) were amplified by PCR primer pairs (arrows). The input represents PCR products obtained from 1% aliquots of chromatin pellets before immunoprecipitation.

PPARγ ligands in cancer research may help to promote their potential use. Dual ligands for PPARα and PPARγ, such as MCC-555, alternatively have been developed to improve treatment of metabolic syndrome, including hyperglycemia and hyperlipidemia. These dual ligands also possess anti-proliferative activities against a variety of cancer cell lines [125, 126] with greater potency than conventional PPARγ-specific ligands. In this report, we used MCC-555 as a PPAR dual ligand and investigated a new molecular target: p21, NAG-1, cyclin D1 and KLF4 in pancreatic cancer cells.

The biological activity of KLF4 in tumorigenesis is controversial. KLF4 is increased in human mammary tumors [156] and oral squamous-cell carcinomas [157], suggesting that overexpression of KLF4 may contribute to tumorigenesis. Conversely, it has been shown that KLF4 is down-regulated during tumorigenesis of the gastrointestinal epithelium [158] and is frequently lost in other human cancer types [159]. Consistent with a tumor suppressor function of KLF4 in colon cancer [160], its overexpression reduces tumorigenesis in pancreatic cancer cells *in vivo* [161]. Moreover, it has been shown that KLF4 inhibits metastasis of several cancers, including pancreatic cancer [162]. Thus, KLF4 may play an important role in pancreas as an anti-tumorigenic protein, but its exact function may be dependent on cell context. Our data support KLF4's anti-proliferative role in this report, showing that KLF4 controls cell cycle inhibitor p21 and pro-apoptotic protein NAG-1.

A study showed that some PPARγ or PPARα/γ agonists regulate the *Klf4* mRNA expression in PPARγ-dependent or independent manner, providing KLF4 as a novel anti-proliferative target of PPARγ ligands in pancreas [163]. From our results, we

identified that MCC-555 affects cyclin D1 expression in a PPARγ-dependent manner; however, KLF4 seems to be regulated by MCC-555 in a PPARγ independent manner (Supplementary Fig. S2.1). Our data also support the view that KLF4 is a key protein that controls cell cycle regulator p21 and pro-apoptotic protein NAG-1 in the presence of MCC-555. We showed that MCC-555 increased KLF4 expression, which results in an increased expression of p21 and NAG-1 expression. This view is in agreement with reports showing that p21 and NAG-1 are the targets of KLF4 in other cancer cells [135, 164]. Interestingly, it has been known that KLF4 regulates cyclin D1 expression, but our data clearly suggest that KLF4 is not involved in cyclin D1 regulation in the presence of MCC-555. It remains unclear, but MCC-555 may affect the modification of KLF4, thereby not binding to the cyclin D1 promoter. Alternatively, MCC-555 has been shown to activate ERK and other kinases [125], and KLF4 could be phosphorylated by these kinases [165], rendering KLF4 activity in cyclin D1 transcriptional regulation. Another possible explanation is KLF4 acetylation. Since KLF4 is acetylated by p300, thereby controlling its activity [166], MCC-555 may affect KLF4 post-translational modification by acetylation, affecting cyclin D1 expression. Finally, PPARγ activation may control more effectively than KLF4 activity in the presence of MCC-555; however, the detail mechanism needs to be elucidated.

We have shown that NAG-1 transgenic mice exhibit resistance to carcinogenic-induced colon and lung adenomas [167, 168], and NAG-1 expression is induced by many cancer chemopreventive compounds [139, 169], indicating that NAG-1 possesses cancer preventive activity and its induction is beneficial. Therefore, NAG-1 expression

induced by MCC-555 may explain the chemopreventive activity of MCC-555 in pancreatic cancer.

2.6 Summary Conclusion

In summary, our data suggest that KLF4 is an upstream molecule that controls NAG-1 and p21 expression by MCC-555 at the transcriptional level, along with the suppression of cyclin D1 by MCC-555. KLF4/NAG-1 and KLF4/p21 affected by MCC-555 are mediated in a PPARγ-independent manner, whereas cyclin D1 suppression by MCC-555 is mediated in a PPARγ-dependent manner (Fig. 2.6).
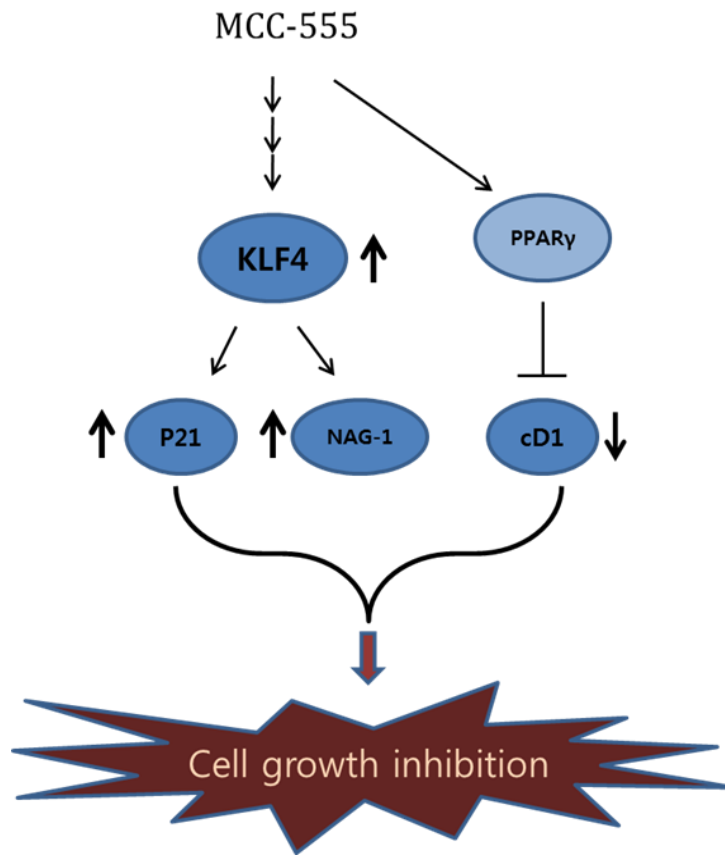
Figure 2.6 Schematic diagram of cell growth inhibition induced by MCC-555 in human pancreatic cancer cells.

MCC-555 inhibits cell growth via multiple pathways. In addition to Cyclin D1 down-regulation via the PPARγ-dependent pathway, KLF4 is up-regulated via the PPARγ-independent pathway that is responsible for the MCC-555-induced NAG-1 and p21 expression, leading to cell growth inhibition in human pancreatic cancer cells.

CHAPTER 3

NAG-1/GDF15 Accumulates in the nucleus and modulates

transcriptional regulation of the Smad pathway

3.1 Abstract

Protein dynamics, modifications, and trafficking are all processes that can modulate protein activity. Accumulating evidence strongly suggests that many proteins play distinctive roles dependent on cellular location. Nonsteroidal anti-inflammatory drug activated gene-1 (NAG-1) is a TGF-β superfamily protein that plays a role in cancer, obesity, and inflammation. NAG-1 is synthesized and cleaved into a mature peptide, which is ultimately secreted into the extracellular matrix (ECM). In this study, we have found that full-length NAG-1 is expressed in not only the cytoplasm and ECM, but also in the nucleus. NAG-1 is dynamically moved to the nucleus, exported into cytoplasm, and further transported into the ECM. We have also found that nuclear NAG-1 contributes to inhibition of the Smad pathway by interrupting the Smad complex. Overall, our study indicates that NAG-1 is localized in the nucleus and provides new evidence that NAG-1 controls transcriptional regulation in the Smad pathway.

3.2 Introduction

The study of genes altered by anti-cancer compounds has great value in regard to cancer chemoprevention and therapeutics. Building on this research, we identified the non-steroidal anti-inflammatory drug (NSAID)-activated gene-1 (*NAG-1*) as a divergent member of the TGF-β superfamily [138]. *NAG-1* has also been identified by other groups using a variety of different cloning strategies and has been called *growth differentiation factor 15 (GDF15)* [170], *placental transformation growth factor-β (PTGFB)* [171], *macrophage inhibitory cytokine-1 (MIC-1)* [172], *prostate-derived factor*

(PDF) [173], and *placental bone morphogenetic protein (PLAB)* [174]. Research to date

has demonstrated that NAG-1 is able to be induced not only by NSAIDs [175], but also

by chemopreventive dietary compounds [169, 176-179] and PPARγ ligands [124, 125,

145, 180]. These compounds affect NAG-1 induction via the tumor suppressor genes

p53, early growth response-1 (EGR-1), and/or via the PI3K/AKT/GSK-3β pathway [120,

124, 181, 182]. Unlike the transcriptional regulation of NAG-1, the principal function,

receptor, and signaling pathway of NAG-1 remain uncertain, and the biological role of

NAG-1 in tumorigenesis remains poorly understood and sometimes contradictory. For

example, NAG-1 plays a role in cancer development and progression, but various

results show it acting as either a pro-tumorigenic or anti-tumorigenic protein [183]. NAG-

1 also controls stress responses, bone formation, hematopoietic development, and

adipose tissue function, as well as contributing to cardiovascular diseases [184-186].

A transgenic mouse was developed in the authors' laboratory that ubiquitously

over-expresses the human *NAG-1* gene [167]. These mice are resistant to chemical-

and genetic-induced cancers and have a decreased systemic inflammatory response

[167, 184, 187]. Furthermore, the transgenic mice weigh less and have less fat, despite

similar food intake as wild-type (WT) littermates, suggesting NAG-1 may act to alter

metabolism, as well [167]. Recently, we reported that NAG-1 modulates metabolic

activity by increasing the expression of key thermogenic and lipolytic genes in adipose

tissue [188]. That study suggested that NAG-1 is also a novel therapeutic target in

preventing and treating obesity and insulin resistance.

NAG-1 is synthesized as a 308-amino acid pro-NAG-1 monomer and then dimerizes by a specific disulfide linkage. The pro-NAG-1 dimer is then cleaved by furin-like proteases at an RXXR site, forming a 112 amino acid C-terminal dimeric protein and pro-peptide.[183] This mature dimeric protein is secreted in the ECM, and can be detected in the blood of humans. Some evidence suggests the pro-NAG-1 dimer binds to the ECM and contributes to latent storage in the stroma [189], but the fate and role of pro-NAG-1 is poorly understood. Experimental evidence clearly confirms the secreted mature dimer has biological activity [188]; however, the multiple forms of NAG-1 present in the cells, their interaction with the cellular system, and their biological activity is unclear. Therefore, there is clearly a need for further study of the molecular mechanisms by which pro-NAG-1 contributes to NAG-1's biological activity.

A number of studies suggest that secreted proteins can localize in the nucleus and exhibit distinctive activity [7, 117]. For example, secreted proteins bFGF and odontogenic ameloblast-associated protein (ODAM) are expressed in the nucleus and cytoplasm, as well as the ECM [190]. Thus, a secreted protein like NAG-1 could also localize and alter molecular events within the nucleus. In this report, we tested this hypothesis and show the trans-localization of pro-NAG-1 into the nucleus followed by its exportation by CRM1. Our results suggest that the cleavage of pro-NAG-1 to the mature form and its subsequent secretion is dependent on translocation into the nucleus. The pro-NAG-1 inside the nucleus altered gene expression and interfered with the TGF-β1-induced Smad signaling pathway, thereby altering cell migration. This is the first study demonstrating the critical importance of NAG-1 nuclear translocation in secretion of the

mature dimer and the first report confirming a biological activity for pro-NAG-1 in the nucleus.

3.3 Materials and Methods

3.3.1 Cell culture and reagents

U2OS and HCT-116 were cultured in McCoy's 5A supplemented with 10% FBS (Hyclone) and 1% penicillin/streptomycin (Lonza). HEK293 cells were cultured in Dulbecco's modified Eagle's medium (DMEM) with 10% FBS and 1% penicillin/streptomycin. The NAG-1 tetracycline-inducible U2OS cell line has been described previously.[191] All cultured cells were maintained at 37°C in humid conditions with 5% CO_2. The following antibodies were purchased from Santa Cruz Biotechnology (Santa Cruz, CA, USA): anti-V5 (sc-271944), anti-CRM1 (sc-5595), anti-tubulin α (sc-8035), anti-lamin A/C (sc-6215), anti-histone H1 (sc-10806), anti-β-actin (sc-47778) and anti-GFP (sc-9996). Anti-Smad2 (#5339), anti-phosphor-smad2 (#3108), anti-smad2/3 (#8685), anti-smad4 (#9515), anti-p21 (#2947), anti-snail (#3879), anti-slug (#9585), anti-hsp90 (#4877) and anti-calnexin (#2679) were purchased from Cell Signaling (Danvers, MA, USA). Recombinant human TGF-β1 (#8915) was also purchased from Cell Signaling. CRM1 inhibitor (leptomycin B, L-6100) was from LC Laboratories (Woburn, MA, USA).

3.3.2 DNA Constructs and transfection

Full-length NAG-1 PCR product amplified from pcDNA3/NAG-1[138] was sub-cloned into pcDNA3.1/V5/His-TOPO vector (Invitrogen, Carlsbad, CA, USA) and pcDNA3.1/CT-GFP-TOPO vector (Invitrogen) to generate the V5/His- and GFP-tagged clones, respectively. All mutant constructs were generated from pNAG1-V5/His or pNAG1-GFP using the QuickChange II site-directed Mutagenesis Kit (Stratagene, Santa Clara, CA, USA). PCR primer sequences are described in Supplementary Table 1, and all DNA constructs used were verified by DNA sequencing. Transient transfections were carried out using either PolyJet (SignaGen, Gaithersburg, MD, USA) or TransIT-2020 transfection reagent (Mirus Bio, Madison, WI, USA) according to the manufacturer's protocol.

3.3.3 Luciferase assay

Cells were seeded on a 12-well plated at a density of 1.0×10^5 cells/well. TGF-β1-inducible reporter constructs *p3TP-luc*, *pPAI-800-luc* (*SERPINE1* promoter), and *pSBE4-luc* were each co-transfected with *pRL-null* vector. After 24 h transfection, cells were stimulated with TGF-β1 for 24 h in serum-free conditions, and then were harvested in 1 x passive lysis buffer (Promega, Madison, WI, USA). Luciferase activity was examined using a DualGlo Luciferase Assay Kit (Promega), and data were normalized by pRL-null luciferase activity.

3.3.4 Subcellular fractionation and immunofluorescence

For subcellular fractionation, either a Nuclear Extract Kit (Active Motif, Carlsbad, CA, USA) or Subcellular Protein Fractionation Kit (Thermo Scientific, Waltham, MA, USA) was used according to the manufacturer's protocol. Proteins for each fraction were subjected to Western blot analysis. For immunofluorescence, cells were plated on a glass bottom culture dish (MatTek, Ashland, MA, USA). After transient transfection, cells were washed twice with phosphate-buffered saline (PBS) and fixed with 4% paraformaldehyde for 15 min. After two PBS washes, cells were permeabilized with PBS containing 0.25% Triton X-100 for 10 min, followed by incubating with 1% bovine serum albumin in PBS for 30 min to block non-specific binding of the antibodies. The cells were incubated with diluted primary antibody overnight followed by incubation with FITC-conjugated secondary antibody (610-602-002, Rockland Immunochemicals, Gilbertsville, PA, USA) for 1 h in the dark. After counterstaining with DAPI, fluorescence was observed at 400 x magnification, with digital enlargement when required.

3.3.5 Western blot and immunoprecipitation

For Western blot, reduced protein samples lysed by RIPA buffer were separated on 8% or 10% SDS-PAGE gels, and transferred to nitrocellulose membranes (Osmonics). The membranes were incubated with a specific primary antibody in TBS containing 0.05% Tween 20 (TSB-T) and 5% nonfat dry milk at 4°C overnight. After three washes with TBS-T, the blots were incubated with horseradish peroxidase-conjugated IgG for 1 h at room temperature, visualized using detection reagent (Thermo

Scientific), and quantified by Scion Image Software (Scion Corp.). To conduct immunoprecipitation analysis, 1 mg of cell extract lysed by modified RIPA buffer (25 mM Tris-Cl pH7.4, 150 mM NaCl, 1 % NP-40, and 5 % glycerol) was incubated with 2 μg primary antibody for 2 h at 4°C on a rotating platform, followed by adding protein A/G PLUS-agarose (Santa Cruz) overnight. Immunoprecipitation was collected by centrifuge at 1000xg for 3 min. After washing five times with modified RIPA buffer, the pellets were resuspended with 50 μL 2XSDS-PAGE sample loading buffer and heated at 95°C for 5 min. Western blot analysis was conducted as described above using 20 μL of the immunoprecipitated samples.

3.3.6 In vitro nuclear import assay

HCT-116 cells were plated on glass coverslips 24 h prior to use. The cells were rinsed three times with transport buffer (TB; 20 mM HEPES, pH 7.3, 110 mM potassium acetate, 2 mM magnesium acetate), and permeabilized for 5 min with complete TB containing 1 mM EGTA, 2 mM DTT, 1 mM PMSF, protease inhibitor cocktail, and 30 μg/mL digitonin on ice. After two washes with TB, the permeabilized cells were incubated in complete TB with HCT-116 cytosol extract, the appropriate GFP-tagged NAG-1 expressed in *in vitro* TNT Quick Coupled Transcription/Translation Systems (Promega), and an ATP regeneration system (0.5 mM ATP and GTP, 5 mM creatine phosphate, and 50 μg/mL creatine kinase). Assays in the absence of an energy-regenerating system were conducted with TB without the ATP regeneration system. For WGA treatments, permeabilized cells were incubated in the presence of 0.05 mg/mL

WGA in TB for 15 min prior to the import reaction. After the import assay, cells were fixed with 4% paraformaldehyde, and fluorescent proteins were analyzed by immunofluorescence assay.

3.3.7 Library preparation and next generation sequencing (NGS)

Inducible U2OS cells were grown in the presence or absence of tetracycline (2 µg/mL) for 2 days. Total RNAs were isolated using E.Z.N.A Total RNA Kit (Omega Bio-Tek, Norcross, GA, USA) following the manufacturer's protocol. An Illumina TruSeq RNA kit (V2; San Diego, CA, USA) was used for library preparation of mRNA-Seq according to the vendor's instruction. Briefly, (poly A+) mRNAs were purified from 1 µg total RNA using poly-T magnetic beads. Messenger RNAs were fragmented to desired lengths by incubating at an elevated temperature (94°C) for 8 min in the presence of metal ions. The RNAs were used as templates for the syntheses of the first- and second-strand cDNAs, which were subsequently subjected to end repair, A-tailing at 3' ends, adapter ligation, and 15-cycle PCR amplifications. During PCR, individual barcodes were incorporated into respective samples to enable sample pooling in subsequent DNA sequencing. Paired-end 100-cycle sequencing of the prepared RNA-Seq libraries were performed on an Illumina HiSeq 2500, following standard protocols of the manufacturer.

3.3.8 NGS Data analysis

Sequence reads were processed using the Tuxedo suite (Baltimore, MD, USA).[192] Briefly, fastq files were aligned to the UCSC human reference genome (hg19) using the TopHat v.2.0.6 software program. The aligned reads were then assembled by Cufflinks v.2.0.2 to produce individual transcripts, followed by Cuffmerge to integrate the reference human genome annotation (GTF transcription annotations from Illumina iGenomes). The output files were then passed onto the Cuffdiff program to create differential expression results.

3.3.9 Real-time qRT-PCR

Total RNA was isolated using an E.Z.N.A Total RNA Kit (Omega Bio-Tek) according to the manufacturer's protocol. Complementary DNA was made from 1 µg isolated RNA using a Verso cDNA synthesis kit (Thermo Scientific) according to the manufacturer's protocol. PCR was carried out using iTaq Universal SYBR Green Supermix (Bio-Rad, Hercules, CA, USA). Primers used for qRT-PCR are provided in Supplementary Table 3. Relative quantities of mRNAs were calculated using the $\Delta\Delta C_t$ method and normalized using human Ribosomal Protein, Large, P0 (RPLP0) as an endogenous control.

3.3.10 Scratch and transwell migration assay

For the scratch migration assay, inducible U2OS cells were plated onto a 6-well plate and cultured to near (> 90%) confluence. Cells were serum starved for 24 h in the

presence or absence of 2 μg/mL tetracycline, and the monolayer was scratched with a

sterile 10 μL-pipette tip. Then serum-free media containing 10 ng/mL of TGF-β1 was

added for 24 h. Phase-contrast images were acquired at 0 and 24 h after the gaps were

created. The cells migrated into the gaps were counted from three different gap regions.

For the transwell migration assay, transfected U2OS cells were resuspended in serum-

free medium, and the cell suspension (4×10^4 cells) was added to the upper transwell

chamber (pore size of 8 μM; Costar; Corning, Corning, NY, USA). Media containing

0.1% serum and TGF-β1 was added to the bottom wells of the chambers. Cells were

incubated for 18 h at 37°C, fixed with 4% paraformaldehyde, and permeabilized by

100% methanol. Cells were then stained with 0.5% crystal violet dissolved in 20%

methanol at room temperature for 15 min. Cells that had not migrated after 18 h were

removed from the upper face of the filters using cotton swabs. Migrated cells were

counted under a light microscope. Images of three different fields were taken for each

membrane.

3.3.11 3D spheroid invasion assay

A 96-well 3D spheroid BME cell invasion assay kit (Cultrex) was used according

to the manufacturer's protocol with minor modification. Briefly, 2,000 cells were

resuspended in serum-free media containing spheroid formation ECM. The cells were

added to a 96-well ultralow attachment round bottom plate, and then incubated for 1 day

to allow cells to assemble into compact spheroids. Invasion matrix was added to each

well, and then the cells were incubated for 1 h prior to adding serum-free media

containing 10 ng/mL TGF-β1. The plate was incubated for 2 days, and spheroids were photographed at 8 x magnification.

3.3.12 DNA pull-down assay

Tetracycline-treated or non-tetracycline-treated inducible U2OS cells grown on a 10-cm dish were stimulated with or without 5 ng/mL of TGF-β1 for 2 h. Whole cell lysates were prepared in lysis buffer (10 mM HEPES pH 7.5, 150 mM NaCl, 1 mM $MgCl2$, 0.5 mM EDTA, 0.5 mM DTT, 0.1% NP-40, 10% glycerol). Lysates were centrifuged at 4°C for 15 min at high speed. Cell lysate (500 μg) was incubated with 5 μg poly(dI-dC) and 1 μg biotinylated SBE oligonucleotides containing Smad binding elements at 4°C for 16 h. DNA-bound proteins were collected with streptavidin beads (G-Biosciences, St. Louis, MO, USA) for 2 h. Beads were collected by centrifugation for 30 s at 3000 g and washed four times with lysis buffer. Then, 2Xsample buffer (50 μL) was added to the beads and boiled for 5 min, followed by Western blotting. The SBE probe sequence for DNA pull-down was Biotine-5'- TCGATAGCCAG-ACAGGTAGCCAGACAGGTAGCCAGACAGGTAGCCAGACAGG-3' [193].

3.3.13 Chromatin immunoprecipitation

For the chromatin immunoprecipitation assay, a MAGnify chromatin immunoprecipitation system (Invitrogen) was used according to the manufacturer's protocol. Briefly, cells were grown to 70~80% confluence in a 150-mm dish. The cells were crosslinked with 1% formaldehyde for 10 min at room temperature. Crosslinking

reactions were quenched with 0.125 M glycine for 5 min at room temperature. The cells were scraped and moved to a 1.5-mL tube, then sonicated for 8 cycles of 15 s on/1 min off. Sheared chromatin was incubated with either Smad2/3 antibody or normal IgG conjugated with beads for 2 h at 4°C. Chromatin-bound DNA was reverse cross-linked and DNA was purified. Purified DNA was subjected to qRT-PCR using the following primer pairs: TIMP3 promoter region, forward 5'- GCAAACAGCAGATGGCTTCC -3' and reverse 5'- CCTTGACTGTGCTTGGTGGA - 3'; SMAD7 promoter region, forward 5'- TTCTGGGAGCTTCTCTGCCC -3' and reverse 5'- GCTCCGGCCTCGTCAC -3'.

3.3.14 Interspecies heterokaryon assay

The human U2OS cells grown in glass bottom dishes were transiently transfected with the pNAG-1/V5/His expression vector. At 24 h post transfection, the U2OS cells were washed with PBS twice, and then an equal number of murine NIH3T3 cells were seeded onto the same glass bottom dishes. After 6 h incubation, cycloheximide (CHX, 100 µg/ml) and 10 nM LMB were added to inhibit protein synthesis and nuclear export of a protein. The co-cultured cells were washed twice with PBS after 2 h and were added with polyethylene glycol MW 8000 (PEG) 50% (w/v) in PBS for 2 min to allow cell fusion, followed by washing twice with serum-free medium containing CHX. The cells were then incubated with complete media (plus CHX along with LMB) for 1 h. After fixation in 4% paraformaldehyde, the cells were counterstained with Hoechst 33258 to distinguish human U2OS nuclei from those of murine NIH3T3 cells.

3.3.15 Statistical analysis

Statistical analysis was performed with the Student unpaired t test. Results were considered statistically significance at $*P < 0.05$, $**P < 0.01$ and $***P < 0.001$.

3.4 Results

3.4.1 Full-length wild-type NAG-1 (pro-NAG-1) translocates to the nucleus

Because emerging evidence suggests that proteins exhibit distinctive activities based on cellular location, we decided to examine whether NAG-1 protein is located in different cellular regions. NAG-1 is first formed as pro-NAG-1 and then cleaved into a pro-peptide and a mature dimer form, which is then secreted into circulation. To investigate the cellular location of NAG-1 and the secretion events, we first used U2OS stable cell lines in which pro-NAG-1 is induced by treatment with tetracycline [191]. Only the pro-NAG-1 was present inside the cells with no mature form observed (Fig. 3.1A). Interestingly, nuclear/cytoplasmic fractionation of U2OS cells demonstrated that pro-NAG-1 was equally expressed in both the cytoplasm and the nucleus in U2OS cells (Fig. 3.1B). Lamin A/C and tubulin α were used as controls for nuclear and cytoplasmic fractions, respectively. To confirm our finding, we constructed expression vectors for GFP- and V5/His-tagged NAG-1 and conducted an immunofluorescence assay to observe subcellular localization of NAG-1 in U2OS cells transiently transfected with the pNAG-1/GFP expression vector. NAG-1 signal (green) was observed in both the nucleus and the cytoplasm with a considerable signal in the ER/Golgi region (Fig. 3.1C).

NAG-1 seemed to be localized in nucleolus; however, NAG-1 expression was not confined to nucleolus, as shown in a co-localization experiment with fibrillarin, a marker for nucleolus expression (Supplementary Fig. S3.1A). To define the location of NAG-1 in more detail, we performed subcellular fractionation, which separates cell components into soluble cytoplasmic extract (CE), membrane extract (ME), soluble nuclear extract (NE), and chromatin-bound protein extract (CB). As shown in Fig. 3.1D, pro-NAG-1 was expressed in both ME and NE fractions. Cell lysates from tet-inducible system and wild-type U2OS cells transiently transfected with the pNAG-1/V5/His expression vector were separated into components. The phenomenon of finding pro-NAG-1 in nuclear fractions is observed both in the transient and stable NAG-1 expressing cells. Endogenous NAG-1 expression is induced by treatment with several anti-cancer compounds in HCT-116 human colorectal cancer cells [138]. As shown in Fig. 3.1E, HCT-116 cells incubated with anticancer compounds for 24 h express endogenous pro-NAG-1 in nucleus, suggesting a rapid translocation into the nucleus. A confocal microscopy analysis supports our finding that NAG-1 is present in the nucleus (Supplementary Fig. S3.1B). Overall, pro-NAG-1 is surprisingly expressed in the nucleus in addition to the membrane fractions, including the vesicle and ER/Golgi apparatus.

Figure 3.1 NAG-1 expression observed in the nuclear fraction.

A, Western blot analysis of tetracycline-inducible U2OS cells. Cells grown in *tet*-free FBS were treated with 2 µg/mL tetracycline for the indicated times. Actin antibody was used for the loading control. **B**, Nuclear and cytoplasmic expression of NAG-1. Cytoplasm and nuclear fractions of inducible U2OS cells were isolated after stimulation with 2 µg/mL tetracycline for 24 h. Expression of NAG-1, lamin A/C (nuclear marker), and tubulin α (cytoplasmic marker) were analyzed by Western blot. **C**, U2OS cells transfected with GFP-tagged NAG-1 (WT) were fixed and analyzed by immunofluorescence with antibodies against GFP as described in the Materials and Methods section. DAPI was used to stain the nuclei. Two independent fields are shown. **D**, Tetracycline-induced U2OS (top panel) and wild-type U2OS cells transfected with NAG-1/V5/His expression vector (bottom panel) were subjected to subcellular fractionation, and Western blot was performed. CE, cytoplasmic extract; ME, membrane extract; NE, nuclear extract; CB, chromatin-bound extract. Markers in each fraction are shown. Sp3 exhibits multiple bands, and a 78 kDa band is shown. **E**, HCT-116 cells were treated with 10 µM of each compound for 24 h and subjected to Western blot analysis. MCC-555 is a PPARγ ligand, whereas SS (sulindac sulfide) and TA (tolfenamic acid) are NSAIDs. DMSO was used for a vehicle.
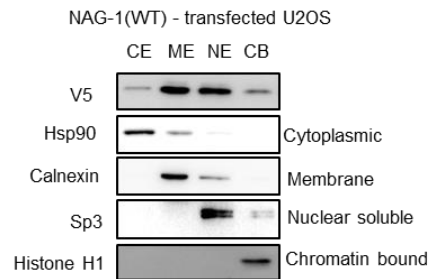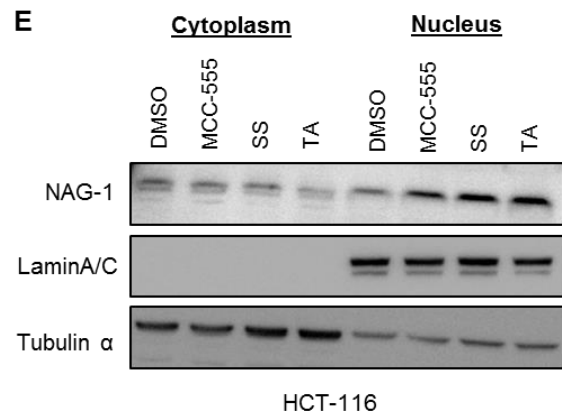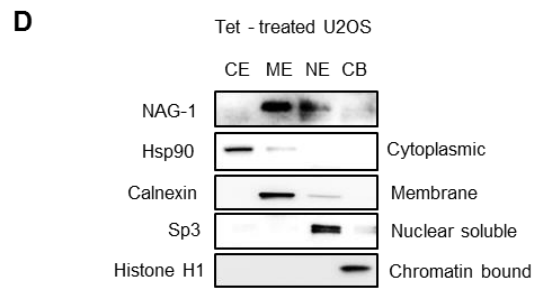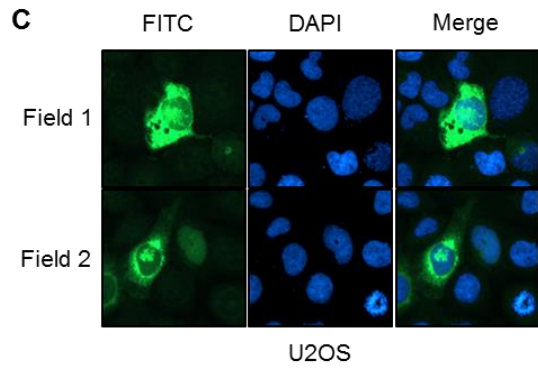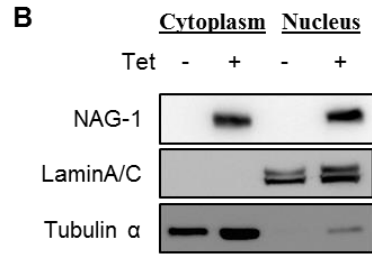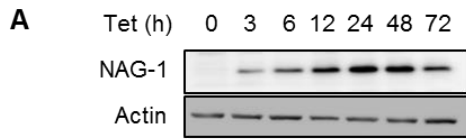
Figure 3.1 Continued.

3.4.2 NAG-1 may contain a non-canonical nuclear localization signal domain and is imported to the nucleus via the nuclear pore complex.

Since NAG-1 does not contain the classical nuclear localization signal (NLS), two independent programs were used to search for the non-classical NLS [194, 195]. Both programs found one potential non-classical NLS (aa 190-197). Another potential NLS (aa 211-218) was selected by only one program. Subsequently, two deletion mutant clones (Δ190-197 and Δ211-218) from the NAG-1/V5/His expression vector were generated (Fig. 3.2A) and expressed in wild-type U2OS and HCT-116 cells. Nuclear/cytoplasmic localization showed that the expression level of the two NAG-1 mutants was higher in the cytoplasmic fraction than in the nucleus, in both cell types (Fig. 3.2A). These data are further confirmed by subcellular fractionation, indicating that Δ190-197 NAG-1 has less NAG-1 expression in the nuclear extraction (Supplementary Fig. S3.2A). Thus, these mutant NAG-1 proteins are still translocated into the nucleus but at a much lower amount, compared to wild-type NAG-1. These results were confirmed by immunofluorescence analysis with NAG-1/GFP construct, indicating that less signal intensity of mutant NAG-1-transfected cells was observed in the nucleus, compared to wild-type NAG-1-transfected cells (Fig. 3.2B). Thus, these two regions, aa 190-197 and aa 211-218, may contribute, at least in part, to translocation of NAG-1 protein from the cytoplasm to the nucleus. It has been reported that a protein can have multiple NLS that may function cooperatively to affect efficient nuclear transport [196, 197]. Since two putative NLS sites exhibit a marginal effect on nuclear entry of NAG-1, serial deletion mutant clones were generated to address this issue. As shown in Fig. 3.2C, none of the clones resulted in a higher ratio of cytoplasmic NAG-1 to nuclear

NAG-1. However, the expression of one NAG-1 mutant clone (Δ2-29 clone) resulted in predominant expression in the nucleus (Fig. 3.2C). To determine whether this translocation requires energy and/or the nuclear pore complex, an in vitro nuclear import assay was performed using NAG-1/GFP fusion proteins. Permeabilized cells lose their transport systems; therefore, cytosolic extract and the ATP/GTP regenerating system were provided to investigate nuclear uptake of NAG-1/GFP. As shown in Fig. 3.2D, NAG-1/GFP protein localized in the nucleus, whereas GFP protein alone did not. These results suggest that NAG-1/GFP does not enter the nucleus by a simple diffusion pathway because of the large size of the NAG-1/GFP protein (more than 60 kDa), and that ATP is required to transport NAG-1 into the nucleus. In addition, inactivation of the nuclear pore complex (NPC) by wheat germ agglutinin (WGA) abolished NAG-1 movement to the nucleus. Since the secreted NAG-1 cannot be absorbed by the cells (Supplementary Fig. S3.2B), only cytoplasmic NAG-1 is subjected to nuclear entry. Taken together, these results indicate that the nuclear entry of NAG-1 is energy-dependent via the nuclear pore complex, and those two sites (190-197 and 211-218), in part, contribute to the nuclear entry of NAG-1.

3.4.3 NAG-1 has a canonical nuclear export signal (NES) mediated by CRM1

Next, we decided to further analyze the 2-29 region of NAG-1, as shown in Fig. 3.2C, in terms of nuclear accumulation of NAG-1. We generated more deletion clones within this region and found that the Δ14-29 clone contains a domain to control

Figure 3.2 NAG-1 moves to the nucleus through a nuclear pore complex in an energy-dependent manner.

A, Schematic diagrams of plasmids encoding different truncated forms of NAG-1, Δ190-197, and Δ211-218. Deletion sequences are presented in the bottom panel. Pro-NAG-1 (Wild-type) is designated at the top: propeptide (yellow), mature peptide (blue), followed by V5 epitope and histidine track (red). C, cytoplasmic and N, nuclear fractions of U2OS (bottom left panel) and HCT-116 (bottom right panel) cells transfected with either WT or two mutant clones were subjected to Western blot. Antibodies against lamin A/C and Tubulin α were used for nuclear and cytoplasm markers, respectively. Intensity ratio for cytoplasmic to nuclear (C/N) expression is shown at the bottom. **B**, Immunofluorescence assay with antibodies against V5 from WT and two mutant NAG-1-transfected U2OS cells. DAPI was used for staining nuclei. Representative fields are shown. **C**, Schematic diagram of serial deletion mutants of NAG-1. HCT-116 cells were transfected with each mutant clone as described in the Materials and Methods section, and Western blot analysis was performed using C and N fractions. Intensity ratio for C/N expression is shown at the bottom. **D**, *In vitro* nuclear import assays of NAG-1/GFP protein. HCT116 cells were permeabilized with digitonin (30 ng/ml) for 5 min and then incubated in a reaction buffer containing cytosol extract and ATP regeneration system with either NAG-1/GFP or GFP protein. For WGA treatment, permeabilized cells were pre-incubated with 0.05 mg/mL WGA for 30 min at room temperature and incubated for 30 min at 37°C with complete reaction buffer. The cells were washed with reaction buffer and then fixed and stained with DAPI. The cells were viewed by fluorescence microscopy. Right panel, expression of in vitro translated GFP and NAG-1/GFP by Western blot.
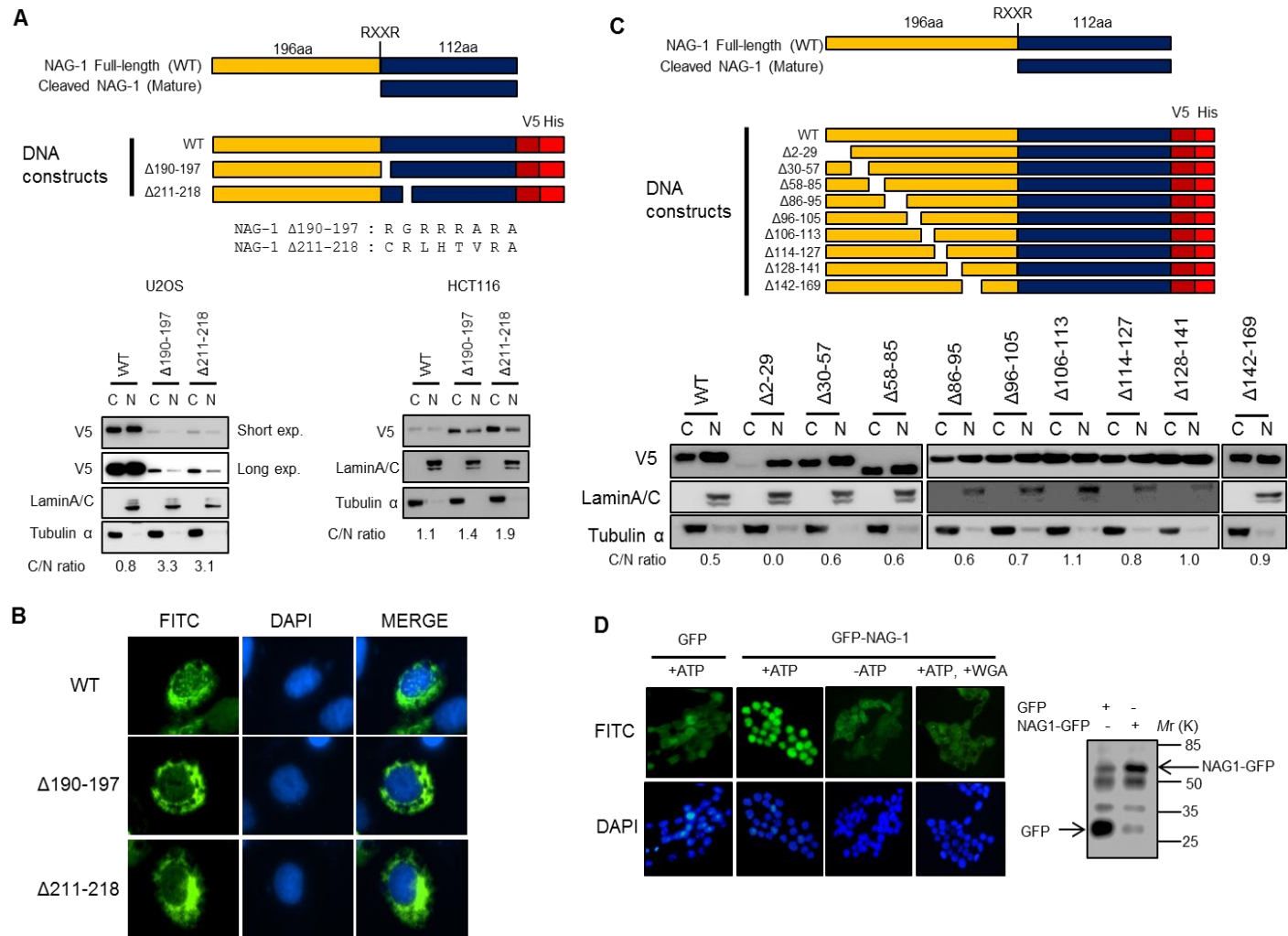
Figure 3.2 Continued.

predominantly nuclear expression of NAG-1 (Supplementary Fig S3.3A, B). We also

generated a glycosylation site mutant clone (N70A) because it has been known that

glycosylation sites may affect nuclear translocation of proteins [198]. This clone showed

an expression pattern of NAG-1 similar to that of wild-type (Supplementary Fig. S3.3A).

As shown in Fig 3.3A, the Δ14-29 clone exhibited higher expression of NAG-1 in the

nucleus (lane 3 vs 7). As a control, we transfected an R193A mutant clone that cannot

be cleaved at the RXXR site and wherein mature NAG-1 cannot form. To elucidate if the

Δ14-29 mutant clone altered secretion of the mature form, conditioned medium from the

same batch used in Fig. 3.3A was purified, and secreted mature NAG-1 was measured

by Western blot analysis. As expected, both pro-NAG-1 and mature NAG-1 (Fig. 3.3B,

lane 2) were detected in pNAG-1/V5 transfected medium, while the R193A clone

secreted only the pro-NAG-1 (Fig. 3.3B, lane 4). However, we could not detect Δ14-29

pro-NAG-1 nor mature NAG-1 in the culture medum (Fig. 3.3B, lane 3). These data

indicate that the Δ14-29 region is necessary for exporting pro-NAG-1 protein to the

cytoplasm from the nucleus and thus no mature NAG-1 is present in the media.

Our results also indicate a putative NES sequence in the Δ14-29 region [199].

Therefore, two mutants (ΔNES and mutNES) were generated to investigate whether the

Δ14-29 region plays a role in nuclear exportation of NAG-1 (Fig. 3.3C). The expression

pattern of NAG-1 in U2OS cells with a ΔNES or mutNES construct showed essentially

nucleus expression with little to no cytoplasm expression in contrast with the wild-type

NAG-1 control (Fig. 3.3C and Supplementary Fig. S3.4A). confirmation of nuclear

expression was obtained with immunofluorescence of U2OS cells transfected with

pNAG/ΔNES/V5 and pNAG/mutNES/V5 constructs (Fig. 3.3D). Chromosome region

maintenance 1 (CRM1; also referred to as exportin1 or Xpo1) is a key protein in

exporting a protein from the nucleus into the cytoplasm [200]. To determine whether

CRM1 is involved in NAG-1 exportation, we added the CRM1 inhibitor leptomycin B

(LMB) to the cells to see nuclear retention of NAG-1. The pro-NAG-1 nuclear

distribution was increased in the cells treated with LMB in a dose-dependent manner

(Supplementary Fig. S3.4B, C and D). Smad4 was used as a control because it is

regulated by CRM1 in exportation out of the nucleus [201]. Finally, we conducted an

immunoprecipitation assay to determine whether pro-NAG-1 physically interacts with

CRM1. As shown in Fig. 3.3E, pro-NAG-1 was indeed immunoprecipitated with CRM1,

suggesting that NAG-1 exportation to the cytoplasm is controlled by CRM1. There is a

possibility that the 14-29 aa region of NAG-1 may have signal sequences for direct

secretion to the extracellular region in addition to those for exportation from the nucleus.

To address this possibility, we observed the level of NAG-1 secretion after LBM

treatment. As expected, LMB treatment blocked NAG-1 secretion, suggesting that the

14-29 aa region is not only for exportation from the nucleus but also for secretion (Fig.

3.3F). To further support the evidence that an NES exists in NAG-1, we employed the

interspecies heterokaryon assay (Supplementary Fig. S3.4E), the results of which

suggested that NAG-1 shuttles between the nucleus and the cytoplasm, and LMB

treatment blocks nucleocytoplasmic shuttling properties of NAG-1.

Figure 3.3 A canonical nuclear export signal (NES) of NAG-1 contributes predominant nuclear expression of NAG-1.

A, HEK293 (left panel) and HCT-116 (right panel) cells were transfected with either control LacZ vector, full-length pNAG-1-V5-WT (FL), or the two mutant clones pNAG-1-V5 Δ14-29 and pNAG-1-V5 R193A. Then the cytoplasm and nuclear fractions were isolated. Western blot analysis was performed against V5, tubulin α, and lamin A/C. **B**, Conditioned media from (**A**) were harvested and concentrated by Corning concentrations (10 kDa MWCO), and 30 µL concentrated conditioned media was analyzed by Western blot with anti-V5 antibody. **C**, A putative NES in the N-terminal domain of NAG-1. The putative NES sequence in human NAG-1 is aligned with NAG-1 in other species, and also compared with the known NES sequences in Smad4, Hsc70, and PKI. Two mutant NAG-1 clones, ΔNES and mutNES, are shown. U2OS cells were transfected with the indicated vectors. Nuclear, N, and cytoplasmic, C, fractions were analyzed using the indicated antibodies as shown at bottom. **D**, U2OS cells were transfected with WT, ΔNES, or mutNES NAG-1-expressing vectors, and immunofluorescence assay was performed with antibodies against V5 (green) with DAPI staining (blue). Scale bars, 10 µm. **E**, *Tet*-inducible U2OS cells were treated with 2 µg/mL tetracycline for 24 h, and cell lysates were isolated with a modified RIPA buffer as described in the Materials and Methods section. The cell lysates were incubated overnight with 2 µg CRM1 or normal IgG antibodies, subjected to immunoprecipitation for 3 h, and then subjected to Western blot analysis using NAG-1 or CRM1 antibodies. The whole cell lysate (WCL) was loaded with 30 µg. **F**, U2OS cells were transfected with pNAG-1/V5/His WT for 6 h, then 10 nM LMB added for 18 h. Conditioned media from the cells was subjected to Western blot analysis.
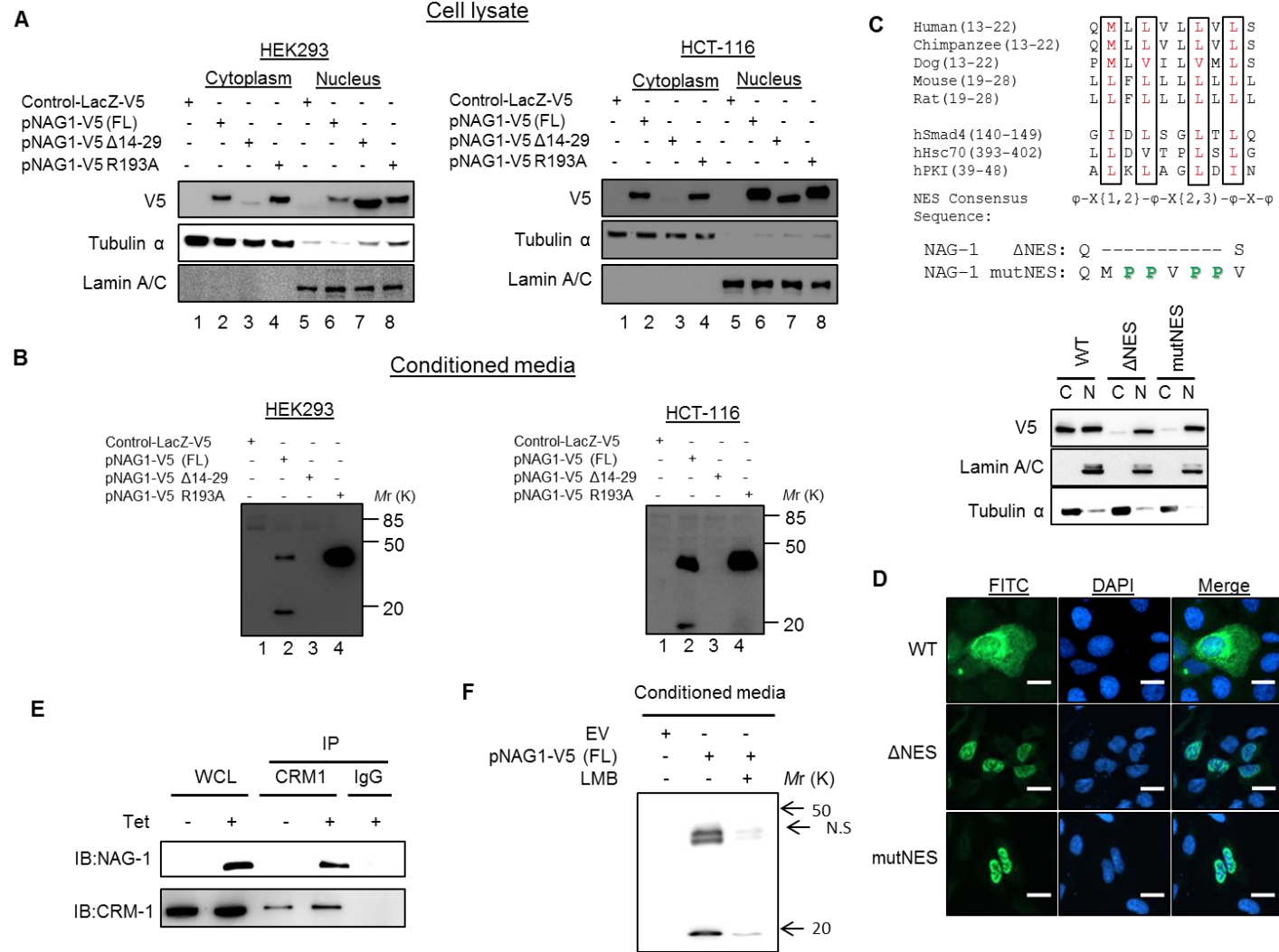
Figure 3.3 Continued.

3.4.4 RNA-seq analysis suggests that NAG-1 inhibits the expression of TGF-β target genes

To date, little is known about the NAG-1 receptor and its downstream pathways. Transcriptome sequencing (RNA-seq) is a promising tool in elucidating downstream effects and/or pathways. To study the effects and downstream pathways of NAG-1, we employed comparative RNA-seq profiling of the transcriptomes using U2OS and *tet-*induced U2OS cells. RNA-seq results revealed 142 differentially expressed genes (Fig. 3.4A). Nineteen of the 142 genes were previously reported to be a potential TGF-β target gene with regard to their relative abundance presented in the heat map (Fig. 3.4B). Ingenuity network analysis was used to identify possible interactions with other genes differentially expressed in our dataset, and suggested NAG-1 expression reduced the expression of several TGF-β1-related genes (Fig. 3.4C). Although we did not treat the cells with TGF-β1 for RNA-seq experiments, U2OS cell lines spontaneously secrete TGF-β1 in an autocrine loop for homeostasis (Supplementary Fig. S3.5). We selected 10 out of 19 genes because they are well-known Smad target genes and confirmed their expression in the cells transfected with pNAG-1/His/V5 expression vector by qRT-PCR (Fig. 3.4D). Except for HMGA1, the expression of NAG-1 inhibited the expression of these downstream targets of TGF-β1, suggesting pro-NAG-1 acts as an inhibitor of the TGF-β1 pathway. To examine further the effect of NAG-1 on the TGF-β signaling pathway, two promoter reporters, *p3TP-Luc* and *pPAI-800-Luc,* were transfected into two TGF-β-responsible U2OS and HEK293 cells with NAG-1 expression vector. NAG-1 expression diminished TGF-β1-mediated Smad

Figure 3.4 NAG-1 modulates TGF-β signaling at the transcriptional level.

A, The scatter plot from RNA-seq data compares the expression of inducible U2OS cells with or without tetracycline. The straight line highlights the general similarities between the two conditions, with the volcano plot (red for up-regulation, green for down-regulation) showing the differentially expressed genes (Supplementary Table 2). **B**, Heat map representation of the mRNA expression profile showing changes in TGF-β downstream target genes between U2OS and tetracycline-treated U2OS cells. Gene expression data were log2 transformed and then normalized prior to generating the heat map for direct comparison of data. Differential expression for each cell is presented. **C**, Schematic representation of Ingenuity network analysis. Gene symbols are in red and green for up- and down-regulation, respectively. Dashed lines show indirect interactions, while continuous lines represent direct interactions, based on Ingenuity's knowledgebase. **D**, Real-time PCR of selected genes from the heat map. Empty vector (EV) or wild-type (WT) NAG-1 was transfected into U2OS cells and total RNAs isolated; then qRT-PCR was performed as described in the Materials and Methods section. The data were normalized by the expression of the housekeeping Ribosomal Protein, Large, P0 (RPLP0) mRNA, and further normalized to the level of the empty vector transfected group, which was set at 1. **E**, Two reporter genes, *p3TP-Luc* and *pPAI-800-Luc* (*SERPINE1 promoter*), were co-transfected with either empty vector or NAG-1-expressing vector into U2OS and HEK293 cells that exhibited an intact TGF-β signaling pathway. Transfected cells were treated with TGF-β1 (10 ng/mL for 24 h), and luciferase activity was measured. The graph shows mean values with ± SD from three replicates. *$P < 0.05$, compared to TGF-β1-treated empty vector-transfected cells.
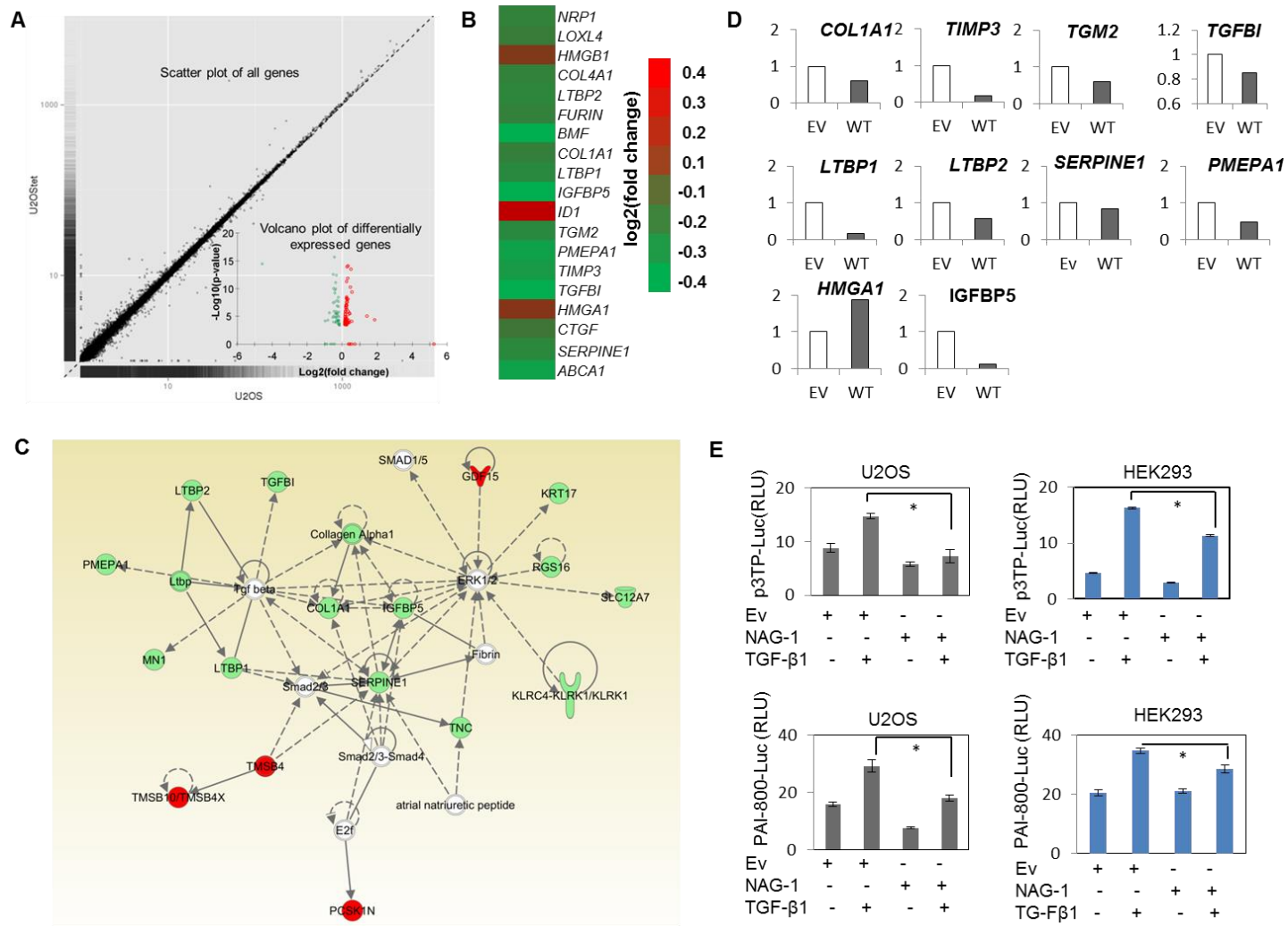
Figure 3.4 Continued.

activities (p3TP-Luc and pPAI-800-Luc) (Fig. 3.4E). Thus, pro-NAG-1 expression inhibits the TGF-β1-mediated Smad signaling pathway at the transcriptional level.

3.4.5 Nuclear NAG-1 mitigates TGF-β signaling via interrupting Smads to DNA binding

To address to what extent NAG-1 is relevant to endogenous Smad target genes, we treated the cells with TGF-β1 and measured the expression of the known TGF-β target genes *SERPINE1, TIMP3, and LTBP1*. Gene expression was suppressed in the presence of NAG-1 and further suppressed in the presence of ΔNES-NAG-1, which is in agreement with a higher level of nuclear pro-NAG-1 (Fig. 3.5A). In U2OS and MCF10A cells (TGF-β1-responding cells), wild-type NAG-1 and mutNES NAG-1 expression inhibited the Smad pathway, as assessed by Smad binding element (SBE) reporter activity (Fig. 3.5B). Similar results were observed in MCF7 cells using *p3TP* and *PAI-1* reporters (Supplementary Fig. S3.6A). Expression of the R193A mutant, which does not produce the mature NAG-1, also inhibited TGF-β-mediated Smad transcriptional activity (Supplementary Fig. S3.6B), supporting the hypothesis that pro-NAG-1, but not mature NAG-1, is involved in the inhibition of Smad signaling.

To further investigate how NAG-1 modulates the TGF-β1 response, we measured the level of phosphorylation of Smad2 in the presence of TGF-β1. Wild-type U2OS cells were transfected with either empty or NAG-1 expression vector and then treated with TGF-β1 for 1 h. Next, the treatment medium was aspirated and fresh

Figure 3.5 Nuclear NAG-1 interrupts DNA binding activity of the Smad complex.
A, Real-time PCR for expression of *SERPINE1*, *TIMP3*, and *LTBP1* genes in the presence of TGF-β1. U2OS cells were transfected with empty (EV), wild-type NAG-1 (WT), or ΔNES NAG-1-expression vectors. Cells were treated with TGF-β1 (2 ng/mL) for 12 h, and gene expression was analyzed by qRT-PCR as described in the Materials and Methods section. The graph shows mean values of fold changes over TGF-β1 treatment. **B**, Wild-type NAG-1 and mutNES-NAG-1 expression decreased Smad binding element (SBE)-containing promoter activity. MCF-10A and U2OS cells were transfected with SBE4 reporter and indicated expression vectors. Cells were treated with TGF-β1 (10 ng/mL) for 24 h and luciferase activity measured. The graph shows mean values ± SD from three replicates. ***$P < 0.001$, compared to TGF-β1-treated empty vector-transfected cells. **C**, U2OS cells were transfected with either empty or wild-type NAG-1 expression vector. After treatment with TGF-β1 (2 ng/mL) for 1 h, the media were replaced with fresh media, and cell lysates were isolated at the indicated time points. Whole cell lysates (30 μg) were subjected to Western blot analysis using p21, phosphor-Smad2, and Smad2 antibodies. **D**, *Tet*-inducible U2OS cells were stimulated with TGF-β1 (2 ng/mL) for the indicated time points, and then cell lysates were subjected to nuclear and cytoplasmic fractionation followed by Western blot with the indicated antibodies. Lamin A/C and tubulin α were used as nucleus and cytoplasm markers, respectively. **E**, DNA pull-down and Western blot with anti-Smad2/3 and anti-Smad4 antibodies. Cell lysates from either U2OS or U2OS-tet cells were incubated with SBE oligo DNA as described in the Materials and Methods section. SBE-bound proteins were reduced in U2OS-tet compared to U2OS (left panel), and similar results were obtained using ectopic NAG-1 expression vectors into U2OS cells (right panel). **F**, *In vivo* binding of Smad2/3 to the TIMP3 or Smad7 promoter in U2OS cells stimulated with TGF-β1 (2 ng/mL) using the ChIP assay. Inducible U2OS cells were stimulated by tetracycline for 24 h (left panel), and wild-type U2OS cells were transfected with either empty vector or NAG-1 expressing vector (right panel). The ChIP assay for endogenous smad2/3 indicates enhanced recruitment of Smad2/3 to the TIMP3 or Smad7 promoter region after simulation with TGF-β1 for 3 h and decreased occupancy on these promoter regions by NAG-1 expression
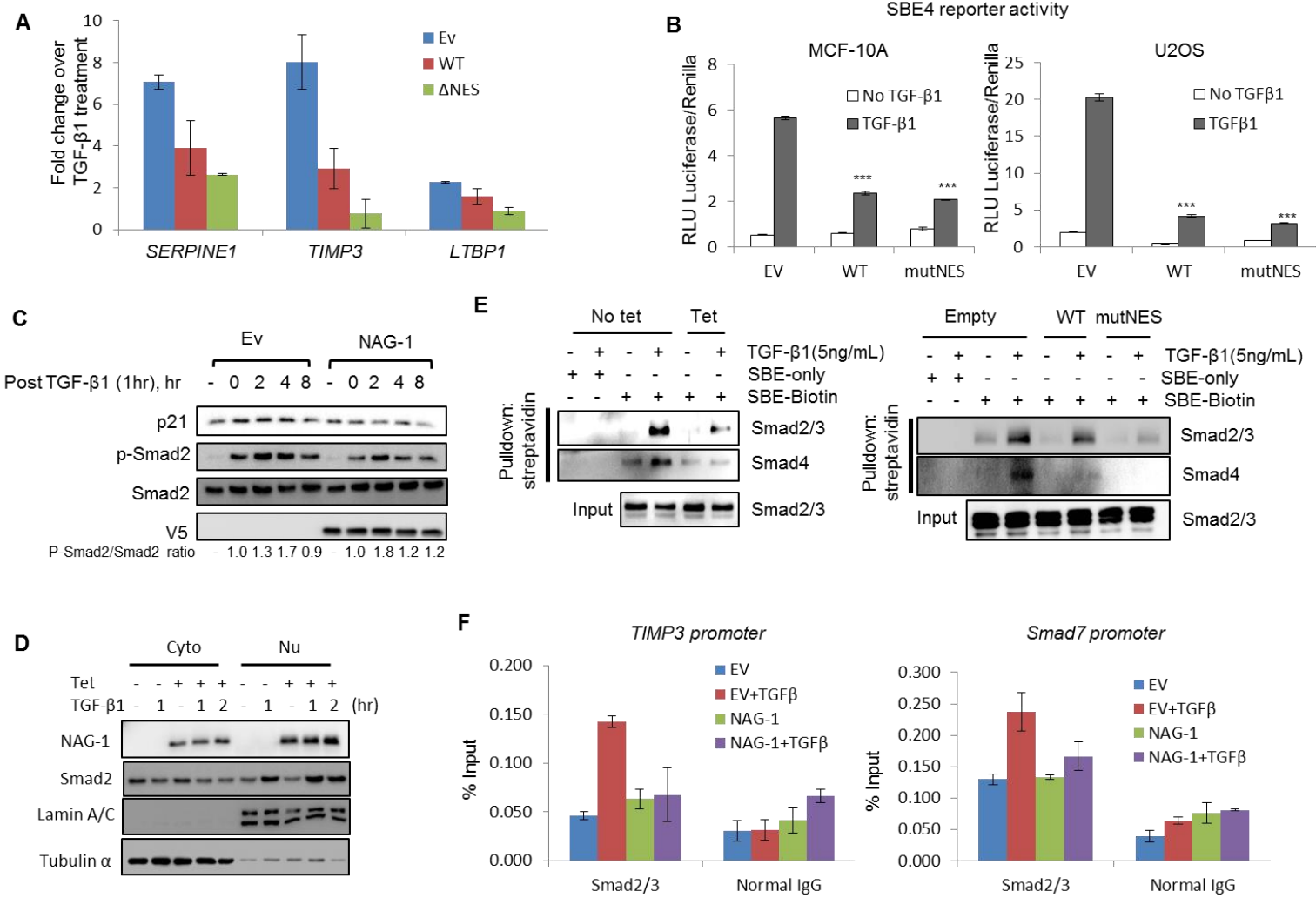
Figure 3.5 Continued.

medium added. The cells were finally harvested in a time course for Western blot analysis. Pro-NAG-1 modulated p21 expression (a TGF-β target gene) in response to TGF-β1 without affecting phosphor-Smad2 signal duration (Fig. 3.5C), suggesting that upon TGF-β1 stimulation, NAG-1 inhibits TGF-β1 signaling without inhibiting phosphorylation of Smad2. To examine if pro-NAG-1 affects the translocation of Smad2 to the nucleus and Smad2 degradation, the distribution of Smad2 was investigated. As shown in Figure 5d, Smad2 distribution was the same in both cytosol (lanes 1, 2 vs 3, 4) and the nucleus (lanes 6, 7 vs 8, 9), regardless of whether NAG-1 was present. Furthermore, this result was confirmed using A549 cells that were transfected with either LacZ or ΔNES NAG-1, and the distribution of Smad2 between cytosol and nucleus was examined (Supplementary Fig. S3.6C). Thus, pro-NAG-1 did not affect Smad2 translocation into the nucleus upon TGF-β1 stimulation or Smad2 degradation. We next explored whether the DNA-binding activity of Smad was diminished by NAG-1 expression. The DNA pull-down assay indicated that SBE binding activity of the Smad complex was diminished when NAG-1 was expressed, implying that NAG-1 may interrupt Smad DNA-binding activity in the nuclear region (Fig. 3.5E, Supplementary Fig. S3.6D). Furthermore, a ChIP assay showed that NAG-1 inhibits binding of Smad to the promoter region of TGF-β target genes (Fig. 3.5F). Taken together, these results suggest that nuclear pro-NAG-1 attenuates TGF-β-mediated Smad signaling through interruption of DNA binding activity of the Smad complex upon TGF-β1 stimulation.

3.4.6 NAG-1 Attenuates TGF-β-induced cell migration

TGF-β1 is a cytokine that increases cell migration and invasion[202]. We next examined if NAG-1 expression altered TGF-β1-induced cell migration. As shown in Fig. 3.6A, NAG-1 expression diminished cell migration into the scratched region in response to TGF-β1. In addition, a trans-well migration assay showed less migration in the NAG-1- or mutNES-NAG-1-expressing cells in comparison to the empty vector-transfected cells (Fig. 3.6B). We employed a 3D culture system to study invasion. Spheroids composed of empty vector-transfected cells exhibited spindle-like protrusions after TGF-β1 treatment; however, spheroids composed of WT-expressing or mutNES-expressing cells did not (Fig. 3.6C). NAG-1 also suppressed expression of snail1 and slug, which are markers for epithelial–mesenchymal transition (EMT) induced by TGF-β1 (Supplementary Fig. S3.7). Overall, NAG-1 expression appeared to suppress EMT and cell invasion activity of TGF-β1 by inhibiting Smad DNA-binding activity.

Figure 3.6 NAG-1 blocks TGF-β1-induced cell migration/invasion.
A, Cell migration assay. *Tet*-inducible U2OS cells were scratched with a pipet tip, and images were taken at 0 and 24 h by phase-contrast microscopy as the cells repopulated the wound. To measure the rate of healing, the area between the wound edges was measured and compared relative to the area of the original wound at t = 0. Dotted lines represent the original wound area. The graph (right panel) shows mean values with ± SD from three replicates (*$P < 0.05$). **B**, Transwell migration assay. Transwell chambers were used to verify migration potential. U2OS cells transfected with the indicated vector were incubated with 10 ng/mL TGF-β1 for 18 h. Cells attached in the lower section were stained with crystal violet and counted under a light microscope. The graph shows mean ± SD of three independent experiments (*$P < 0.05$ and **$P < 0.01$). **C**, U2OS cells transfected with either empty, wild-type NAG-1, or mutNES NAG-1 were prepared and subjected to an *in vitro* 3-D spheroid cell invasion assay as described in the Materials and Methods section. The green arrow indicates cells invading the surrounding invasion matrix
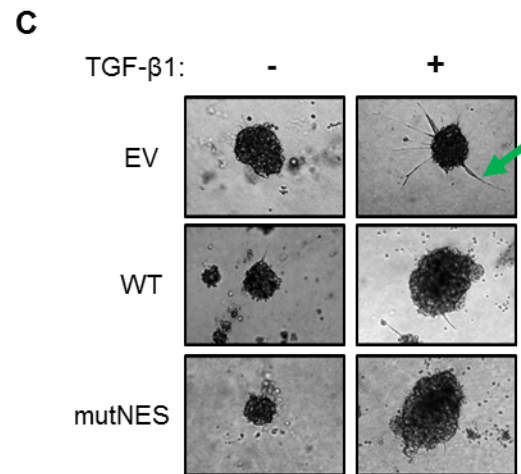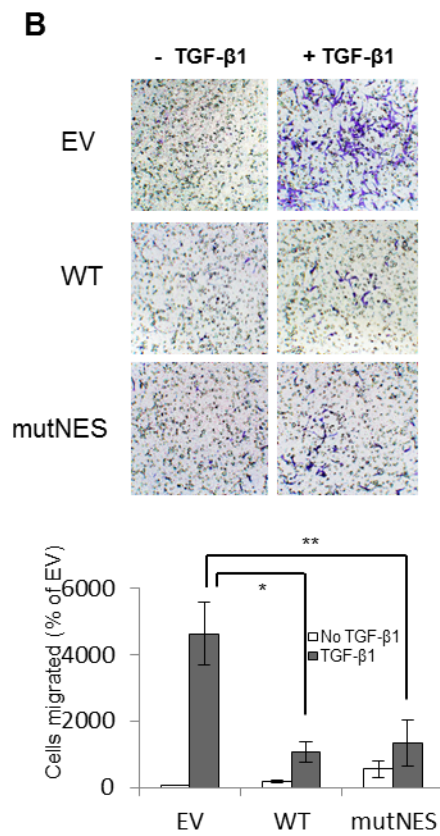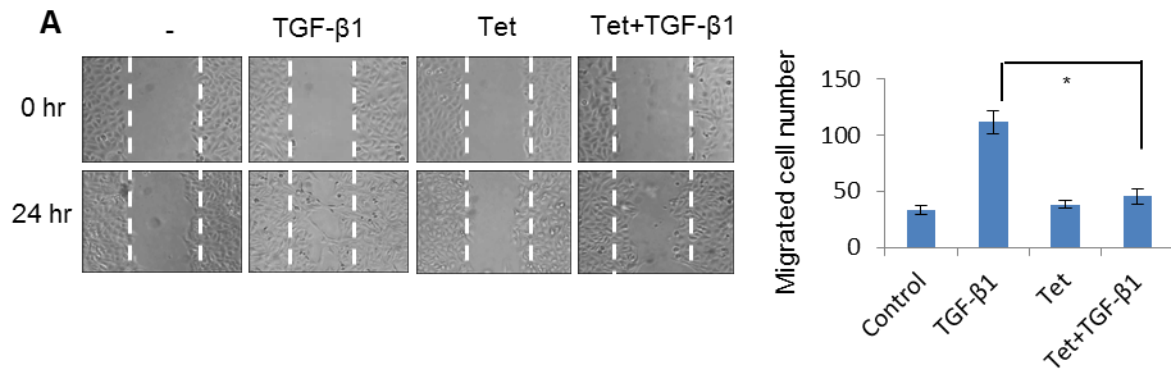
Figure 3.6 Continued.

3.5 Discussion

Multiple cellular localizations of protein give rise to multiple functions or integrate signals from different locations to fulfill one biological outcome [41, 75, 190, 203]. NAG-1 is a secreted TGF-β superfamily member, and plays a role as a cytokine to affect several biological activities through an unknown receptor. While working on cellular NAG-1 movement, we discovered that NAG-1 is significantly expressed in the nucleus and affects transcriptional regulation of the Smad complex. NAG-1 expression is altered by a variety of signals, such as those from cytokines (IL-1β, TNF-α, macrophage colony-stimulating factor) [172], radiation [171], tissue injury [204], anoxia [205], and many chemopreventive/chemotherapeutic chemicals [206], suggesting NAG-1 signaling may be important for maintaining cellular homeostasis. In addition, NAG-1 is a target gene of several transcription factors, such as p53 [171, 207], NF-κB [208], Sp1 [141], and Egr-1 [120]. However, downstream signaling pathways affected by NAG-1 remain to be discovered.

Although *in vitro* assays show different results, the results from NAG-1 over-expression in NAG-Tg mice and NAG-1 depletion in NAG-1 knockout mice consistently support the notion for anti-tumorigenic activity [167, 168, 209]. Some possible explanations for the contradictory activity of NAG-1 *in vitro* include: 1) NAG-1's different functions in the different cancer types, 2) an unidentified role of pro-NAG-1 in cells, and 3) the contribution of NAG-1 binding proteins or receptors in different cells. In fact, there are many examples of other proteins having dual biological functions in different cancer types and microenvironments. For example, EGR-1 has been shown to be associated

with pro-tumorigenic activity in prostate cancer [210], whereas EGR-1 acts like a tumor suppressor protein in other cancers [211]. 15-lipooxygenase-1 (LOX-1) is another example; LOX-1 acts as a tumor suppressor in colorectal cancer and a pro-tumorigenic protein in prostate cancer [212, 213]. Thus, the fact that NAG-1 shows dual functions in carcinogenesis is not surprising. Lack of knowledge of NAG-1's receptor and/or binding proteins is a large hurdle to studying its signaling pathway; however, a couple of reports have suggested that NAG-1 may be involved in TGF-β receptor-mediated signaling [171, 214]. Based on our data, we were surprised to find that NAG-1 expressed in the nucleus, and that nuclear NAG-1 inhibited the TGF-β1-induced Smad complex, thereby inhibiting expression of Smad target genes. This observation consistently occurred in different cell lines. Therefore, our data suggest that inhibition of the Smad pathway by nuclear NAG-1 expression may provide a new avenue to support NAG-1's role in anti-tumorigenesis.

Our results suggest that NAG-1 could translocate into the nucleus through an active transport system (Fig. 3.2D); however, we have yet to define the precise mechanisms involved in its nuclear importation. It is likely that multiple pathways or a novel pathway may affect NAG-1 movement to the nucleus since two potential mutations partially affected NAG-1 importation, and no canonical NLS signals were found in the NAG-1 full-length peptide sequences (Fig. 3.2A and B). The TGF-β superfamily member BMP2 has been observed in a truncated form in the nucleus [215]; however, the current study is the first report that a full-length TGF-β superfamily protein expresses in the nucleus and plays a role in transcription. Nuclear importation of NAG-1

requires energy and carrier proteins. GFP by itself was not able to enter nuclei (Fig. 3.2D); however, NAG-1/GFP was imported into the nucleus as examined by an *in vitro* import assay. Depleting the energy generation system and NPC inhibitor WGA treatment in the permeabilized cells reduced nuclear uptake of NAG-1, suggesting that NAG-1 nuclear entry occurs through the NPC in an energy-dependent manner. Given that NAG-1 lacks a classical NLS region and requires the NPC for translocation, nuclear localization of NAG-1 likely requires interaction with a partner that contains the NLS domain [216]. Indeed, nuclear importation of protein can be mediated by multiple transport receptors [196, 197], or a protein can directly interact with a component of nuclear pore proteins containing armadillo repeats [217]. Thus, it is likely that a portion of NAG-1 is exposed to the cytoplasm while another portion of NAG-1 is embedded in ER/Golgi for being recognized by a transporter, as seen in EGFR nuclear importation [218]. Although we have not ruled out these possibilities, our data indicate that two sites (190-197 and 211-218) play a role, at least in part, in importing NAG-1 to the nucleus. Further experiments are necessary to define the molecular mechanism of nuclear transport and specifically, the exact component of import machinery for NAG-1.

In comparison to the importation mechanism of NAG-1, we were able to investigate in greater detail NAG-1 exportation to the cytoplasm. NAG-1 export was mediated by a LMB-sensitive, CRM1-dependent pathway, which requires a functional domain to be recognized by CRM1. Sequence analysis showed that the canonical, leucine-rich NES was present within the N-terminal region of NAG-1. If this site were deleted or mutated, then NAG-1 was retained in the nucleus of the cells. We also

observed that NAG-1 physically bound to CRM1; however, we cannot exclude the possibility that other nuclear proteins that supply NES may help NAG-1 exportation. Interestingly, we could not find secreted mature NAG-1 in the culture media when NAG-1 was retained in the nucleus. It is likely that one of the secretion pathways of NAG-1 must pass through the nucleus prior to processing to the mature form. Vesicles are required for NAG-1 secretion, and the vesicle containing NAG-1 may form at the nuclear membrane; therefore, an NES sequence may play a pivotal role in vesicle formation. Indeed, our results show that NAG-1 is localized in the ER/Golgi region in the cytoplasm, not as a soluble cytosolic fraction (Fig. 3.1D) and that this localization is dependent upon sequences in the N-terminal domain, a region that contains an NES sequence (Fig. 3.3C). Notably, there is a possibility that anti-tumorigenic activity of NAG-1 may occur with nuclear NAG-1, whereas secreted mature NAG-1 protein may possess pro-tumorigenic activity. This is supported by previous reports indicating that recombinant NAG-1 increases kinase pathways in some cancer cells [219]. Although further mechanistic studies are required to define the exact biological activity of nuclear NAG-1 and secreted mature NAG-1, our data clearly show that nuclear NAG-1 causes inhibition of cell migration and invasion, as assessed by experiments with mutants.

The biological role of NAG-1 nuclear-cytoplasmic shuttling remains to be established. In this study, we found that nuclear NAG-1 could control the strength of TGF-β1-mediated Smad signaling. It remains to be clarified how nuclear NAG-1 modulates the DNA binding capacity of the Smad complex, even though it has been known that various factors and cellular context attenuate Smad-mediated transcription.

One possible way is that NAG-1 might bind directly to DNA (SBE) to compete with Smad, although no DNA binding motif has been identified in the NAG-1 sequence. To test this hypothesis, we employed ChIP-seq to see if any DNA fragments were pulled down with NAG-1. It is not likely that NAG-1 directly binds to conserved SBE, since we have not identified any genes related to the SBE-containing promoter. Another possibility is that NAG-1 may bind to phosphor-Smad2, thereby inhibiting Smad binding activity. However, we could not find any direct physical interaction between Samd2/3/4 and NAG-1 (Supplementary Fig. S3.8). Our data rather imply that NAG-1 somehow interrupts the Smad complex in the nucleus by unknown mechanism(s). Smad proteins may need an additional transcription factor or co-factor to strongly occupy their target DNA [43, 220]. Thus, NAG-1 might disrupt the formation of the Smad complex upon TGF-β1 stimulation, or NAG-1 might somehow facilitate ADP-ribosylation, which dissociates the Smad complex from DNA, leading to attenuation of a Smad-specific gene response [221].

Our data show that all the cells tested tended to express NAG-1 in varying amounts in both the cytoplasm and nucleus (Fig. 3.3A). This provides a model that could demonstrate strategies for therapeutic intervention in disease states in which "inappropriate" localization of protein is believed to contribute to disease development [222, 223]. It remains to be elucidated whether more transformed tumor cells activate mechanisms that allow increased nuclear import or decreased nuclear export of NAG-1. We are currently developing an antibody that recognizes the N-terminal region of NAG-1 to examine NAG-1 expression in the nucleus of human tissue samples and to

determine whether more nuclear staining of NAG-1 is associated with a better prognosis in cancer patients.

3.6 Summary Conclusion

In summary, our data indicate that the pro-NAG-1 was expressed in the nucleus and appears to play a role in transcriptional regulation by disturbing the Smad complex. In addition, nuclear retention resulted in an absence of secreted mature NAG-1. The schematic diagram in Fig. 3.7 represents the proposed model of the molecular mechanism of nuclear-cytoplasmic NAG-1 shuttling through active transport and nuclear NAG-1 attenuating TGF-β signaling through interruption of DNA binding of the Smad complex upon TGF-β stimulation. In addition, the novel role of NAG-1 in the nucleus may help lead to the development of new drugs that facilitate the retention of NAG-1 in the nucleus or to the development of novel diagnostic tools for assessing cancer progression.
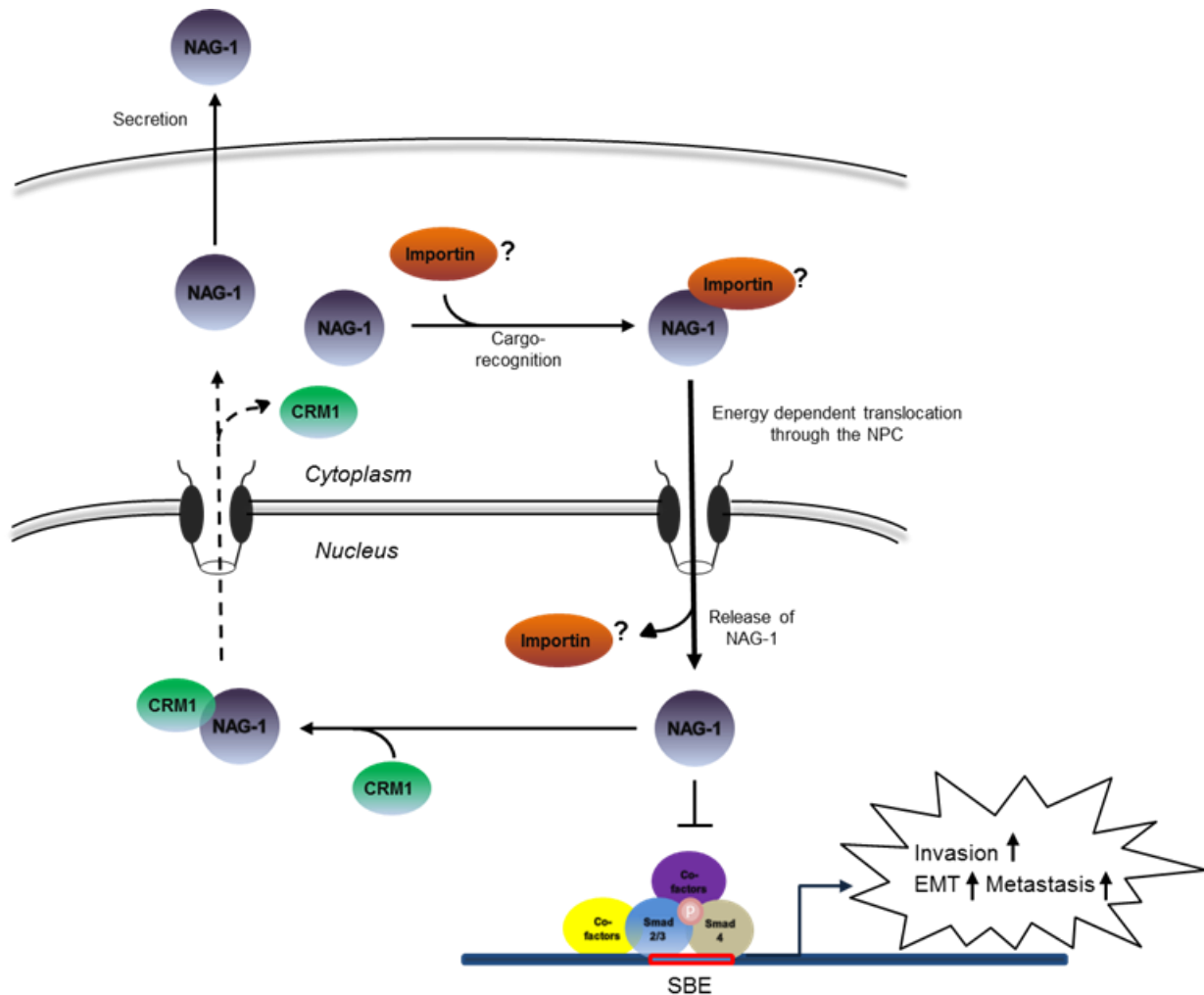
Figure 3.7 A proposed model for nuclear-cytoplasmic shutting and the function of NAG-1 in the nucleus.

Cytoplasmic NAG-1 is recognized by import machinery and enters the nucleus via the NPC in an energy-dependent manner. In the nucleus, NAG-1 interrupts the DNA binding capacity of the Smad complex giving rise to attenuation of Smad signaling. Nuclear NAG-1 interacts with CRM1 for export out of the nucleus. NAG-1 is secreted by an unknown secretory pathway and likely binds to an unidentified receptor.

CONCLUSION

The studies presented in this dissertation contribute to the better understanding of regulatory mechanism that control NAG-1 expression in response to PPARγ-ligand and identify nuclear NAG-1 that may decipher the molecular basis of NAG-1's dual effects in cancer. Our findings will pave the way for the new avenue in future studies which attempt to understand how NAG-1 coordinates with the intracellular signaling component(s) such as KLF4 and PPARγ to modulate a proper cellular response at a given cellular context and how nuclear NAG-1 participates in regulating gene expression which is either negative or positive in tumor cell growth and survival based on cellular context. This work will shed light on the relationship between nuclear NAG-1 and tumorigenesis that could suggest NAG-1 may be served as a potential biomarker/or a therapeutic target for the diagnosis and treatment during cancer progression

REFERENCES

[1] M.R. Bootcov, A.R. Bauskin, S.M. Valenzuela, A.G. Moore, M. Bansal, X.Y. He, H.P. Zhang, M. Donnellan, S. Mahler, K. Pryor, B.J. Walsh, R.C. Nicholson, W.D. Fairlie, S.B. Por, J.M. Robbins, S.N. Breit, MIC-1, a novel macrophage inhibitory cytokine, is a divergent member of the TGF-β superfamily, Proceedings of the National Academy of Sciences, 94 (1997) 11514-11519.

[2] P.-X. Li, J. Wong, A. Ayed, D. Ngo, A.M. Brade, C. Arrowsmith, R.C. Austin, H.J. Klamut, Placental Transforming Growth Factor-β Is a Downstream Mediator of the Growth Arrest and Apoptotic Response of Tumor Cells to DNA Damage and p53 Overexpression, Journal of Biological Chemistry, 275 (2000) 20127-20135.

[3] V.M. Paralkar, A.L. Vail, W.A. Grasser, T.A. Brown, H. Xu, S. Vukicevic, H.Z. Ke, H. Qi, T.A. Owen, D.D. Thompson, Cloning and Characterization of a Novel Member of the Transforming Growth Factor-β/Bone Morphogenetic Protein Family, Journal of Biological Chemistry, 273 (1998) 13760-13767.

[4] M. Böttner, M. Laaff, B. Schechinger, G. Rappold, K. Unsicker, C. Suter-Crazzolara, Characterization of the rat, mouse, and human genes of growth/differentiation factor-15/macrophage inhibiting cytokine-1 (GDF-15/MIC-1), Gene, 237 (1999) 105-111.

[5] R. Hromas, M. Hufford, J. Sutton, D. Xu, Y. Li, L. Lu, PLAB, a novel placental bone morphogenetic protein, Biochimica et Biophysica Acta (BBA) - Gene Structure and Expression, 1354 (1997) 40-44.

[6] J. Massagué, TGF² in Cancer, Cell, 134 (2008) 215-230.

[7] N. Planque, Nuclear trafficking of secreted factors and cell-surface receptors: new pathways to regulate cell proliferation and differentiation, and involvement in cancers, Cell Communication and Signaling, 4 (2006) 7.

[8] S.J. Baek, L.C. Wilson, T.E. Eling, Resveratrol enhances the expression of non-steroidal anti-inflammatory drug-activated gene (NAG-1) by increasing the expression of p53, Carcinogenesis, 23 (2002) 425-432.

[9] A. Krones-Herzig, S. Mittal, K. Yule, H. Liang, C. English, R. Urcis, T. Soni, E.D. Adamson, D. Mercola, Early Growth Response 1 Acts as a Tumor Suppressor In vivo and In vitro via Regulation of p53, Cancer Research, 65 (2005) 5133-5143.

[10] V. Baron, G. De Gregorio, A. Krones-Herzig, T. Virolle, A. Calogero, R. Urcis, D. Mercola, Inhibition of Egr-1 expression reverses transformation of prostate cancer cells in vitro and in vivo, Oncogene, 22 (0000) 4194-4204.

[11] S.J. Baek, J.-S. Kim, J.B. Nixon, R.P. DiAugustine, T.E. Eling, Expression of NAG-1, a Transforming Growth Factor-β Superfamily Member, by Troglitazone Requires the Early Growth Response Gene EGR-1, Journal of Biological Chemistry, 279 (2004) 6883-6892.

[12] T. Hai, M.G. Hartman, The molecular biology and nomenclature of the activating transcription factor/cAMP responsive element binding family of transcription factors: activating transcription factor proteins and homeostasis, Gene, 273 (2001) 1-11.

[13] S.-H. Lee, C. Krisanapun, S.J. Baek, NSAID-activated gene-1 as a molecular target for capsaicin-induced apoptosis through a novel molecular mechanism involving GSK3β, C/EBPβ and ATF3, Carcinogenesis, 31 (2010) 719-728.

[14] J.A. Segre, C. Bauer, E. Fuchs, Klf4 is a transcription factor required for establishing the barrier function of the skin, Nat Genet, 22 (1999) 356-360.

[15] L.A. Garrett-Sinha, H. Eberspaecher, M.F. Seldin, B. de Crombrugghe, A Gene for a Novel Zinc-finger Protein Expressed in Differentiated Epithelial Cells and Transiently in Certain Mesenchymal Cells, Journal of Biological Chemistry, 271 (1996) 31384-31390.

[16] X. Chen, D.C. Johns, D.E. Geiman, E. Marban, D.T. Dang, G. Hamlin, R. Sun, V.W. Yang, Krüppel-like Factor 4 (Gut-enriched Krüppel-like Factor) Inhibits Cell Proliferation by Blocking G1/S Progression of the Cell Cycle, Journal of Biological Chemistry, 276 (2001) 30423-30428.

[17] D. Wei, M. Kanai, S. Huang, K. Xie, Emerging role of KLF4 in human gastrointestinal cancer, Carcinogenesis, 27 (2005) 23-31.

[18] D. Wei, W. Gong, M. Kanai, C. Schlunk, L. Wang, J.C. Yao, T.-T. Wu, S. Huang, K. Xie, Drastic Down-regulation of Krüppel-Like Factor 4 Expression Is Critical in Human Gastric Cancer Development and Progression, Cancer Research, 65 (2005) 2746-2754.

[19] J.P. Katz, N. Perreault, B.G. Goldstein, L. Actman, S.R. McNally, D.G. Silberg, E.E. Furth, K.H. Kaestner, Loss of Klf4 in mice causes altered proliferation and differentiation and precancerous changes in the adult stomach, Gastroenterology, 128 (2005) 935-945.

[20] M. Cekanova, S.H. Lee, M.F. McEntee, S.J. Baek, MCC-555-induced NAG-1 expression is mediated in part by KLF4, European journal of pharmacology, 637 (2010) 30-37.

[21] D.A. Brown, R.L. Ward, P. Buckhaults, T. Liu, K.E. Romans, N.J. Hawkins, A.R. Bauskin, K.W. Kinzler, B. Vogelstein, S.N. Breit, MIC-1 Serum Level and Genotype: Associations with Progress and Prognosis of Colorectal Carcinoma, Clinical Cancer Research, 9 (2003) 2642-2650.

[22] Y. Zhong, C. Krisanapun, S.-H. Lee, T. Nualsanit, C. Sams, P. Peungvicha, S.J. Baek, Molecular targets of apigenin in colorectal cancer cells: Involvement of p21, NAG-1 and p53, European Journal of Cancer, 46 (2010) 3365-3374.

[23] S.J. Baek, R. Okazaki, S.-H. Lee, J. Martinez, J.-S. Kim, K. Yamaguchi, Y. Mishina, D.W. Martin, A. Shoieb, M.F. McEntee, T.E. Eling, Nonsteroidal Anti-Inflammatory Drug-Activated Gene-1 Over Expression in Transgenic Mice Suppresses Intestinal Neoplasia, Gastroenterology, 131 (2006) 1553-1560.

[24] T. Liu, A.R. Bauskin, J. Zaunders, D.A. Brown, S. Pankurst, P.J. Russell, S.N. Breit, Macrophage Inhibitory Cytokine 1 Reduces Cell Adhesion and Induces Apoptosis in Prostate Cancer Cells, Cancer Research, 63 (2003) 5034-5040.

[25] J.R. Lambert, J.A. Kelly, M. Shim, W.E. Huffer, S.K. Nordeen, S.J. Baek, T.E. Eling, M.S. Lucia, Prostate derived factor in human prostate cancer cells: Gene induction by vitamin D via a p53-dependent mechanism and inhibition of prostate cancer cell growth, Journal of Cellular Physiology, 208 (2006) 566-574.

[26] S. Senapati, S. Rachagani, K. Chaudhary, S.L. Johansson, R.K. Singh, S.K. Batra, Overexpression of macrophage inhibitory cytokine-1 induces metastasis of human prostate cancer cells through the FAK-RhoA signaling pathway, Oncogene, 29 (2010) 1293-1302.

[27] S.-J. Chen, D. Karan, S.L. Johansson, F.-F. Lin, J. Zeckser, A.P. Singh, S.K. Batra, M.-F. Lin, Prostate-derived factor as a paracrine and autocrine factor for the proliferation of androgen receptor-positive human prostate cancer cells, The Prostate, 67 (2007) 557-571.

[28] A.R. Bauskin, D.A. Brown, T. Kuffner, H. Johnen, X.W. Luo, M. Hunter, S.N. Breit, Role of Macrophage Inhibitory Cytokine-1 in Tumorigenesis and Diagnosis of Cancer, Cancer Research, 66 (2006) 4983-4986.

[29] J.B. Welsh, L.M. Sapinoso, S.G. Kern, D.A. Brown, T. Liu, A.R. Bauskin, R.L. Ward, N.J. Hawkins, D.I. Quinn, P.J. Russell, R.L. Sutherland, S.N. Breit, C.A. Moskaluk, H.F. Frierson, G.M. Hampton, Large-scale delineation of secreted protein biomarkers overexpressed in cancer tissue and serum, Proceedings of the National Academy of Sciences, 100 (2003) 3410-3415.

[30] M. Parras-Molto, F. Campos-Laborie, J. Garcia-Dieguez, M. Rodriguez-Grinolo, A. Perez-Pulido, Classification of protein motifs based on subcellular localization uncovers evolutionary relationships at both sequence and functional levels, BMC Bioinformatics, 14 (2013) 229.

[31] C.J. Jeffery, Moonlighting proteins, Trends in Biochemical Sciences, 24 (1999) 8-11.

[32] C.J. Jeffery, Moonlighting proteins: old proteins learning new tricks, Trends in Genetics, 19 (2003) 415-417.

[33] C.J. Jeffery, Moonlighting proteins-an update, Molecular BioSystems, 5 (2009) 345-350.

[34] D.H.E.W. Huberts, I.J. van der Klei, Moonlighting proteins: An intriguing mode of multitasking, Biochimica et Biophysica Acta (BBA) - Molecular Cell Research, 1803 (2010) 520-525.

[35] J.-P. Kruse, W. Gu, Modes of p53 Regulation, Cell, 137 609-622.

[36] T. Riley, E. Sontag, P. Chen, A. Levine, Transcriptional control of human p53-regulated genes, Nature Rev. Mol. Cell Biol., 9 (2008) 402-412.

[37] J.E. Chipuk, L. Bouchier-Hayes, T. Kuwana, D.D. Newmeyer, D.R. Green, PUMA couples the nuclear and cytoplasmic proapoptotic function of p53, Science, 309 (2005) 1732-1735.

[38] H. You, K. Yamamoto, T.W. Mak, Regulation of transactivation-independent proapoptotic activity of p53 by FOXO3a, Proc. Natl Acad. Sci. USA, 103 (2006) 9051-9056.

[39] N.D. Marchenko, S. Wolff, S. Erster, K. Becker, U.M. Moll, Monoubiquitylation promotes mitochondrial p53 translocation, EMBO J., 26 (2007) 923-934.

[40] J.E. Chipuk, Direct activation of Bax by p53 mediates mitochondrial membrane permeabilization and apoptosis, Science, 303 (2004) 1010-1014.

[41] D.R. Green, G. Kroemer, Cytoplasmic functions of the tumour suppressor p53, Nature, 458 (2009) 1127-1130.

[42] R.S. Foo, Regulation of p53 tetramerization and nuclear export by ARC, Proc. Natl Acad. Sci. USA, 104 (2007) 20826-20831.

[43] J. Massagué, J. Seoane, D. Wotton, Smad transcription factors, Genes & Development, 19 (2005) 2783-2810.

[44] R.J. Akhurst, A. Hata, Targeting the TGF[beta] signalling pathway in disease, Nat Rev Drug Discov, 11 (2012) 790-811.

[45] C.S. Hill, Nucleocytoplasmic shuttling of Smad proteins, Cell Res, 19 (2009) 36-46.

[46] Alan C. Mullen, David A. Orlando, Jamie J. Newman, J. Lovén, Roshan M. Kumar, S. Bilodeau, J. Reddy, Matthew G. Guenther, R.P. DeKoter, Richard A. Young, Master Transcription Factors Determine Cell-Type-Specific Responses to TGF-β Signaling, Cell, 147 (2011) 565-576.

[47] D.R. Warner, M.M. Pisano, E.A. Roberts, R.M. Greene, Identification of three novel Smad binding proteins involved in cell polarity, FEBS Letters, 539 167-173.

[48] L.R. Ellis, D.R. Warner, R.M. Greene, M.M. Pisano, Interaction of Smads with collagen types I, III, and V, Biochemical and Biophysical Research Communications, 310 (2003) 1117-1123.

[49] R. Quéré, G. Karlsson, F. Hertwig, M. Rissler, B. Lindqvist, T. Fioretos, P. Vandenberghe, M.L. Slovak, J. Cammenga, S. Karlsson, Smad4 binds Hoxa9 in the cytoplasm and protects primitive hematopoietic cells against nuclear activation by Hoxa9 and leukemia transformation, 2011.

[50] A. Zwijsen, K. Verschueren, D. Huylebroeck, New intracellular components of bone morphogenetic protein/Smad signaling cascades, FEBS Letters, 546 (2003) 133-139.

[51] J.S. Isaacs, W. Xu, L. Neckers, Heat shock protein 90 as a molecular target for cancer therapeutics, Cancer Cell, 3 (2003) 213-217.

[52] L. Whitesell, S.L. Lindquist, HSP90 and the chaperoning of cancer, Nat Rev Cancer, 5 (2005) 761-772.

[53] X. Wang, X. Song, W. Zhuo, Y. Fu, H. Shi, Y. Liang, M. Tong, G. Chang, Y. Luo, The regulatory mechanism of Hsp90α secretion and its function in tumor malignancy, Proceedings of the National Academy of Sciences, 106 (2009) 21288-21293.

[54] X. Song, X. Wang, W. Zhuo, H. Shi, D. Feng, Y. Sun, Y. Liang, Y. Fu, D. Zhou, Y. Luo, The Regulatory Mechanism of Extracellular Hsp90α on Matrix Metalloproteinase-2 Processing and Tumor Angiogenesis, Journal of Biological Chemistry, 285 (2010) 40039-40049.

[55] B.K. Eustace, T. Sakurai, J.K. Stewart, D. Yimlamai, C. Unger, C. Zehetmeier, B. Lain, C. Torella, S.W. Henning, G. Beste, B.T. Scroggins, L. Neckers, L.L. Ilag, D.G. Jay, Functional proteomic screens reveal an essential extracellular role for hsp90[alpha] in cancer cell invasiveness, Nat Cell Biol, 6 (2004) 507-514.

[56] M.W. Hance, K. Dole, U. Gopal, J.E. Bohonowych, A. Jezierska-Drutel, C.A. Neumann, H. Liu, I.P. Garraway, J.S. Isaacs, Secreted Hsp90 Is a Novel Regulator of the Epithelial to Mesenchymal Transition (EMT) in Prostate Cancer, Journal of Biological Chemistry, 287 (2012) 37732-37744.

[57] P. Csermely, T. Schnaider, C. So˝ti, Z. Prohászka, G. Nardai, The 90-kDa Molecular Chaperone Family: Structure, Function, and Clinical Applications. A Comprehensive Review, Pharmacology & Therapeutics, 79 (1998) 129-168.

[58] J. Trepel, M. Mollapour, G. Giaccone, L. Neckers, Targeting the dynamic HSP90 complex in cancer, Nat Rev Cancer, 10 (2010) 537-549.

[59] L. Lorand, R.M. Graham, Transglutaminases: crosslinking enzymes with pleiotropic functions, Nat Rev Mol Cell Biol, 4 (2003) 140-156.

[60] D. Park, S. Choi, K.-S. Ha, Transglutaminase 2: a multi-functional protein in multiple subcellular compartments, Amino Acids, 39 (2010) 619-631.

[61] L. Cao, D.N. Petrusca, M. Satpathy, H. Nakshatri, I. Petrache, D. Matei, Tissue transglutaminase protects epithelial ovarian cancer cells from cisplatin-induced apoptosis by promoting cell survival signaling, Carcinogenesis, 29 (2008) 1893-1900.

[62] S.E. Iismaa, M.-J. Wu, N. Nanda, W.B. Church, R.M. Graham, GTP Binding and Signaling by Gh/Transglutaminase II Involves Distinct Residues in a Unique GTP-binding Pocket, Journal of Biological Chemistry, 275 (2000) 18259-18265.

[63] S. Mishra, L.J. Murphy, Tissue Transglutaminase Has Intrinsic Kinase Activity: IDENTIFICATION OF TRANSGLUTAMINASE 2 AS AN INSULIN-LIKE GROWTH FACTOR-BINDING PROTEIN-3 KINASE, Journal of Biological Chemistry, 279 (2004) 23863-23868.

[64] A.P. Mann, A. Verma, G. Sethi, B. Manavathi, H. Wang, J.Y. Fok, A.B. Kunnumakkara, R. Kumar, B.B. Aggarwal, K. Mehta, Overexpression of Tissue Transglutaminase Leads to Constitutive Activation of Nuclear Factor-κB in Cancer Cells: Delineation of a Novel Pathway, Cancer Research, 66 (2006) 8788-8795.

[65] X. Peng, Y. Zhang, H. Zhang, S. Graner, J.F. Williams, M.L. Levitt, A. Lokshin, Interaction of tissue transglutaminase with nuclear transport protein importin-α3, FEBS Letters, 446 (1999) 35-39.

[66] M. Lesort, K. Attanavanich, J. Zhang, G.V.W. Johnson, Distinct Nuclear Localization and Activity of Tissue Transglutaminase, Journal of Biological Chemistry, 273 (1998) 11991-11994.

[67] S. Oliverio, A. Amendola, F. Di Sano, M.G. Farrace, L. Fesus, Z. Nemes, L. Piredda, A. Spinedi, M. Piacentini, Tissue transglutaminase-dependent posttranslational modification of the retinoblastoma gene product in promonocytic cells undergoing apoptosis, Molecular and Cellular Biology, 17 (1997) 6040-6048.

[68] A.J. Filiano, C.D.C. Bailey, J. Tucholski, S. Gundemir, G.V.W. Johnson, Transglutaminase 2 protects against ischemic insult, interacts with HIF1β, and attenuates HIF1 signaling, The FASEB Journal, 22 (2008) 2662-2675.

[69] H. Tatsukawa, Y. Fukaya, G. Frampton, A. Martinez–Fuentes, K. Suzuki, T.F. Kuo, K. Nagatsuma, K. Shimokado, M. Okuno, J. Wu, S. Iismaa, T. Matsuura, H. Tsukamoto, M.A. Zern, R.M. Graham, S. Kojima, Role of Transglutaminase 2 in Liver Injury via Cross-linking and Silencing of Transcription Factor Sp1, Gastroenterology, 136 (2009) 1783-1795.e1710.

[70] S. Mishra, A. Saleh, P.S. Espino, J.R. Davie, L.J. Murphy, Phosphorylation of Histones by Tissue Transglutaminase, Journal of Biological Chemistry, 281 (2006) 5532-5538.

[71] R.J. Collighan, M. Griffin, Transglutaminase 2 cross-linking of matrix proteins: biological significance and medical applications, Amino Acids, 36 (2009) 659-670.

[72] S.S. Akimov, A.M. Belkin, Cell surface tissue transglutaminase is involved in adhesion and migration of monocytic cells on fibronectin, 2001.

[73] D. Telci, Z. Wang, X. Li, E.A.M. Verderio, M.J. Humphries, M. Baccarini, H. Basaga, M. Griffin, Fibronectin-Tissue Transglutaminase Matrix Rescues RGD-impaired Cell Adhesion through Syndecan-4 and β1 Integrin Co-signaling, Journal of Biological Chemistry, 283 (2008) 20937-20947.

[74] C. Tristan, N. Shahani, T.W. Sedlak, A. Sawa, The diverse functions of GAPDH: Views from different subcellular compartments, Cellular Signalling, 23 (2011) 317-323.

[75] M.A. Sirover, Subcellular dynamics of multifunctional protein regulation: Mechanisms of GAPDH intracellular translocation, Journal of Cellular Biochemistry, 113 (2012) 2193-2200.

[76] M.R. Hara, N. Agrawal, S.F. Kim, M.B. Cascio, M. Fujimuro, Y. Ozeki, M. Takahashi, J.H. Cheah, S.K. Tankou, L.D. Hester, C.D. Ferris, S.D. Hayward, S.H. Snyder, A. Sawa, S-nitrosylated GAPDH initiates apoptotic cell death by nuclear translocation following Siah1 binding, Nat Cell Biol, 7 (2005) 665-674.

[77] N. Sen, M.R. Hara, M.D. Kornberg, M.B. Cascio, B.-I. Bae, N. Shahani, B. Thomas, T.M. Dawson, V.L. Dawson, S.H. Snyder, A. Sawa, Nitric oxide-induced nuclear GAPDH activates p300/CBP and mediates apoptosis, Nat Cell Biol, 10 (2008) 866-873.

[78] S. Azam, N. Jouvet, A. Jilani, R. Vongsamphanh, X. Yang, S. Yang, D. Ramotar, Human Glyceraldehyde-3-phosphate Dehydrogenase Plays a Direct Role in Reactivating Oxidized Forms of the DNA Repair Enzyme APE1, Journal of Biological Chemistry, 283 (2008) 30632-30641.

[79] R.-P. Dai, F.-X. Yu, S.-R. Goh, H.-W. Chng, Y.-L. Tan, J.-L. Fu, L. Zheng, Y. Luo, Histone 2B (H2B) Expression Is Confined to a Proper NAD+/NADH Redox Status, Journal of Biological Chemistry, 283 (2008) 26894-26901.

[80] N.A. Demarse, S. Ponnusamy, E.K. Spicer, E. Apohan, J.E. Baatz, B. Ogretmen, C. Davies, Direct Binding of Glyceraldehyde 3-Phosphate Dehydrogenase to Telomeric DNA Protects Telomeres against Chemotherapy-Induced Rapid Degradation, Journal of Molecular Biology, 394 (2009) 789-803.

[81] D.K.H. Chou, J.E. Evans, F.B. Jungalwala, Identity of nuclear high-mobility-group protein, HMG-1, and sulfoglucuronyl carbohydrate-binding protein, SBP-1, in brain, Journal of Neurochemistry, 77 (2001) 120-131.

[82] M.E. Bianchi, A. Agresti, HMG proteins: dynamic players in gene regulation and differentiation, Current Opinion in Genetics & Development, 15 (2005) 496-506.

[83] M.T. Lotze, K.J. Tracey, High-mobility group box 1 protein (HMGB1): nuclear weapon in the immune arsenal, Nat Rev Immunol, 5 (2005) 331-342.

[84] H. Wang, O. Bloom, M. Zhang, J.M. Vishnubhakat, M. Ombrellino, J. Che, A. Frazier, H. Yang, S. Ivanova, L. Borovikova, K.R. Manogue, E. Faist, E. Abraham, J. Andersson, U. Andersson, P.E. Molina, N.N. Abumrad, A. Sama, K.J. Tracey, HMG-1 as a Late Mediator of Endotoxin Lethality in Mice, Science, 285 (1999) 248-251.

[85] G.P. Sims, D.C. Rowe, S.T. Rietdijk, R. Herbst, A.J. Coyle, HMGB1 and RAGE in Inflammation and Cancer, Annual Review of Immunology, 28 (2010) 367-388.

[86] K.R. Diener, N. Al-Dasooqi, E.L. Lousberg, J.D. Hayball, The multifunctional alarmin HMGB1 with roles in the pathophysiology of sepsis and cancer, Immunol Cell Biol, 91 (2013) 443-450.

[87] A. Abe, T. Kuwata, C. Yamauchi, Y. Higuchi, A. Ochiai, High Mobility Group Box1 (HMGB1) released from cancer cells induces the expression of pro-inflammatory cytokines in peritoneal fibroblasts, Pathology International, 64 (2014) 267-275.

[88] B.M. Gumbiner, Regulation of cadherin-mediated adhesion in morphogenesis, Nat Rev Mol Cell Biol, 6 (2005) 622-634.

[89] J.M. Halbleib, W.J. Nelson, Cadherins in development: cell adhesion, sorting, and tissue morphogenesis, Genes & Development, 20 (2006) 3199-3214.

[90] F.H. Brembeck, M. Rosário, W. Birchmeier, Balancing cell adhesion and Wnt signaling, the key role of β-catenin, Current Opinion in Genetics & Development, 16 (2006) 51-59.

[91] X. Qian, T. Karpova, A.M. Sheppard, J. McNally, D.R. Lowy, E-cadherin-mediated adhesion inhibits ligand-dependent activation of diverse receptor tyrosine kinases, 2004.

[92] K. Polyak, R.A. Weinberg, Transitions between epithelial and mesenchymal states: acquisition of malignant and stem cell traits, Nat Rev Cancer, 9 (2009) 265-273.

[93] M. Yilmaz, G. Christofori, Mechanisms of Motility in Metastasizing Cells, Molecular Cancer Research, 8 (2010) 629-642.

[94] E.C. Ferber, M. Kajita, A. Wadlow, L. Tobiansky, C. Niessen, H. Ariga, J. Daniel, Y. Fujita, A Role for the Cleaved Cytoplasmic Domain of E-cadherin in the Nucleus, Journal of Biological Chemistry, 283 (2008) 12691-12700.

[95] R. Chetty, S. Serra, S.L. Asa, Loss of Membrane Localization and Aberrant Nuclear E-cadherin Expression Correlates With Invasion in Pancreatic Endocrine Tumors, The American Journal of Surgical Pathology, 32 (2008) 413-419 410.1097/PAS.1090b1013e31813547f31813548.

[96] J.M. David, A.K. Rajasekaran, Dishonorable Discharge: The Oncogenic Roles of Cleaved E-Cadherin Fragments, Cancer Research, 72 (2012) 2917-2923.

[97] L.J. Inge, S.P. Barwe, J. D'Ambrosio, J. Gopal, K. Lu, S. Ryazantsev, S.A. Rajasekaran, A.K. Rajasekaran, Soluble E-cadherin promotes cell survival by activating epidermal growth factor receptor, Experimental Cell Research, 317 (2011) 838-848.

[98] Y. Shi, J. Massagué, Mechanisms of TGF-β Signaling from Cell Membrane to the Nucleus, Cell, 113 (2003) 685-700.

[99] C. Liu, P. Xu, S. Lamouille, J. Xu, R. Derynck, TACE-Mediated Ectodomain Shedding of the Type I TGF-β Receptor Downregulates TGF-β Signaling, Molecular cell, 35 (2009) 26-36.

[100] Y. Mu, R. Sundar, N. Thakur, M. Ekman, S.K. Gudey, M. Yakymovych, A. Hermansson, H. Dimitriou, M.T. Bengoechea-Alonso, J. Ericsson, C.-H. Heldin, M. Landstrom, TRAF6 ubiquitinates TGF[beta] type I receptor to promote its cleavage and nuclear translocation in cancer, Nat Commun, 2 (2011) 330.

[101] M. Chandra, S. Zang, H. Li, L.J. Zimmerman, J. Champer, A. Tsuyada, A. Chow, W. Zhou, Y. Yu, H. Gao, X. Ren, R.-J. Lin, S.E. Wang, Nuclear Translocation of Type I Transforming Growth Factor β Receptor Confers a Novel Function in RNA Processing, Molecular and Cellular Biology, 32 (2012) 2183-2195.

[102] S.-Y. Lin, K. Makino, W. Xia, A. Matin, Y. Wen, K.Y. Kwong, L. Bourguignon, M.-C. Hung, Nuclear localization of EGF receptor and its potential new role as a transcription factor, Nat Cell Biol, 3 (2001) 802-808.

[103] H.W. Lo, M.C. Hung, Nuclear EGFR signalling network in cancers: linking EGFR pathway to cell cycle progression, nitric oxide pathway and patient survival, Br J Cancer, 94 (0000) 184-188.

[104] S.-C. Hsu, M.-C. Hung, Characterization of a Novel Tripartite Nuclear Localization Sequence in the EGFR Family, Journal of Biological Chemistry, 282 (2007) 10432-10440.

[105] Y.N. Wang, H. Wang, H. Yamaguchi, H.J. Lee, H.H. Lee, M.C. Hung, COPI-mediated retrograde trafficking from the Golgi to the ER regulates EGFR nuclear transport, Biochemical and Biophysical Research Communications, 399 (2010) 498-504.

[106] Y.N. Wang, H.H. Lee, H.J. Lee, Y. Du, H. Yamaguchi, M.C. Hung, Membrane-bound trafficking regulates nuclear transport of integral epidermal growth factor receptor (EGFR) and ErbB-2, Journal of Biological Chemistry, 287 (2012) 16869-16879.

[107] H.-W. Lo, M. Ali-Seyed, Y. Wu, G. Bartholomeusz, S.-C. Hsu, M.-C. Hung, Nuclear-cytoplasmic transport of EGFR involves receptor endocytosis, importin β1 and CRM1, Journal of Cellular Biochemistry, 98 (2006) 1570-1583.

[108] E.R. Eldredge, G.M. Korf, T.A. Christensen, D.C. Connolly, M.J. Getz, N.J. Maihle, Activation of c-fos gene expression by a kinase-deficient epidermal growth factor receptor, Molecular and Cellular Biology, 14 (1994) 7527-7534.

[109] N. Hanada, H.-W. Lo, C.-P. Day, Y. Pan, Y. Nakajima, M.-C. Hung, Co-regulation of B-Myb expression by E2F1 and EGF receptor, Molecular Carcinogenesis, 45 (2006) 10-17.

[110] H.-W. Lo, S.-C. Hsu, M. Ali-Seyed, M. Gunduz, W. Xia, Y. Wei, G. Bartholomeusz, J.-Y. Shih, M.-C. Hung, Nuclear interaction of EGFR and STAT3 in the activation of the iNOS/NO pathway, Cancer Cell, 7 (2005) 575-589.

[111] K. Kessenbrock, V. Plaks, Z. Werb, Matrix Metalloproteinases: Regulators of the Tumor Microenvironment, Cell, 141 (2010) 52-67.

[112] A. Page-McCaw, A.J. Ewald, Z. Werb, Matrix metalloproteinases and the regulation of tissue remodelling, Nat Rev Mol Cell Biol, 8 (2007) 221-233.

[113] F. Mannello, V. Medda, Nuclear localization of Matrix metalloproteinases, Progress in Histochemistry and Cytochemistry, 47 (2012) 27-58.

[114] J.A. Kwan, C.J. Schulze, W. Wang, H. Leon, M. Sariahmetoglu, M. Sung, J. Sawicka, D.E. Sims, G. Sawicki, R. Schulz, Matrix metalloproteinase-2 (MMP-2) is present in the nucleus of cardiac myocytes and is capable of cleaving poly (ADP-ribose) polymerase (PARP) in vitro, The FASEB journal : official publication of the Federation of American Societies for Experimental Biology, 18 (2004) 690-692.

[115] K. Si-Tayeb, A. Monvoisin, C. Mazzocco, S. Lepreux, M. Decossas, G. Cubel, D. Taras, J.-F. Blanc, D.R. Robinson, J. Rosenbaum, Matrix Metalloproteinase 3 Is Present in the Cell Nucleus and Is Involved in Apoptosis, The American Journal of Pathology, 169 (2006) 1390-1401.

[116] T. Eguchi, S. Kubota, K. Kawata, Y. Mukudai, J. Uehara, T. Ohgawara, S. Ibaragi, A. Sasaki, T. Kuboki, M. Takigawa, Novel transcription factor-like function of human matrix metalloproteinase 3 regulating the CTGF/CCN2 gene, Molecular and Cellular Biology, 28 (2008) 2391-2413.

[117] D.J. Marchant, C.L. Bellac, T.J. Moraes, S.J. Wadsworth, A. Dufour, G.S. Butler, L.M. Bilawchuk, R.G. Hendry, A.G. Robertson, C.T. Cheung, J. Ng, L. Ang, Z. Luo, K. Heilbron, M.J. Norris, W. Duan, T. Bucyk, A. Karpov, L. Devel, D. Georgiadis, R.G. Hegele, H. Luo, D.J. Granville, V. Dive, B.M. McManus, C.M. Overall, A new transcriptional role for matrix metalloproteinase-12 in antiviral immunity, Nat Med, 20 (2014) 493-502.

[118] N. Bardeesy, R.A. DePinho, Pancreatic cancer biology and genetics, Nat Rev Cancer, 2 (2002) 897-909.

[119] A.F. Hezel, A.C. Kimmelman, B.Z. Stanger, N. Bardeesy, R.A. Depinho, Genetics and biology of pancreatic ductal adenocarcinoma, Genes Dev, 20 (2006) 1218-1249.

[120] S.J. Baek, J.S. Kim, J.B. Nixon, R.P. DiAugustine, T.E. Eling, Expression of NAG-1, a transforming growth factor-beta superfamily member, by troglitazone requires the early growth response gene EGR-1, J Biol Chem, 279 (2004) 6883-6892.

[121] M. Cekanova, J.S. Yuan, X. Li, K. Kim, S.J. Baek, Gene alterations by peroxisome proliferator-activated receptor gamma agonists in human colorectal cancer cells, Int J Oncol, 32 (2008) 809-819.

[122] E. Osawa, A. Nakajima, K. Wada, S. Ishimine, N. Fujisawa, T. Kawamori, N. Matsuhashi, T. Kadowaki, M. Ochiai, H. Sekihara, H. Nakagama, Peroxisome proliferator-activated receptor gamma ligands suppress colon carcinogenesis induced by azoxymethane in mice, Gastroenterology, 124 (2003) 361-367.

[123] S. Wei, S.K. Kulp, C.S. Chen, Energy restriction as an antitumor target of thiazolidinediones, J Biol Chem, 285 (2010) 9780-9791.

[124] S.J. Baek, L.C. Wilson, L.C. Hsi, T.E. Eling, Troglitazone, a peroxisome proliferator-activated receptor gamma (PPAR gamma) ligand, selectively induces the early growth response-1 gene independently of PPAR gamma. A novel mechanism for its anti-tumorigenic activity, J Biol Chem, 278 (2003) 5845-5853.

[125] K. Yamaguchi, M. Cekanova, M.F. McEntee, J.H. Yoon, S.M. Fischer, I.B. Renes, I. Van Seuningen, S.J. Baek, Peroxisome proliferator-activated receptor ligand MCC-555 suppresses intestinal polyps in ApcMin/+ mice via extracellular signal-regulated kinase and peroxisome proliferator-activated receptor-dependent pathways, Molecular cancer therapeutics, 7 (2008) 2779-2787.

[126] K. Yamaguchi, S.H. Lee, T.E. Eling, S.J. Baek, A novel peroxisome proliferator-activated receptor gamma ligand, MCC-555, induces apoptosis via posttranscriptional regulation of NAG-1 in colorectal cancer cells, Molecular cancer therapeutics, 5 (2006) 1352-1361.

[127] O.P. Lazarenko, S.O. Rzonca, L.J. Suva, B. Lecka-Czernik, Netoglitazone is a PPAR-gamma ligand with selective effects on bone and fat, Bone, 38 (2006) 74-84.

[128] R. Upton, P.S. Widdowson, S. Ishii, H. Tanaka, G. Williams, Improved metabolic status and insulin sensitivity in obese fatty (fa/fa) Zucker rats and Zucker Diabetic Fatty (ZDF) rats treated with the thiazolidinedione, MCC-555, British Journal of Pharmacology, 125 (1998) 1708-1714.

[129] L. Pickavance, P.S. Widdowson, P. King, S. Ishii, H. Tanaka, G. Williams, The development of overt diabetes in young Zucker Diabetic Fatty (ZDF) rats and the effects of chronic MCC-555 treatment, British Journal of Pharmacology, 125 (1998) 767-770.

[130] M.J. Reginato, S.T. Bailey, S.L. Krakow, C. Minami, S. Ishii, H. Tanaka, M.A. Lazar, A Potent Antidiabetic Thiazolidinedione with Unique Peroxisome Proliferator-activated Receptor γ-activating Properties, Journal of Biological Chemistry, 273 (1998) 32679-32684.

[131] T. Kumagai, T. Ikezoe, D. Gui, J. O'Kelly, X.J. Tong, F.J. Cohen, J.W. Said, H.P. Koeffler, RWJ-241947 (MCC-555), a unique peroxisome proliferator-activated receptor-gamma ligand with antitumor activity against human prostate cancer in vitro and in beige/nude/ X-linked immunodeficient mice and enhancement of apoptosis in myeloma cells induced by arsenic trioxide, Clin Cancer Res, 10 (2004) 1508-1520.

[132] D.C. Liu, C.B. Zang, H.Y. Liu, K. Possinger, S.G. Fan, E. Elstner, A novel PPAR alpha/gamma dual agonist inhibits cell growth and induces apoptosis in human glioblastoma T98G cells, Acta pharmacologica Sinica, 25 (2004) 1312-1319.

[133] S. Chintharlapalli, S. Papineni, S. Safe, 1,1-bis(3'-indolyl)-1-(p-substitutedphenyl)methanes inhibit growth, induce apoptosis, and decrease the androgen receptor in LNCaP prostate cancer cells through peroxisome proliferator-activated receptor gamma-independent pathways, Mol Pharmacol, 71 (2007) 558-569.

[134] S.D. Cho, S. Chintharlapalli, M. Abdelrahim, S. Papineni, S. Liu, J. Guo, P. Lei, A. Abudayyeh, S. Safe, 5,5'-Dibromo-bis(3'-indolyl)methane induces Kruppel-like factor 4 and p21 in colon cancer cells, Mol Cancer Ther, 7 (2008) 2109-2120.

[135] M. Cekanova, S.-H. Lee, M.F. McEntee, S.J. Baek, MCC-555-induced NAG-1 expression is mediated in part by KLF4, European Journal of Pharmacology, 637 (2010) 30-37.

[136] B.D. Rowland, D.S. Peeper, KLF4, p21 and context-dependent opposing forces in cancer, Nat Rev Cancer, 6 (2006) 11-23.

[137] J.L. Shie, Z.Y. Chen, M. Fu, R.G. Pestell, C.C. Tseng, Gut-enriched Kruppel-like factor represses cyclin D1 promoter activity through Sp1 motif, Nucleic Acids Res, 28 (2000) 2969-2976.

[138] S.J. Baek, K.S. Kim, J.B. Nixon, L.C. Wilson, T.E. Eling, Cyclooxygenase inhibitors regulate the expression of a TGF-beta superfamily member that has proapoptotic and antitumorigenic activities, Mol Pharmacol, 59 (2001) 901-908.

[139] S.H. Lee, C. Krisanapun, S.J. Baek, NSAID-activated gene-1 as a molecular target for capsaicin-induced apoptosis through a novel molecular mechanism involving GSK3beta, C/EBPbeta and ATF3, Carcinogenesis, 31 (2010) 719-728.

[140] T. Nualsanit, P. Rojanapanthu, W. Gritsanapan, S.H. Lee, D. Lawson, S.J. Baek, Damnacanthal, a noni component, exhibits antitumorigenic activity in human colorectal cancer cells, J Nutr Biochem, (2011).

[141] S.J. Baek, J.M. Horowitz, T.E. Eling, Molecular cloning and characterization of human nonsteroidal anti-inflammatory drug-activated gene promoter. Basal transcription is mediated by Sp1 and Sp3, J Biol Chem, 276 (2001) 33384-33392.

[142] H.A. Elrod, S.-Y. Sun, PPARγ and Apoptosis in Cancer, PPAR Research, 2008 (2008) 1-12.

[143] L. Cerquetti, C. Sampaoli, D. Amendola, B. Bucci, L. Masuelli, R. Marchese, S. Misiti, A. De Venanzi, M. Poggi, V. Toscano, A. Stigliano, Rosiglitazone induces autophagy in H295R and cell cycle deregulation in SW13 adrenocortical cancer cells, Exp Cell Res, 317 (2011) 1397-1410.

[144] S. Kim, J.-J. Lee, D.S. Heo, PPARγ ligands induce growth inhibition and apoptosis through p63 and p73 in human ovarian cancer cells, Biochem Biophys Res Commun, 406 (2011) 389-395.

[145] S. Chintharlapalli, S. Papineni, S.J. Baek, S. Liu, S. Safe, 1,1-Bis(3'-indolyl)-1-(p-substitutedphenyl)methanes are peroxisome proliferator-activated receptor gamma agonists but decrease HCT-116 colon cancer cell survival through receptor-independent activation of early growth response-1 and nonsteroidal anti-inflammatory drug-activated gene-1, Mol Pharmacol, 68 (2005) 1782-1792.

[146] J. Hong, I. Samudio, S. Liu, M. Abdelrahim, S. Safe, Peroxisome proliferator-activated receptor gamma-dependent activation of p21 in Panc-28 pancreatic cancer cells involves Sp1 and Sp4 proteins, Endocrinology, 145 (2004) 5774-5785.

[147] R. Nasrallah, J. Clark, J. Corinaldi, G. Paris, P. Miura, B.J. Jasmin, R.L. Hébert, Thiazolidinediones alter growth and epithelial cell integrity, independent of PPAR-γ and MAPK activation, in mouse M1 cortical collecting duct cells, Am J Physiol Renal Physiol, 298 (2010) F1105-F1112.

[148] D.J. Graham, C.R. Drinkard, D. Shatin, Incidence of idiopathic acute liver failure and hospitalized liver injury in patients treated with troglitazone, Am J Gastroenterol, 98 (2003) 175-179.

[149] G. Eibl, M.N. Wente, H.A. Reber, O.J. Hines, Peroxisome Proliferator-Activated Receptor γ Induces Pancreatic Cancer Cell Apoptosis, Biochemical and Biophysical Research Communications, 287 (2001) 522-529.

[150] T. Ohta, A. Elnemr, M. Yamamoto, I. Ninomiya, S. Fushida, G. Nishimura, T. Fujimura, H. Kitagawa, M. Kayahara, K. Shimizu, S. Yi, K. Miwa, Thiazolidinedione, a peroxisome proliferator-activated receptor-gamma ligand, modulates the E-cadherin/beta-catenin system in a human pancreatic cancer cell line, BxPC-3, Int J Oncol, 21 (2002) 37-42.

[151] Y. Bren-Mattison, V. Van Putten, D. Chan, R. Winn, M.W. Geraci, R.A. Nemenoff, Peroxisome proliferator-activated receptor-gamma (PPAR(gamma)) inhibits tumorigenesis by reversing the undifferentiated phenotype of metastatic non-small-cell lung cancer cells (NSCLC), Oncogene, 24 (2005) 1412-1422.

[152] S. Vignati, V. Albertini, A. Rinaldi, I. Kwee, C. Riva, R. Oldrini, C. Capella, F. Bertoni, G.M. Carbone, C.V. Catapano, Cellular and molecular consequences of peroxisome proliferator-activated receptor-gamma activation in ovarian cancer cells, Neoplasia, 8 (2006) 851-861.

[153] E. Elstner, C. Muller, K. Koshizuka, E.A. Williamson, D. Park, H. Asou, P. Shintaku, J.W. Said, D. Heber, H.P. Koeffler, Ligands for peroxisome proliferator-activated receptorgamma and retinoic acid receptor inhibit growth and induce apoptosis of human breast cancer cells in vitro and in BNX mice, Proc Natl Acad Sci U S A, 95 (1998) 8806-8811.

[154] S.E. Nissen, K. Wolski, Effect of Rosiglitazone on the Risk of Myocardial Infarction and Death from Cardiovascular Causes, N Engl J Med, 356 (2007) 2457-2471.
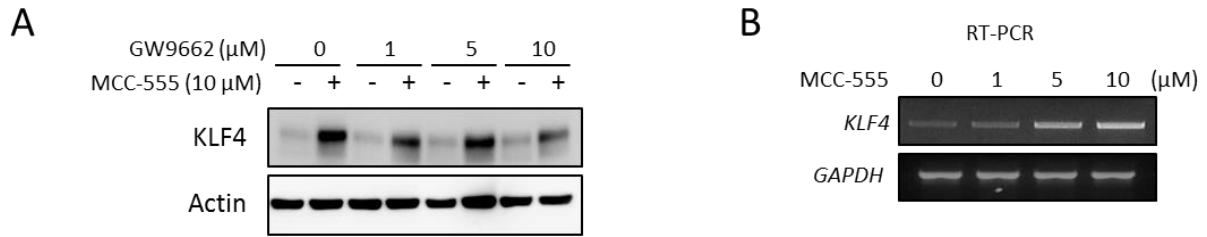
[155] J.H. Choi, A.S. Banks, J.L. Estall, S. Kajimura, P. Bostrom, D. Laznik, J.L. Ruas, M.J. Chalmers, T.M. Kamenecka, M. Bluher, P.R. Griffin, B.M. Spiegelman, Anti-diabetic drugs inhibit obesity-linked phosphorylation of PPARgamma by Cdk5, Nature, 466 (2010) 451-456.

[156] K.W. Foster, A.R. Frost, P. McKie-Bell, C.Y. Lin, J.A. Engler, W.E. Grizzle, J.M. Ruppert, Increase of GKLF messenger RNA and protein expression during progression of breast cancer, Cancer Res, 60 (2000) 6488-6495.

[157] K.W. Foster, S. Ren, I.D. Louro, S.M. Lobo-Ruppert, P. McKie-Bell, W. Grizzle, M.R. Hayes, T.R. Broker, L.T. Chow, J.M. Ruppert, Oncogene expression cloning by retroviral transduction of adenovirus E1A-immortalized rat kidney RK3E cells: transformation of a host with epithelial features by c-MYC and the zinc finger protein GKLF, Cell Growth Differ, 10 (1999) 423-434.

[158] W. Zhao, I.M. Hisamuddin, M.O. Nandan, B.A. Babbin, N.E. Lamb, V.W. Yang, Identification of Kruppel-like factor 4 as a potential tumor suppressor gene in colorectal cancer, Oncogene, 23 (2004) 395-402.

[159] D. Wei, W. Gong, M. Kanai, C. Schlunk, L. Wang, J.C. Yao, T.T. Wu, S. Huang, K. Xie, Drastic down-regulation of Kruppel-like factor 4 expression is critical in human gastric cancer development and progression, Cancer Res, 65 (2005) 2746-2754.

[160] D.T. Dang, X. Chen, J. Feng, M. Torbenson, L.H. Dang, V.W. Yang, Overexpression of Kruppel-like factor 4 in the human colon cancer cell line RKO leads to reduced tumorigenecity, Oncogene, 22 (2003) 3424-3430.

[161] F. Zammarchi, M. Morelli, M. Menicagli, C. Di Cristofano, K. Zavaglia, A. Paolucci, D. Campani, P. Aretini, U. Boggi, F. Mosca, A. Cavazzana, L. Cartegni, G. Bevilacqua, C.M. Mazzanti, KLF4 is a Novel Candidate Tumor Suppressor Gene in Pancreatic Ductal Carcinoma, Am J Pathol, 178 (2011) 361-372.

[162] D. Wei, M. Kanai, Z. Jia, X. Le, K. Xie, Krüppel-like Factor 4 Induces p27Kip1 Expression in and Suppresses the Growth and Metastasis of Human Pancreatic Cancer Cells, Cancer Res, 68 (2008) 4631-4639.

[163] S. Chintharlapalli, S. Papineni, S. Liu, I. Jutooru, G. Chadalapaka, S.D. Cho, R.S. Murthy, Y. You, S. Safe, 2-cyano-lup-1-en-3-oxo-20-oic acid, a cyano derivative of betulinic acid, activates peroxisome proliferator-activated receptor gamma in colon and pancreatic cancer cells, Carcinogenesis, 28 (2007) 2337-2346.

[164] Y.C. Chew, G. Adhikary, G.M. Wilson, E.A. Reece, R.L. Eckert, Protein Kinase C (PKC) δ Suppresses Keratinocyte Proliferation by Increasing p21Cip1 Level by a KLF4 Transcription Factor-dependent Mechanism, Journal of Biological Chemistry, 286 (2011) 28772-28782.

[165] N. Ohnesorge, D. Viemann, N. Schmidt, T. Czymai, D. Spiering, M. Schmolke, S. Ludwig, J. Roth, M. Goebeler, M. Schmidt, Erk5 Activation Elicits a Vasoprotective Endothelial Phenotype via Induction of Krüppel-like Factor 4 (KLF4), J Biol Chem, 285 (2010) 26199-26210.

[166] P.M. Evans, W. Zhang, X. Chen, J. Yang, K.K. Bhakat, C. Liu, Krüppel-like Factor 4 Is Acetylated by p300 and Regulates Gene Transcription via Modulation of Histone Acetylation, J Biol Chem, 282 (2007) 33994-34002.

[167] S.J. Baek, R. Okazaki, S.H. Lee, J. Martinez, J.S. Kim, K. Yamaguchi, Y. Mishina, D.W. Martin, A. Shoieb, M.F. McEntee, T.E. Eling, Nonsteroidal anti-inflammatory drug-activated gene-1 over expression in transgenic mice suppresses intestinal neoplasia, Gastroenterology, 131 (2006) 1553-1560.

[168] M. Cekanova, S.H. Lee, R.L. Donnell, M. Sukhthankar, T.E. Eling, S.M. Fischer, S.J. Baek, Nonsteroidal anti-inflammatory drug-activated gene-1 expression inhibits urethane-induced pulmonary tumorigenesis in transgenic mice, Cancer Prev Res (Phila Pa), 2 (2009) 450-458.

[169] S.J. Baek, J.S. Kim, F.R. Jackson, T.E. Eling, M.F. McEntee, S.H. Lee, Epicatechin gallate-induced expression of NAG-1 is associated with growth inhibition and apoptosis in colon cancer cells, Carcinogenesis, 25 (2004) 2425-2432.

[170] M. Bottner, M. Laaff, B. Schechinger, G. Rappold, K. Unsicker, C. Suter-Crazzolara, Characterization of the rat, mouse, and human genes of growth/differentiation factor-15/macrophage inhibiting cytokine-1 (GDF-15/MIC-1), Gene, 237 (1999) 105-111.

[171] P.X. Li, J. Wong, A. Ayed, D. Ngo, A.M. Brade, C. Arrowsmith, R.C. Austin, H.J. Klamut, Placental transforming growth factor-beta is a downstream mediator of the growth arrest and apoptotic response of tumor cells to DNA damage and p53 overexpression, J Biol Chem, 275 (2000) 20127-20135.

[172] M.R. Bootcov, A.R. Bauskin, S.M. Valenzuela, A.G. Moore, M. Bansal, X.Y. He, H.P. Zhang, M. Donnellan, S. Mahler, K. Pryor, B.J. Walsh, R.C. Nicholson, W.D. Fairlie, S.B. Por, J.M. Robbins, S.N. Breit, MIC-1, a novel macrophage inhibitory cytokine, is a divergent member of the TGF-beta superfamily, Proc Natl Acad Sci U S A, 94 (1997) 11514-11519.
[173] V.M. Paralkar, A.L. Vail, W.A. Grasser, T.A. Brown, H. Xu, S. Vukicevic, H.Z. Ke, H. Qi, T.A. Owen, D.D. Thompson, Cloning and characterization of a novel member of the transforming growth factor-beta/bone morphogenetic protein family, J Biol Chem, 273 (1998) 13760-13767.
[174] R. Hromas, M. Hufford, J. Sutton, D. Xu, Y. Li, L. Lu, PLAB, a novel placental bone morphogenetic protein., Biochim Biophys ACTA, 1354 (1997) 40-44.
[175] S.J. Baek, L.C. Wilson, C.H. Lee, T.E. Eling, Dual function of nonsteroidal anti-inflammatory drugs (NSAIDs): inhibition of cyclooxygenase and induction of NSAID-activated gene, J Pharmacol Exp Ther, 301 (2002) 1126-1131.
[176] S.H. Lee, M. Cekanova, S.J. Baek, Multiple mechanisms are involved in 6-gingerol-induced cell growth arrest and apoptosis in human colorectal cancer cells, Mol Carcinog, 47 (2008) 197-208.
[177] S.H. Lee, J.S. Kim, K. Yamaguchi, T.E. Eling, S.J. Baek, Indole-3-carbinol and 3,3'-diindolylmethane induce expression of NAG-1 in a p53-independent manner, Biochem Biophys Res Commun, 328 (2005) 63-69.
[178] S.H. Lee, K. Yamaguchi, J.S. Kim, T.E. Eling, S. Safe, Y. Park, S.J. Baek, Conjugated linoleic acid stimulates an anti-tumorigenic protein NAG-1 in an isomer specific manner, Carcinogenesis, 27 (2006) 972-981.
[179] M.H. Yang, J. Kim, I.A. Khan, L.A. Walker, S.I. Khan, Nonsteroidal anti-inflammatory drug activated gene-1 (NAG-1) modulators from natural products as anti-cancer agents, Life Sci, (2014).
[180] K.W. Min, X. Zhang, T. Imchen, S.J. Baek, A peroxisome proliferator-activated receptor ligand MCC-555 imparts anti-proliferative response in pancreatic cancer cells by PPARgamma-independent up-regulation of KLF4, Toxicology and applied pharmacology, 263 (2012) 225-232.
[181] S.-H. Lee, J.H. Bahn, C.K. Choi, N.C. Whitlock, A.E. English, S. Safe, S.J. Baek, ESE-1/EGR-1 pathway plays a role in tolfenamic acid-induced apoptosis in colorectal cancer cells, Mol Cancer Ther, 7 (2008) 3739-3750.
[182] K. Yamaguchi, S.H. Lee, T.E. Eling, S.J. Baek, Identification of nonsteroidal anti-inflammatory drug-activated gene (NAG-1) as a novel downstream target of phosphatidylinositol 3-kinase/AKT/GSK-3beta pathway, J Biol Chem, 279 (2004) 49617-49623.
[183] X. Wang, S.J. Baek, T.E. Eling, The diverse roles of nonsteroidal anti-inflammatory drug activated gene (NAG-1/GDF15) in cancer, Biochemical Pharmacology, 85 (2013) 597-606.
[184] J.M. Kim, J.P. Kosak, J.K. Kim, G. Kissling, D.R. Germolec, D.C. Zeldin, J.A. Bradbury, S.J. Baek, T. Eling, NAG-1/GDF15 Transgenic Mouse Has Less White Adipose Tissue and a Reduced Inflammatory Response, Mediators of Inflammation, 2013 (2013) 641851.
[185] H. Johnen, T. Kuffner, D.A. Brown, B.J. Wu, R. Stocker, S.N. Breit, Increased expression of the TGF-b superfamily cytokine MIC-1/GDF15 protects ApoE(-/-) mice from the development of atherosclerosis, Cardiovascular pathology : the official journal of the Society for Cardiovascular Pathology, (2012).
[186] L. Macia, V.W. Tsai, A.D. Nguyen, H. Johnen, T. Kuffner, Y.C. Shi, S. Lin, H. Herzog, D.A. Brown, S.N. Breit, A. Sainsbury, Macrophage inhibitory cytokine 1 (MIC-1/GDF15) decreases food intake, body weight and improves glucose tolerance in mice on normal & obesogenic diets, PLoS ONE, 7 (2012) e34868.
[187] M. Cekanova, S.H. Lee, R.L. Donnell, M. Sukhthankar, T.E. Eling, S.M. Fischer, S.J. Baek, Nonsteroidal anti-inflammatory drug-activated gene-1 expression inhibits urethane-induced pulmonary tumorigenesis in transgenic mice, Cancer Prev Res (Phila), 2 (2009) 450-458.
[188] K. Chrysovergis, X. Wang, J. Kosak, S.H. Lee, J.S. Kim, J.F. Foley, G. Travlos, S. Singh, S.J. Baek, T.E. Eling, NAG-1/GDF-15 prevents obesity by increasing thermogenesis, lipolysis and oxidative metabolism, Int J Obes, (2014).
[189] A.R. Bauskin, D.A. Brown, S. Junankar, K.K. Rasiah, S. Eggleton, M. Hunter, T. Liu, D. Smith, T. Kuffner, G.J. Pankhurst, H. Johnen, P.J. Russell, W. Barret, P.D. Stricker, J.J. Grygiel, J.G. Kench, S.M.

Henshall, R.L. Sutherland, S.N. Breit, The propeptide mediates formation of stromal stores of PROMIC-1: role in determining prostate cancer outcome, Cancer Res, 65 (2005) 2330-2336.

[190] H.-K. Lee, D.-S. Lee, H.-M. Ryoo, J.-T. Park, S.-J. Park, H.-S. Bae, M.-I. Cho, J.-C. Park, The odontogenic ameloblast-associated protein (ODAM) cooperates with RUNX2 and modulates enamel mineralization via regulation of MMP-20, Journal of Cellular Biochemistry, 111 (2010) 755-767.

[191] S.J. Baek, L.C. Wilson, T.E. Eling, Resveratrol enhances the expression of non-steroidal anti-inflammatory drug-activated gene (NAG-1) by increasing the expression of p53, Carcinogenesis, 23 (2002) 425-432.

[192] C. Trapnell, A. Roberts, L. Goff, G. Pertea, D. Kim, D.R. Kelley, H. Pimentel, S.L. Salzberg, J.L. Rinn, L. Pachter, Differential gene and transcript expression analysis of RNA-seq experiments with TopHat and Cufflinks, Nature protocols, 7 (2012) 562-578.

[193] M. Inui, A. Manfrin, A. Mamidi, G. Martello, L. Morsut, S. Soligo, E. Enzo, S. Moro, S. Polo, S. Dupont, M. Cordenonsi, S. Piccolo, USP15 is a deubiquitylating enzyme for receptor-activated SMADs, Nat Cell Biol, 13 (2011) 1368-1375.

[194] A. Nguyen Ba, A. Pogoutse, N. Provart, A. Moses, NLStradamus: a simple Hidden Markov Model for nuclear localization signal prediction, BMC Bioinformatics, 10 (2009) 202.

[195] S. Kosugi, M. Hasebe, N. Matsumura, H. Takashima, E. Miyamoto-Sato, M. Tomita, H. Yanagawa, Six Classes of Nuclear Localization Signals Specific to Different Binding Grooves of Importin α, Journal of Biological Chemistry, 284 (2009) 478-485.

[196] M. Theodore, Y. Kawai, J. Yang, Y. Kleshchenko, S.P. Reddy, F. Villalta, I.J. Arinze, Multiple Nuclear Localization Signals Function in the Nuclear Import of the Transcription Factor Nrf2, Journal of Biological Chemistry, 283 (2008) 8984-8994.

[197] I. Waldmann, S. Wälde, R.H. Kehlenbach, Nuclear Import of c-Jun Is Mediated by Multiple Transport Receptors, Journal of Biological Chemistry, 282 (2007) 27685-27692.

[198] C.-P. Chan, T.-Y. Mak, K.-T. Chin, I.O.-L. Ng, D.-Y. Jin, N-linked glycosylation is required for optimal proteolytic activation of membrane-bound transcription factor CREB-H, Journal of Cell Science, 123 (2010) 1438-1448.

[199] S. Kosugi, M. Hasebe, M. Tomita, H. Yanagawa, Nuclear Export Signal Consensus Sequences Defined Using a Localization-Based Yeast Selection System, Traffic, 9 (2008) 2053-2062.

[200] S. Hutten, R.H. Kehlenbach, CRM1-mediated nuclear export: to the pore and beyond, Trends in Cell Biology, 17 (2007) 193-201.

[201] C.E. Pierreux, F.J. Nicolás, C.S. Hill, Transforming Growth Factor β-Independent Shuttling of Smad4 between the Cytoplasm and Nucleus, Molecular and Cellular Biology, 20 (2000) 9041-9054.

[202] J. Massague, TGF[beta] signalling in context, Nat Rev Mol Cell Biol, 13 (2012) 616-630.

[203] T.-F. Kuo, H. Tatsukawa, S. Kojima, New insights into the functions and localization of nuclear transglutaminase 2, FEBS Journal, 278 (2011) 4756-4767.

[204] T.A. Zimmers, X. Jin, E.C. Hsiao, S.A. McGrath, A.F. Esquela, L.G. Koniaris, Growth differentiation factor-15/macrophage inhibitory cytokine-1 induction after kidney and lung injury, Shock, 23 (2005) 543-548.

[205] M. Albertoni, P.H. Shaw, M. Nozaki, S. Godard, M. Tenan, M.F. Hamou, D.W. Fairlie, S.N. Breit, V.M. Paralkar, N. de Tribolet, E.G. Van Meir, M.E. Hegi, Anoxia induces macrophage inhibitory cytokine-1 (MIC-1) in glioblastoma cells independently of p53 and HIF-1, Oncogene, 21 (2002) 4212-4219.

[206] S.J. Baek, T.E. Eling, Changes in gene expression contribute to cancer prevention by COX inhibitors, Prog Lipid Res, 45 (2006) 1-16.

[207] M. Tan, Y. Wang, K. Guan, Y. Sun, PTGF-beta, a type beta transforming growth factor (TGF-beta) superfamily member, is a p53 target gene that inhibits tumor cell growth via TGF-beta signaling pathway, Proc Natl Acad Sci U S A, 97 (2000) 109-114.

[208] M. Shim, T.E. Eling, Protein kinase C-dependent regulation of NAG-1/placental bone morphogenic protein/MIC-1 expression in LNCaP prostate carcinoma cells, J Biol Chem, 280 (2005) 18636-18642.

[209] T.A. Zimmers, J.C. Gutierrez, L.G. Koniaris, Loss of GDF-15 abolishes sulindac chemoprevention in the ApcMin/+ mouse model of intestinal cancer, J Cancer Res Clin Oncol, 136 (2010) 571-576.

[210] D. Gitenay, V.T. Baron, Is EGR1 a potential target for prostate cancer therapy?, Future Oncology, 5 (2009) 993-1003.

[211] V. Baron, E.D. Adamson, A. Calogero, G. Ragona, D. Mercola, The transcription factor Egr1 is a direct regulator of multiple tumor suppressors including TGF[beta]1, PTEN, p53, and fibronectin, Cancer Gene Ther, 13 (2005) 115-124.

[212] I. Shureiqi, S.M. Lippman, Lipoxygenase Modulation to Reverse Carcinogenesis, Cancer Res, 61 (2001) 6307-6312.

[213] S.B. Shappell, S.J. Olson, S.E. Hannah, S. Manning, R.L. Roberts, N. Masumori, M. Jisaka, W.E. Boeglin, V. Vader, D.S. Dave, M.F. Shook, T.Z. Thomas, C.D. Funk, A.R. Brash, R.J. Matusik, Elevated Expression of 12/15-Lipoxygenase and Cyclooxygenase-2 in a Transgenic Mouse Model of Prostate Carcinoma, Cancer Res, 63 (2003) 2256-2267.

[214] J. Xu, T.R. Kimball, J.N. Lorenz, D.A. Brown, A.R. Bauskin, R. Klevitsky, T.E. Hewett, S.N. Breit, J.D. Molkentin, GDF15/MIC-1 Functions As a Protective and Antihypertrophic Factor Released From the Myocardium in Association With SMAD Protein Activation, Circ Res, 98 (2006) 342-350.

[215] J. Felin, J. Mayo, T. Loos, J.D. Jensen, D. Sperry, S. Gaufin, C. Meinhart, J. Moss, L. Bridgewater, Nuclear variants of bone morphogenetic proteins, BMC Cell Biology, 11 (2010) 20.

[216] G.J. Lindeman, S. Gaubatz, D.M. Livingston, D. Ginsberg, The subcellular localization of E2F-4 is cell-cycle dependent, Proceedings of the National Academy of Sciences, 94 (1997) 5095-5100.

[217] M. Sharma, C. Jamieson, M. Johnson, M.P. Molloy, B.R. Henderson, Specific Armadillo Repeat Sequences Facilitate β-Catenin Nuclear Transport in Live Cells via Direct Binding to Nucleoporins Nup62, Nup153, and RanBP2/Nup358, Journal of Biological Chemistry, 287 (2012) 819-831.

[218] Y.N. Wang, H. Yamaguchi, J.M. Hsu, M.C. Hung, Nuclear trafficking of the epidermal growth factor receptor family membrane proteins, Oncogene, 29 (2010) 3997-4006.

[219] J.P. Joshi, N.E. Brown, S.E. Griner, R. Nahta, Growth differentiation factor 15 (GDF15)-mediated HER2 phosphorylation reduces trastuzumab sensitivity of HER2-overexpressing breast cancer cells, Biochem Pharmacol, 82 (2011) 1090-1099.

[220] R. Janknecht, N.J. Wells, T. Hunter, TGF-β-stimulated cooperation of Smad proteins with the coactivators CBP/p300, Genes & Development, 12 (1998) 2114-2119.

[221] P. Lönn, L.P. van der Heide, M. Dahl, U. Hellman, C.-H. Heldin, A. Moustakas, PARP-1 Attenuates Smad-Mediated Transcription, Molecular cell, 40 (2010) 521-532.

[222] J.G. Turner, J. Dawson, D.M. Sullivan, Nuclear export of proteins and drug resistance in cancer, Biochemical Pharmacology, 83 (2012) 1021-1032.

[223] T.R. Kau, J.C. Way, P.A. Silver, Nuclear transport and cancer: from mechanism to intervention, Nat Rev Cancer, 4 (2004) 106-117.

Appendix: Supplementary Figures and Tables

A

GW9662 (µM)   0   1   5   10
MCC-555 (10 µM) -   +   -   +   -   +   -   +

KLF4

Actin

B   RT-PCR

MCC-555   0   1   5   10   (µM)

KLF4

GAPDH

Supplementary Figure S2.1 KLF4 RNA is increased in the presence of MCC-555, KLF4 induction by MCC-555 appears to not involve PPARγ activation.
A, BxPC-3 cells were pretreated with GW9662 for 30 min at the indicated dose and then the cells were treated with 10 µM of MCC-555 for 24 h. Total proteins were isolated for Western blot analysis. Equal loading was confirmed by Actin. **B**, Total RNAs were isolated from BxPC-3 cells after MCC-555 treatment. The expression of transcripts for KLF4 was analyzed by RT-PCR. GAPDH was used as control transcript.

A, FITC (NAG-1) · TRICT Fibrillarin · DAPI · MERGE · Field 1 · Field 2
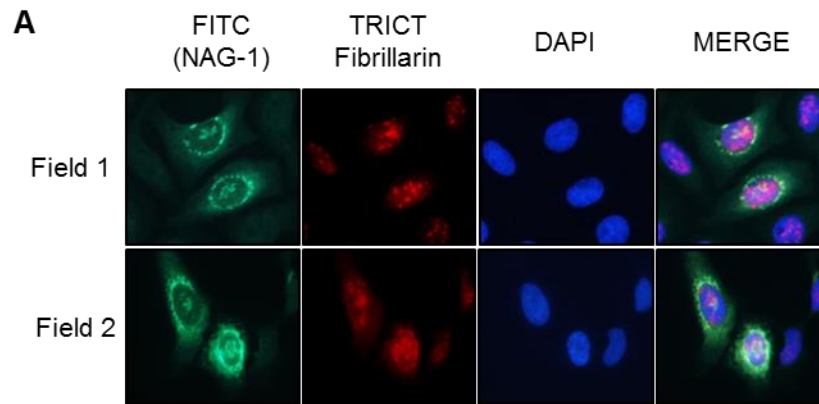
B
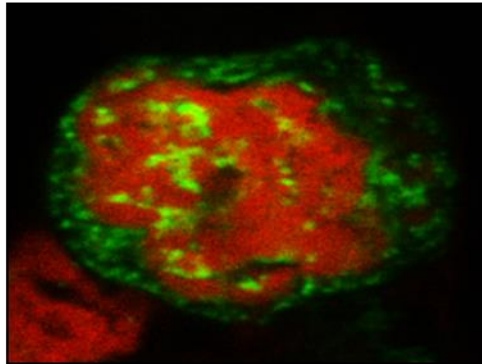
Supplementary Figure S3.1 Nuclear localization of NAG-1.

A, Immunofluorescence for fibrillarin. U2OS cells transfected with GFP-tagged NAG-1 (WT) were fixed and analyzed by immunofluorescence with antibodies against GFP and fibrillarin, as described in the Materials and Methods section. DAPI was used to stain the nuclei. Two independent fields are shown. **B**, Confocal microscope image of subcellular localization of NAG-1. HCT-116 cells were transfected with pNAG1-GFP expression vector, and the cells were counterstained with propium iodide. A representative picture is shown. A confocal microscope (Leica, TCS SP2) was used and Leica software (version 2.61) was used to collect the images.
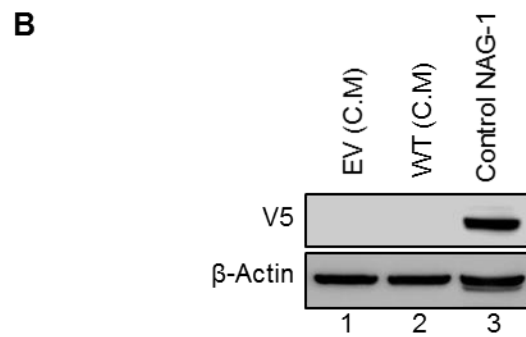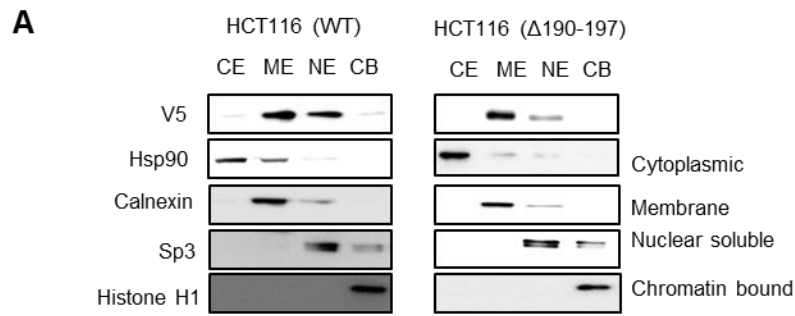
Supplementary Figure S3.2 Cytoplasmic NAG-1 is subjected to nuclear translocation.

A, Wildtype U2OS cells transfected with either pNAG-1/V5/His WT expression vector or pNAG-1/V5/His Δ190-197 were subjected to subcellular fractionation, and Western blot was performed. CE, cytoplasmic extract; ME, membrane extract; NE, nuclear extract; CB, chromatin-bound extract. Markers in each fraction are shown. **B**, U2OS cells were treated with the conditioned media of HCT-116 cells from Fig. 3.3B for 24 h, and cell lysates were isolated in RIPA buffer followed by Western blot analysis. Cell lysate pNAG-1/V5/His WT transfected cells were loaded as a control (lane 3).
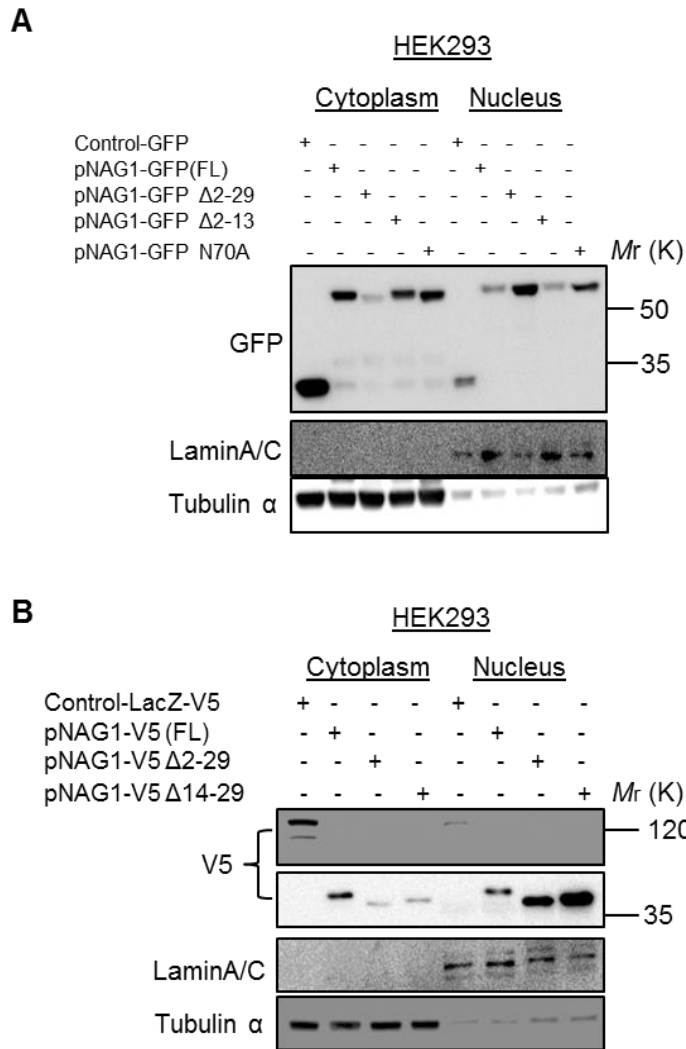
Supplementary Figure S3.3 NAG-1 has a nuclear retention signal within aa 14-29.
A, HEK293 cells were transfected with GFP, NAG-1/GFP expression vector, or the mutant constructs that are conjugated with GFP. Both cytoplasm and nuclear fractions were isolated, and Western blot analysis was performed against GFP, tubulin α, and lamin A/C. **B**, HEK293 cells were transfected with LacZ expression vector or indicated NAG-1 expression vectors conjugated with V5. Both cytoplasm and nuclear fractions were isolated, and Western blot analysis was performed against V5, tubulin α, and lamin A/C.

Supplementary Figure S3.4 NAG-1 possesses a nuclear export signal (NES).
A, U2OS and HCT-116 cells were transfected with mutNES clone, and subcellular fraction was isolated. Western blot analysis was performed using antibodies against V5, Hsp90, calnexin, Sp3, or histone H1. CE, cytoplasmic extract; ME, membrane extract; NE, nuclear extract; CB, chromatin bound extract. **B**, *Tet*-inducible U2OS cells were treated with 2 µg/mL tetracycline for 16 h, and cells were treated with CRM1 inhibitor LMB for 5 h with various doses. Cytoplasmic fraction was isolated, and Western blot was performed using antibodies against NAG-1 and tubulin α. **C**, HEK293 cells were transfected with pNAG-1/V5/His WT expression vector, and the cells were treated with LMB for 5 h at various doses. The nuclear fraction was isolated, and Western blot was performed using antibodies against V5, Smad4, and lamin A/C. **D**, HEK293 cells transfected with NAG-1/V5 expression vector with or without 10 nM LMB treatment for 5 h were subjected to immunofluorescence assay. NAG-1/V5 was detected by FITC conjugated secondary antibody (green), and the nuclei were stained with DAPI (blue). **E**, Effect of LMB on shuttling of NAG-1. Interspecies heterokaryons were prepared and viewed as described in the Materials and Methods section. The murine NIH3T3 nuclei gave a characteristic staining of intranuclear bodies (speckles), and the human U2OS nuclei displayed a diffuse pattern, indicated by the arrows.

A

U2OS (mutNES)

CE ME NE CB

V5
Hsp90 — Cytoplasmic
Calnexin — Membrane
Sp3 — Nuclear soluble
Histone H1 — Chromatin bound

HCT116 (mutNES)

CE ME NE CB

V5
Hsp90 — Cytoplasmic
Calnexin — Membrane
Sp3 — Nuclear soluble
Histone H1 — Chromatin bound

B

2 µg/mL tet (16 h)

Cytoplasm

LMB (nM) 0 1 10 20

NAG-1
Tubulin α

C

HEK293

Nucleus

NAG-1-WT-V5 + + + +
LMB (nM) - 1 10 20

V5
Smad4
Lamin A/C

D

-LMB +LMB

FITC
DAPI
MERGE

E

-LMB +LMB

NAG-1
Hoechst 33258
Merge

Supplementary Figure S3.4 Continued.

113
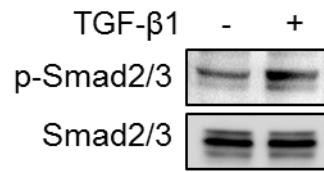
Supplementary Figure S3.5. U2OS cells express the phosphorylated form of Smad2 in the absence of TGF-β1 treatment.

U2OS cells were starved in serum-free media for 24 h and then were stimulated with 2 ng/mL TGF-β1 for 1 h in serum-free condition. Cell lysates were subjected to Western blot analysis. Phosphor-Smad2 and total Smad2/3 antibodies were used.

Supplementary Figure S3.6 NAG-1 attenuates TGF-β signaling without affecting Smad2 phosphorylation.

A, MCF7 cells were transfected with either *3TP* or *PAI-1 (800 bp promoter)* reporter constructs with the indicated expression vectors, and luciferase was measured. **B**, MCF-10A cells were transfected with *SBE4* reporter with indicated NAG-1 expression vectors, followed by luciferase assay. Mean values with SD from three replicates are shown. $*P < 0.05$, $***P < 0.001$, compared to TGF-β1-treated empty vector-transfected cells. **C**, A549 cells were transfected with control LacZ expression vector or pNAG-1-V5/His ΔNES expression vector. After treatment with TGF-β1 (2 ng/mL) for 1 h, the media were replaced with fresh media containing 10 μM cycloheximide (CHX), and cell lysates were isolated at the indicated time points followed by subcellular fractionation. Cytoplasmic and nuclear fractions were subjected to Western blot analysis using pSmad2 and Smad2 antibodies. **D**, DNA pull-down followed by Western analysis with anti-Smad2/3 and anti-Smad4 antibodies. Cell lysates from either empty vector or wildtype-NAG-1 expression vector were transfected into MCF-10A cells incubated with SBE oligos, as described in Materials and Methods. SBE-bound Smad proteins were reduced in NAG-1-expressing MCF-10A cells compared to empty vector-transfected MCF-10A cells.
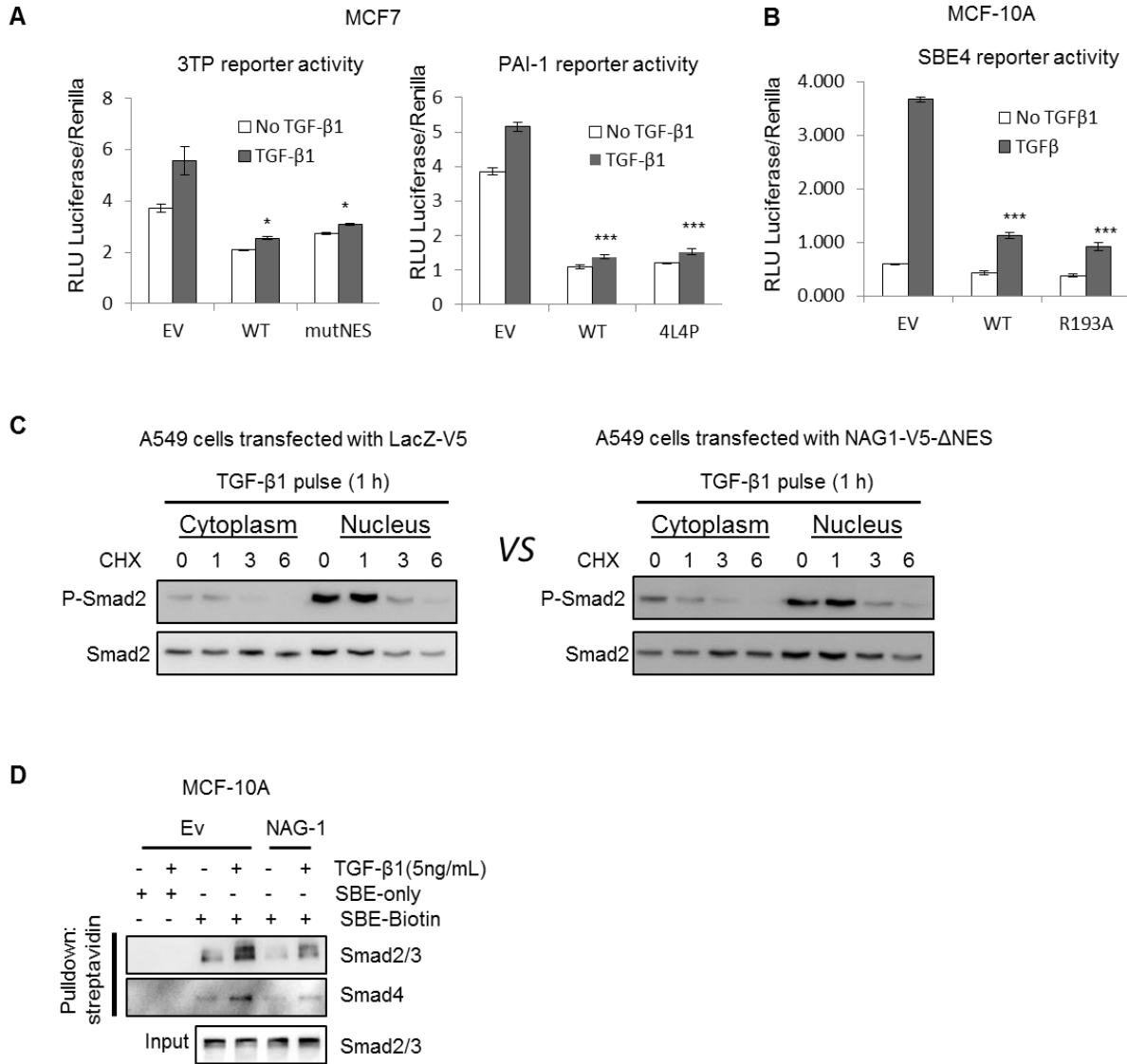
Supplementary Figure S3.6 Continued.
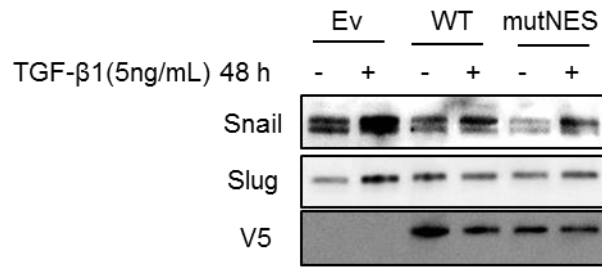
Supplementary Figure S3.7 NAG-1 attenuates TGF-β1-induced EMT marker.
MDA-MB-231cells were transfected with the indicated vectors and then were stimulated with TGF-β1 for 48 h. Whole cell lysates (30 µg) were subjected to Western blot with anti-Snail, anti-Slug, and anti-V5 antibodies.
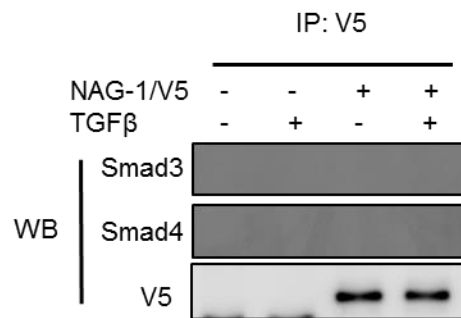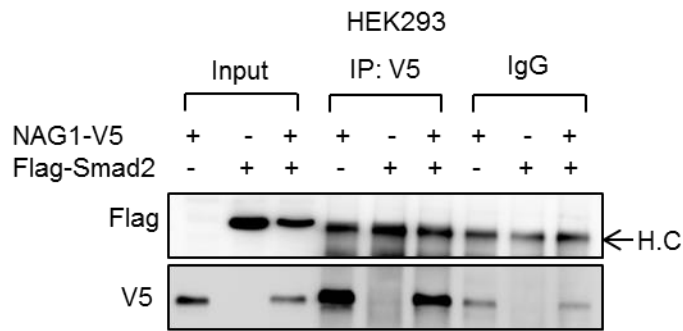
Supplementary Figure S3.8 NAG-1 does not bind to Smad2/3/4.
A, HEK293 cells were transfected with pNAG-1/V5/His WT NAG-1 and Flag-tagged Smad2 expression vector. Cell lysates were subjected to immunoprecipitation using 2 µg V5 or normal IgG antibodies, and then subjected to Western blot analysis using Flag or V5 antibodies. The whole cell lysate (WCL) was loaded with 30 µg. **B**, HEK293 cells were transfected with pNAG-1/V5/His WT NAG-1 expression vector; then the cells were stimulated with 2 ng/ml TGF-β1 for 3 h. Cell lysates were subjected to immunoprecipitation using 2 µg V5 antibody followed by Western blot analysis using Smad3 or Smad4 antibodies

Supplementary Table S3.1. Primer sequences used to construct plasmids in this study.

Construct	Direction	Sequence (5'-3')
NAG-1-GFP-WT	Forward	GCCATGCCCGGGCAAGAACTC
	Reverse	ATATGCAGTGGCAGTCTTTGGC
NAG-1-GFP-Δ2-29	Forward	CACAGCCATGCTGTCTCTGGCCGAGGCGAG
	Reverse	CCAGAGACAGCATGGCTGTGCAGGTTGCCC
NAG-1-GFP-Δ2-13	Forward	CTGCACAGCCATGCTCCTGGTGTTGCTGGT
	Reverse	CCAGGAGCATCATGGCTGTGCAGGTTGCCC
NAG-1-GFP-N70A	Forward	GCTGCGGGCCGCCCAGAGCTGGGAAGATTCGA
	Reverse	TCGAATCTTCCCAGCTCTGGGCGGCCCGCAGC
NAG-1-V5-WT	Forward	GACAATGCCCGGGCAAGAACT
	Reverse	ATATGCAGTGGCAGTCTTTGGC
NAG-1-V5-Δ190-197	Forward	GCAAGCCGCCCGCAACGGGGACCACTGTCC
	Reverse	CCCCGTTGCGGGCGGCTTGCGGCCGCAAGT
NAG-1-V5-Δ211-218	Forward	CGGGCGTTGCTCGCTGGAAGACCTGGGCTG
	Reverse	CTTCCAGCGAGCAACGCCCGGGCCCGAGCG
NAG-1-V5-Δ2-29	Forward	TGGGACAATGCTGTCTCTGGCCGAGGCGAG
	Reverse	CCAGAGACAGCATTGTCCCAAGCTTAACTA
NAG-1-V5-Δ30-57	Forward	TGGGGGCGCCAAACGCTACGAGGACCTGCT
	Reverse	CGTAGCGTTTGGCGCCCCCATGCGGCAGCC
NAG-1-V5-Δ58-85	Forward	AGAGTTGCGGGTCCGGATACTCACGCCAGA
	Reverse	GTATCCGGACCCGCAACTCTCGGAATCTGG
NAG-1-V5-Δ86-95	Forward	GGCCCCTGCAGGATCCGGCGGCCACCTGCA
	Reverse	CGCCGGATCCTGCAGGGGCCGGGACGAGGT
NAG-1-V5-Δ96-105	Forward	AGTGCGGCTGTCTCGGGCCGCCCTTCCCGA
	Reverse	CGGCCCGAGACAGCCGCACTTCTGGCGTGA
NAG-1-V5-Δ106-113	Forward	CCTGCGTATCCTCCCCGAGGCCTCCCGCCT
	Reverse	CCTCGGGGAGGATACGCAGGTGCAGGTGGC
NAG-1-V5-Δ114-127	Forward	TCCCGAGGGGTCCCCGACGGCGTCAAGGTC
	Reverse	CCGTCGGGGACCCCTCGGGAAGGGCGGCCC
NAG-1-V5-Δ128-141	Forward	GTTCCGGCTGCGGCGTCAGCTCAGCCTTGC
	Reverse	GCTGACGCCGCAGCCGGAACAGAGCCCGGT
NAG-1-V5-Δ142-169	Forward	ACGACCGCTGCTGGCAGAATCTTCGTCCGC
	Reverse	ATTCTGCCAGCAGCGGTCGTGTCACGTCCC
NAG-1-V5-Δ14-29	Forward	TGGCTCTCAGCTGTCTCTGGCCGAGGCGAG
	Reverse	CCAGAGACAGCTGAGAGCCATTCACCGTCC
NAG-1-V5-R193A	Forward	CAGGGGGCGCGCCAGAGCGCGTGCGCGCAACG
	Reverse	CGTTGCGCGCACGCGCTCTGGCGCGCCCCCTG
NAG-1-V5-ΔNES	Forward	TGGCTCTCAGTCGTGGCTGCCGCATGGGGG
	Reverse	GCAGCCACGACTGAGAGCCATTCACCGTCC
NAG-1-V5-mutNES	Forward	CTCTCAGATGCCCCCGGTGCCGCCCGTGCTCTCGTGGCTG
	Reverse	CAGCCACGAGAGCACGGGCGGCACCGGGGGCATCTGAGAG

Supplementary Table S3.2 Differentially expressed genes under U2OS and U2OS-tet condition.

Gene	Locus	Sample 1	Sample 2	Status	Value 1	Value 2	log2 (fold change)	Test stat	P value	Q value	significant
RPE65	chr1:68851224-68915642	U2OS	U2OStet	OK	50.0103	59.5349	0.251508	-5.92584	3.11E-09	2.19E-06	yes
ATP13A2	chr1:17312452-17338423	U2OS	U2OStet	OK	19.4523	15.6498	-0.31379	4.66955	3.02E-06	0.00101	yes
EBNA1BP2	chr1:43629844-43720029	U2OS	U2OStet	OK	133.414	148.138	0.151041	-3.82183	0.000132463	0.02233	yes
NES	chr1:156638555-156647189	U2OS	U2OStet	OK	26.5665	23.781	-0.1598	3.59639	0.000322663	0.04391	yes
ANKRD36BP1	chr1:16819525416822234 3	U2OS	U2OStet	OK	3.15888	2.65061	-0.25309	3.97624	7.00E-05	0.01347	yes
RGS16	chr1:18256775718257354 8	U2OS	U2OStet	OK	13.3078	10.7221	-0.31168	4.79532	1.62E-06	0.00059	yes
TNNT2	chr1:20132814120134680 5	U2OS	U2OStet	OK	10.2585	13.7161	0.419053	-3.83183	0.000127195	0.02163	yes
C1orf35	chr1:22828842722829102 2	U2OS	U2OStet	OK	8.86745	11.3399	0.354821	-3.86768	0.000109876	0.0192	yes
RPS24	chr10:7979351779816571	U2OS	U2OStet	OK	2414.31	2640.85	0.129394	-3.62123	0.000293203	0.04134	yes
NRP1	chr10:33466418-33623920	U2OS	U2OStet	OK	20.2058	17.4308	-0.21313	3.71141	0.000206104	0.03129	yes
LOXL4	chr10:100007372-10002801 2	U2OS	U2OStet	OK	36.3558	32.0409	-0.18227	3.74878	0.000177696	0.02845	yes
-	chr10:33269656-33371081	U2OS	U2OStet	OK	5.30518	4.54118	-0.22434	3.98668	6.70E-05	0.01315	yes
GALNTL4	chr11:11292420-11643596	U2OS	U2OStet	OK	4.4756	2.28591	-0.96932	12.4881	0	0	yes
MIR612	chr11:65201219-65213004	U2OS	U2OStet	OK	0.448262	0.27093	-0.7264	4.72271	2.33E-06	0.00081	yes
CCDC85B	chr11:65657874-65659106	U2OS	U2OStet	OK	23.4042	33.4995	0.517373	-7.60004	2.95E-14	3.75E-11	yes

Supplementary Table S3.2 Continued.

Gene	Location										
GALNTL4	chr11:11292420-11643596	U2OS	U2OStet	OK	12.6261	6.83109	-0.88622	9.907	0	0	Yes
CCDC34	chr11:27351057-27384795	U2OS	U2OStet	OK	21.5285	26.2257	0.284735	-4.13379	3.57E-05	0.0085	yes
H2AFX	chr11:118964584-118966177	U2OS	U2OStet	OK	136.859	160.963	0.234035	-5.83948	5.24E-09	3.56E-06	yes
PTMS	chr12:6875540-6880118	U2OS	U2OStet	OK	406.393	457.4	0.170582	-4.79486	1.63E-06	0.00059	yes
GABARAPL1	chr12:10365488-10375724	U2OS	U2OStet	OK	54.675	47.9905	-0.18813	4.01602	5.92E-05	0.01212	yes
KLRK1	chr12:10515570-10562745	U2OS	U2OStet	OK	51.8896	41.3405	-0.32789	4.00674	6.16E-05	0.01248	yes
CNTN1	chr12:41086243-41466213	U2OS	U2OStet	OK	8.54818	6.47264	-0.40126	5.51954	3.40E-08	1.75E-05	yes
PA2G4	chr12:56498102-56507694	U2OS	U2OStet	OK	135.414	149.879	0.146421	-3.78167	0.000155781	0.0258	yes
RPL41	chr12:56510373-56511616	U2OS	U2OStet	OK	3897.42	4354.86	0.160106	-4.57509	4.76E-06	0.00144	yes
TUBA1A	chr12:49578582-49582861	U2OS	U2OStet	OK	177.573	203.035	0.193315	-5.1941	2.06E-07	8.72E-05	yes
LRIG3	chr12:59265936-59314337	U2OS	U2OStet	OK	11.2591	8.80464	-0.35475	4.28307	1.84E-05	0.00468	yes
FLJ44054	chr13:114586609-114629142	U2OS	U2OStet	OK	66.7944	58.9236	-0.18088	3.98432	6.77E-05	0.01315	yes
HMGB1	chr13:31032878-31040081	U2OS	U2OStet	OK	378.835	419.79	0.148099	-4.35111	1.35E-05	0.00363	yes
SLITRK6	chr13:86366921-86373483	U2OS	U2OStet	OK	0.534355	0.27587	-0.9538	4.00393	6.23E-05	0.01249	yes
COL4A1	chr13:110801309-110959496	U2OS	U2OStet	OK	38.3841	33.131	-0.21233	5.55266	2.81E-08	1.52E-05	yes
FRMD6	chr14:51955854-52197444	U2OS	U2OStet	OK	40.3315	35.644	-0.17825	3.72671	0.000193995	0.0305	yes
SNAPC1	chr14:62228931-62263146	U2OS	U2OStet	OK	131.496	170.306	0.37311	-8.46904	0	0	yes
SMOC1	chr14:70346113-70499083	U2OS	U2OStet	OK	6.85399	5.41703	-0.33944	3.84588	0.00012012	0.0208	yes
JDP2	chr14:75894508-75939714	U2OS	U2OStet	OK	7.81831	9.69454	0.310315	-3.77742	0.000158462	0.0258	yes

Supplementary Table S3.2 Continued.

SLIRP	chr14:781 74424-78183941	U2OS	U2OSte t	OK	323.35	365.9 62	0.1786	-3.712 64	0.00020 5105	0.031 29	Yes
CRIP2	chr14:105 941130-10594650 0	U2OS	U2OStet	OK	40.343 6	46.96 48	0.2192 39	-3.807 45	0.00014 0408	0.023 46	yes
-	chr14:503 26419-50329569	U2OS	U2OStet	OK	88.353 8	60.88 24	-0.5372 7	11.40 39	0	0	yes
BMP4	chr14:544 16454-54423554	U2OS	U2OStet	OK	13.887 7	18.58 03	0.4199 68	-4.707 83	2.50E-06	0.000 85	yes
LTBP2	chr14:749 64885-75079337	U2OS	U2OStet	OK	14.383 3	12.25 76	-0.2307 3	4.039 41	5.36E-05	0.011 22	yes
AHNAK2	chr14:105 403441-10544469 4	U2OS	U2OStet	OK	12.804 1	11.52 34	-0.1520 4	3.579 85	0.00034 3797	0.046 45	yes
THBS1	chr15:398 73279-39889668	U2OS	U2OStet	OK	32.504 6	28.45 36	-0.1920 4	4.783 33	1.72E-06	0.000 61	yes
CHAC1	chr15:412 45635-41248717	U2OS	U2OStet	OK	7.4383 7	10.10 87	0.4425 44	-4.651 31	3.30E-06	0.001 08	yes
DUT	chr15:486 23620-48635570	U2OS	U2OStet	OK	75.449 6	86.89 43	0.2037 49	-4.174 39	2.99E-05	0.007 2	yes
FURIN	chr15:914 11884-91426687	U2OS	U2OStet	OK	50.943 6	44.14 6	-0.2066 2	5.193 81	2.06E-07	8.72E -05	yes
BMF	chr15:403 80056-40401221	U2OS	U2OStet	OK	7.2859 7	5.347 53	-0.4462 5	4.839 32	1.30E-06	0.000 49	yes
COX5A	chr15:752 12616-75230495	U2OS	U2OStet	OK	157.58 6	177.2 6	0.1697 29	3.710 37	0.00020 6954	0.031 29	yes
RPS17	chr15:828 21160-82824865	U2OS	U2OStet	OK	1163.2	1379. 55	0.2461 05	6.903 51	5.07E-12	5.09E -09	yes
ATP6V0C	chr16:256 3726-2570224	U2OS	U2OStet	OK	83.715 5	98.63 28	0.2365 73	-3.985 6	6.73E-05	0.013 15	yes
MT2A	chr16:566 42477-56643409	U2OS	U2OStet	OK	1164.6 8	1320. 76	0.1814 33	4.893 6	9.90E-07	0.000 38	yes
MT1E	chr16:566 59584-56661024	U2OS	U2OStet	OK	355.52 4	400.2 67	0.1710 14	-3.950 35	7.80E-05	0.014 72	yes
RPL13	chr16:896 26746-89634370	U2OS	U2OStet	OK	144.89 3	163.6 45	0.1755 82	-3.664	0.00024 831	0.036 39	yes
RPS2	chr16:201 2061-2014827	U2OS	U2OStet	OK	2576.6 3	2832. 3	0.1364 86	3.946 56	7.93E-05	0.014 81	yes
PFN1	chr17:484 8946-4851825	U2OS	U2OStet	OK	905.56 1	1007. 07	0.1532 73	-4.412 85	1.02E-05	0.002 86	yes

Supplementary Table S3.2 Continued.

Gene	Location										
KRT17	chr17:39775691-39781043	U2OS	U2OStet	OK	92.1375	82.6933	-0.15602	3.67753	0.000235503	0.03533	Yes
C1QL1	chr17:43037060-43045644	U2OS	U2OStet	OK	72.07663	91.6376	0.346414	-4.85375	1.21E-06	0.00046	yes
COL1A1	chr17:48261456-48279000	U2OS	U2OStet	OK	112.428	97.7037	-0.20251	5.82227	5.81E-09	3.81E-06	yes
-	chr18:76566211-76580175	U2OS	U2OStet	OK	13.156	15.5836	0.244306	-5.80345	6.50E-09	4.13E-06	yes
RPS15	chr19:1438362-1440492	U2OS	U2OStet	OK	637.677	733.575	0.202117	-5.3185	1.05E-07	4.86E-05	yes
OAZ1	chr19:2269519-2273487	U2OS	U2OStet	OK	459.216	507.073	0.14302	-4.03238	5.52E-05	0.01143	yes
TRAPPC5	chr19:7745706-7747748	U2OS	U2OStet	OK	34.6711	44.87	0.372017	-4.05195	5.08E-05	0.01091	yes
RPL18A	chr19:17970730-17974124	U2OS	U2OStet	OK	832.075	911.643	0.131755	-3.6567	0.00025548	0.03715	yes
GDF15	chr19:18496967-18499986	U2OS	U2OStet	OK	49.2736	1925.45	5.28824	-114.252	0	0	yes
UBA52	chr19:18682371-18688270	U2OS	U2OStet	OK	146.052	161.38	0.143981	-3.59724	0.000321608	0.04391	yes
-	chr19:30074963-30083332	U2OS	U2OStet	OK	0.636652	0.36587	-0.79917	4.05569	5.00E-05	0.01091	yes
FTL	chr19:49468565-49470136	U2OS	U2OStet	OK	785.472	857.697	0.126909	-3.64911	0.000263149	0.03798	yes
FAM108A1	chr19:1876974-1885518	U2OS	U2OStet	OK	26.9541	32.1732	0.255357	-3.57352	0.000352219	0.04725	yes
CTXN1	chr19:7989380-7991051	U2OS	U2OStet	OK	24.4743	30.4756	0.316387	-4.56293	5.04E-06	0.0015	yes
C19orf43	chr19:12841453-12845529	U2OS	U2OStet	OK	85.2514	102.243	0.262206	-5.30411	1.13E-07	5.14E-05	yes
GADD45GIP1	chr19:13064971-13068050	U2OS	U2OStet	OK	55.0329	65.6681	0.254899	-4.20604	2.60E-05	0.00635	yes
JUND	chr19:18390562-18392432	U2OS	U2OStet	OK	51.7795	62.5369	0.272326	-5.73197	9.93E-09	5.91E-06	yes
LRFN1	chr19:39797456-39811499	U2OS	U2OStet	OK	13.6311	15.966	0.228099	-3.7696	0.000163513	0.0264	yes
SLC1A5	chr19:47278136-47291842	U2OS	U2OStet	OK	55.6713	64.88	0.220839	-4.28812	1.80E-05	0.00464	yes
LBH	chr2:30454396-30482899	U2OS	U2OStet	OK	38.7842	33.7861	-0.19904	4.36921	1.25E-05	0.00339	yes

Supplementary Table S3.2 Continued.

LTBP1	chr2:3317 1602- 33624575	U2OS	U2OSte t	OK	16.338 9	13.69 16	- 0.2550 3	3.964 19	7.36E- 05	0.014 03	Yes
MTHFD2	chr2:7442 5689- 74442424	U2OS	U2OStet	OK	109.63 5	124.7 29	0.1860 92	- 4.212 67	2.52E- 05	0.006 24	yes
TMSB10	chr2:8513 2762- 85133799	U2OS	U2OStet	OK	1996.8 1	2201	0.1404 64	- 4.098 13	4.17E- 05	0.009 68	yes
LOC44090 5	chr2:1307 83571- 13082478 4	U2OS	U2OStet	OK	2.1061 5	1.683 28	- 0.3233 4	4.624 89	3.75E- 06	0.001 17	yes
TNFAIP6	chr2:1522 14105- 15223656 2	U2OS	U2OStet	OK	5.8843 2	4.069 31	- 0.5320 9	4.328 08	1.50E- 05	0.003 93	yes
NOP58	chr2:2031 30514- 20316838 4	U2OS	U2OStet	OK	75.611 7	83.88 47	0.1497 97	- 3.673 86	0.00023 8912	0.035 48	yes
PTMA	chr2:2325 73234- 23257825 0	U2OS	U2OStet	OK	824.17	905.7 95	0.1362 44	- 3.878 56	0.00010 5076	0.018 53	yes
SNRPG	chr2:7050 8505- 70520869	U2OS	U2OStet	OK	356.55 5	413.4 76	0.2136 77	- 5.162 07	2.44E- 07	0.000 1	yes
LINC0011 6	chr2:1109 69105- 11098051 7	U2OS	U2OStet	OK	7.0947 4	8.990 87	0.3417 1	- 3.778 16	0.00015 7994	0.025 8	yes
LIMS3	chr2:1111 60495- 11123065 2	U2OS	U2OStet	OK	1.9338 5	0.082 35	- 4.5535 2	7.957 11	1.78E- 15	2.82E -12	yes
IGFBP5	chr2:2175 36827- 21756027 2	U2OS	U2OStet	OK	29.852 3	21.99 58	- 0.4406 2	10.67 94	0	0	yes
EPHA4	chr2:2222 82746- 22243977 4	U2OS	U2OStet	OK	1.9933 3	1.437 41	- 0.4717 1	4.418 36	9.95E- 06	0.002 83	yes
ID1	chr20:301 93085- 30194317	U2OS	U2OStet	OK	107.23	145.3 31	0.4386 32	- 8.915 74	0	0	yes
CEBPB	chr20:488 07119- 48809227	U2OS	U2OStet	OK	15.109 9	17.87 89	0.2427 71	- 3.619 54	0.00029 5131	0.041 34	yes
-	chr20:571 97836- 57210985	U2OS	U2OStet	OK	5.6984 4	4.269 81	-0.4164	6.311 94	2.76E- 10	2.19E -07	yes
RPS21	chr20:609 62120- 60963576	U2OS	U2OStet	OK	1541.6 6	1715	0.1537 24	- 4.224 21	2.40E- 05	0.006 01	yes
CST3	chr20:236 14293- 23618574	U2OS	U2OStet	OK	78.154	89.74 03	0.1994 38	- 3.631 15	0.00028 2162	0.040 11	yes

Supplementary Table S3.2 Continued.

TGM2	chr20:367 56863-36793700	U2OS	U2OStet	OK	19.0493	15.9769	-0.25375	4.46147	8.14E-06	0.00239	Yes
PMEPA1	chr20:562 23447-56286592	U2OS	U2OStet	OK	25.0607	19.3473	-0.3733	6.73062	1.69E-11	1.61E-08	yes
PSMA7	chr20:607 11790-60718474	U2OS	U2OStet	OK	464.14	508.518	0.131739	-3.6724	0.00024028	0.03548	yes
-	chr20:572 11326-57218179	U2OS	U2OStet	OK	1.07683	0.77355	-0.47723	3.90803	9.31E-05	0.01661	yes
-	chr21:982 5436-9826332	U2OS	U2OStet	OK	52.6068	77.6733	0.562169	3.93863	8.19E-05	0.01516	yes
MIF	chr22:242 35896-24241117	U2OS	U2OStet	OK	1143.53	1385.34	0.276748	-7.72916	1.09E-14	1.48E-11	yes
TIMP3	chr22:329 08539-33454377	U2OS	U2OStet	OK	19.8074	15.7429	-0.33134	7.15985	8.08E-13	9.05E-10	yes
ATF4	chr22:399 16568-39918691	U2OS	U2OStet	OK	330.381	370.346	0.164746	-4.63089	3.64E-06	0.00116	yes
MN1	chr22:281 32565-28198388	U2OS	U2OStet	OK	30.1175	25.3892	-0.24639	4.05882	4.93E-05	0.01091	yes
BHLHE40	chr3:5021 096-5026865	U2OS	U2OStet	OK	17.0303	14.5697	-0.22514	4.04045	5.33E-05	0.01122	yes
LMCD1	chr3:8543 484-8609806	U2OS	U2OStet	OK	11.9364	9.50559	-0.32852	3.90886	9.27E-05	0.01661	yes
CCDC72	chr3:4848 1685-48485537	U2OS	U2OStet	OK	462.879	535.171	0.209363	-5.10424	3.32E-07	0.00013	yes
-	chr3:1106 05903-11069024 3	U2OS	U2OStet	OK	20.3358	18.2178	-0.15868	3.60785	0.000308741	0.04293	yes
H1FX	chr3:1290 33613-12904341 2	U2OS	U2OStet	OK	129.898	151.375	0.220745	-5.36982	7.88E-08	3.85E-05	yes
SERP1	chr3:1502 59779-15030380 3	U2OS	U2OStet	OK	31.2551	36.0892	0.207474	-3.63617	0.000276722	0.03964	yes
HMGB2	chr4:1742 52526-17425559 5	U2OS	U2OStet	OK	104.463	123.437	0.240782	-5.36272	8.20E-08	3.90E-05	yes
RHOBTB3	chr5:9506 3687-95132071	U2OS	U2OStet	OK	48.4892	54.3196	0.163809	-3.72502	0.00019653	0.0305	yes
TGFBI	chr5:1353 64583-13539950 7	U2OS	U2OStet	OK	31.2223	23.1096	-0.43409	8.09872	6.66E-16	1.15E-12	yes

SLC12A7	chr5:1050488-1112392	U2OS	U2OStet	OK	33.5048	27.6413	-0.27755	5.62238	1.88E-08	1.09E-05	Yes
PLK2	chr5:57749809-57755966	U2OS	U2OStet	OK	43.1773	50.8841	0.236943	-5.54921	2.87E-08	1.52E-05	yes
TBCA	chr5:76986994-77072185	U2OS	U2OStet	OK	85.1154	97.8317	0.200882	-3.72726	0.000193574	0.0305	yes
HMGA1	chr6:34204576-34214010	U2OS	U2OStet	OK	266.58	301.212	0.176211	-4.10874	3.98E-05	0.00936	yes
IER3	chr6:30710975-30712327	U2OS	U2OStet	OK	58.5764	48.3121	-0.27794	5.25117	1.51E-07	6.70E-05	yes
-	chr6:44608572-44621571	U2OS	U2OStet	OK	16.5315	11.7753	-0.48946	5.45211	4.98E-08	2.50E-05	yes
CTGF	chr6:132269316-132272518	U2OS	U2OStet	OK	77.6613	69.8194	-0.15357	3.7221	0.000197574	0.0306	yes
SLC2A12	chr6:134308718-134373789	U2OS	U2OStet	OK	7.50797	5.63796	-0.41325	6.09759	1.08E-09	7.89E-07	yes
CITED2	chr6:139693396-139695785	U2OS	U2OStet	OK	55.9886	69.8478	0.319081	-7.09193	1.32E-12	1.40E-09	yes
EZR	chr6:159186772-159240456	U2OS	U2OStet	OK	49.1065	54.6956	0.155511	-3.60215	0.000315591	0.04357	yes
FSCN1	chr7:5632435-5646287	U2OS	U2OStet	OK	118.606	131.692	0.150986	-4.0667	4.77E-05	0.01069	yes
CLDN4	chr7:73245192-73247015	U2OS	U2OStet	OK	30.9854	24.0884	-0.36325	6.36613	1.94E-10	1.61E-07	yes
SERPINE1	chr7:100769956-100782547	U2OS	U2OStet	OK	22.4485	18.9229	-0.24648	4.61296	3.97E-06	0.00122	yes
CAV1	chr7:116164838-116201239	U2OS	U2OStet	OK	121.754	153.646	0.33565	-7.77471	7.55E-15	1.11E-11	yes
-	chr7:57920454-57929601	U2OS	U2OStet	OK	7.13588	9.96256	0.481424	-6.5672	5.13E-11	4.65E-08	yes
SPDYE7P	chr7:72333317-72339655	U2OS	U2OStet	OK	3.96852	2.86021	-0.47248	6.39477	1.61E-10	1.39E-07	yes
ASNS	chr7:97481428-97501854	U2OS	U2OStet	OK	40.9043	47.6367	0.219822	-4.05106	5.10E-05	0.01091	yes
EIF4EBP1	chr8:37888019-37917883	U2OS	U2OStet	OK	74.3734	89.1871	0.262048	-5.02997	4.91E-07	0.00019	yes

Supplementary Table S3.2 Continued.

ZMAT4	chr8:40388110-40755343	U2OS	U2OStet	OK	0.46997	1.74857	1.89554	-4.09483	4.22E-05	0.0097	Yes
PABPC1	chr8:101715143-101734315	U2OS	U2OStet	OK	610.245	668.341	**0.131197**	-3.8373	0.000124394	0.02135	**yes**
ANXA1	chr9:75766780-75785307	U2OS	U2OStet	OK	327.944	360.829	**0.137864**	-3.90733	9.33E-05	0.01661	**yes**
PSAT1	chr9:80912058-80945009	U2OS	U2OStet	OK	27.0889	33.2947	**0.297588**	-5.57133	2.53E-08	1.42E-05	**yes**
MRPL41	chr9:140446308-140447007	U2OS	U2OStet	OK	88.6464	111.916	**0.336281**	-5.77516	7.69E-09	4.72E-06	yes
TMEM2	chr9:74298281-74383822	U2OS	U2OStet	OK	18.8444	16.4445	**-0.19653**	4.38101	1.18E-05	0.00326	**yes**
ABCA1	chr9:107543056-107694762	U2OS	U2OStet	OK	1.9841	1.52911	**-0.37579**	4.34643	1.38E-05	0.00366	**yes**
TNC	chr9:117781853-117881330	U2OS	U2OStet	OK	32.4589	28.6507	**-0.18005**	4.07784	4.55E-05	0.01031	yes
RPL35	chr9:127615754-127624240	U2OS	U2OStet	OK	858.713	951.244	**0.147639**	-3.91793	8.93E-05	0.01636	**yes**
XAGE1A,XAGE1E	chrX:52238809-52243953	U2OS	U2OStet	OK	120.244	76.7833	**-0.6471**	8.80437	0	0	**yes**
XAGE1C,XAGE1D	chrX:52511760-52516904	U2OS	U2OStet	OK	122.227	86.126	**-0.50504**	7.18372	6.78E-13	8.08E-10	yes
PCSK1N	chrX:48689505-48693960	U2OS	U2OStet	OK	14.1463	21.1719	**0.581733**	-6.25284	4.03E-10	3.07E-07	**yes**
XAGE1C	chrX:52255219-52260363	U2OS	U2OStet	OK	210.471	308.648	**0.552339**	-10.945	0	0	**yes**
XAGE1A,XAGE1D	chrX:52528159-52533303	U2OS	U2OStet	OK	103.765	175.515	**0.758277**	-12.5288	0	0	**yes**
XAGE1C	chrX:52541053-52546197	U2OS	U2OStet	OK	73.705	56.8792	**-0.37386**	4.64691	3.37E-06	0.00109	yes
BCYRN1	chrX:70430034-70948962	U2OS	U2OStet	OK	225.264	645.53	**1.51886**	-4.44083	8.96E-06	0.00259	**yes**

Supplementary Table S3.3. Primer sets for real-time RT-PCR in this study.

Gene	Direction	Sequence (5'-3')
COL1A1	Forward	GTCCTGTCGGCCCTGTTG
	Reverse	CTTCTCTTGAGGTGGCTGGG
TIMP3	Forward	ATGGCAAGATGTACACGGGG
	Reverse	GGGGTCTGTGGCATTGATGA
TGM2	Forward	TACGATGCGCCCTTTGTCTT
	Reverse	GTGTTGTTGGTGATGTGGGC
TGFBI	Forward	TAACGGCCAGTACACGCTTT
	Reverse	TGGCTGTGGACACATCAGAC
LTBP1	Forward	GGGATGGGGAGATAACTGCG
	Reverse	TTTCTGACGCATCCAGGACC
LTBP2	Forward	AAGTGACCCCCTCCACTGAT
	Reverse	ATCACACTCGCAGTGGTACG
SERPINE1	Forward	GCCAGTGGAAGACTCCCTTC
	Reverse	CTCTAGGGGCTTCCTGAGGT
PMEPA1	Forward	CCTCAGAAGGATGCCTGTGG
	Reverse	CCAGCCTGGCACTATCCATC
HMGA1	Forward	GGAAAAGGACGGCACTGAGA
	Reverse	GAGGACTCCTGCGAGATGC
IGFBP5	Forward	AACGAAAAGAGCTACCGCGA
	Reverse	GGGAAGGTTTGCACTGCTTT
RPLP0	Forward	AATCTCCAGGGGCACCATTG
	Reverse	ATCTGCAGACAGACACTGGC

VITA

Kyung-Won Min was born in South Korea. He joined the Cell Biology Laboratory at the National Kangneung University in South Korea as an ungraduated student worker in August 2005. In February of 2007 he graduated from the National Kangneung University in South Korea with a bachelor's degree in Biology. In 2007 he returned to the Cell Biology Laboratory as a graduate student assistant. In February of 2009 he graduated with a master's degree. He joined the Environmental Carcinogenesis Laboratory at the University of Tennessee Veterinary College as a graduate student seeking PhD degree. He completed his dissertation in the fall of 2014.